DYNAMIC OPTIMIZATION OF MULTI-UNIT SYSTEMS UNDER FAILURE CONDITIONS

DYNAMIC OPTIMIZATION OF MULTI-UNIT SYSTEMS UNDER FAILURE CONDITIONS

by

Anthony K.S. Balthazaar, B.Eng.

A Thesis
Submitted to the School of Graduate Studies
in Partial Fulfillment of the Requirements
for the Degree
Master of Applied Science

McMaster University

MASTER OF APPLIED SCIENCE (2005) McMaster University

(Chemical Engineering) Hamilton, Ontario, Canada

TITLE:	Dynamic Optimization of Multi-Unit Systems Under Failure Conditions
AUTHOR:	Anthony K.S. Balthazaar, B.Eng. (McMaster University, Canada)
SUPERVISOR:	Dr. C.L.E. Swartz
NUMBER OF PAGES:	xx, 168

ABSTRACT

Shutdowns in a chemical processing plant are detrimental both to plant economics and critical product characteristics. These situations can be due to routine maintenance, or due to the more extreme case of equipment failure due to wear. Nevertheless, both are cases of non-normal plant operation, and are often unavoidable. These situations are complicated further when many units are linked, and subjected to a high degree of integration. In this case, the shutdown of any unit within the plant can have immediate and potentially severe impacts on other areas of the operation. Since these events are unavoidable, the challenge is to minimize their economic impact through careful design of operating practices, and potentially plant design retrofits.

This thesis focuses on developing generic and systematic methods of determining economically optimal operating policies and plant designs in the face of failures in multi-unit operations. This includes determining the optimal trajectory of critical plant variables (flows through units, flows between units, buffer tank levels, etc.), as well as determining whether plant design changes would improve plant economics during such events. Such ventures lead to mixed-integer dynamic optimization (MIDO) problems.

A dynamic model of the process is presented, accounting for the major flows of process materials through units, between units, as well as the accumulation of these in the intermediate buffer capacities. The approach used was to assume that the processing units operated at pseudo-steady-state, with dynamics confined to the intermediate buffer capacities. All models developed were based on a combination of empirical and fundamental elements. For use of the model in an optimization study, a simultaneous approach, in which the differential equations are discretized and included as equality constraints, was employed. This yielded a nonlinear optimization problem involving

only algebraic equations. Optimal responses to scenarios involving planned maintenance shutdowns, as well as unplanned shutdowns (unit failures) were computed, with plant economics used as the merit function. Sensitivity to parameters such as preparation time, shutdown length, and restoration time were studied. In all cases, it was desired to maximize plant economics, while maintaining a smooth operation. While several methods are available for use in a multi-criterion optimization problem, a two-tiered approach was developed and applied in which the plant economics were maximized first, and input usage subsequently minimized as a secondary objective.

After identifying key failure scenarios through a review of industrial data and downtime reports, a multiple-model formulation was developed involving the probability distribution of failure scenarios. Optimal steady-state operating levels for the buffer capacities were computed. This formulation is then extended to a mixed-integer programming problem in which the addition of extra buffer capacity is included as a decision variable.

ACKNOWLEDGEMENTS

I wish to express my gratitude to Dr. Christopher L.E. Swartz for his patience and guidance during the pursuit of my Master's degree.

To Drs. Thomas E. Marlin and Andrew N. Hrymak. Thank you for your teachings and advice through, not only my days as a graduate student, but also during my undergraduate days at McMaster.

I would like to acknowledge and say thank you for the generous funding provided by McMaster University, the McMaster Advanced Control Consortium, the Ontario Graduate Scholarship Program, the Ontario Graduate Scholarships in Science and Technology Program, and Dr. and Mrs. Naresh Sinha.

To all of my friends that have supported me during my days at McMaster. Thank you especially to Dave Rapone, Janaki Logendran, Lavan Kalaichelvam and rest of the 29 Thorndale Crews from 1999–2005. Thank you also to my fellow graduate students, especially Benoit Cardin, Richard MacRosty, Mark-John Bruwer, Art Tinson, and Karen Yeung. Benny, thank you for all the games of squash, many conversations about non-research topics. Richie, thank you for all the coffee breaks and talks.

To the many members of my extended family. Special thank you's must be extended to Uncle Aubrey, Aunty Clare, Shane, and Brandon. Thank you for providing me with a home away from home. To Keith, thank you for you support and for being a second brother to me.

To Uncle Siva and Aunty Nithiya. Thank you for welcoming me into your family during the past couple of years. To Nisha – thank you for your support and encouragement, as well as your love. To Tania and Bob, and Tyronne - thank you for all of

your support through my university days. Last, but certainly not least, thank you to my parents, Anthony and Marie Balthazaar. Thank you for all of the drives to and from McMaster throughout my university days, the home-cooked meals, and for all of your love and support.

Table of Contents

List of Figures

List of Tables

Chapter 1

Introduction

1.1 Motivation and Goals

Failures in a chemical plant are detrimental to both plant economics and critical product characteristics. This situation is complicated further when the units are subjected to a high degree of integration, because the failure of one unit can have immediate and potentially severe impacts on other areas of the plant. Since these events are often unavoidable, the goal is to minimize their impacts through careful design of operating practices. The goal of this research is to develop generic and systematic methods to determine optimal operating policies and plant designs in the face of failures in multi-unit operations. This includes determining the optimal trajectory of critical plant variables (flows through units, flows between units, buffer tank levels, etc.) as well as determining whether the addition of extra storage capacities would aid in the event of the failures that are typical for the plant being investigated. Such scenarios can become mixed-integer dynamic optimization (MIDO) problems.

The Kraft Pulp and Paper process provides an interesting application of the above ideas. The Kraft mill is a highly integrated network of various production departments, with many of the departments bordered by intermediate storage capacities. Since the departments interact through the flows of material and energy, disturbances in one area of the plant can propagate to other areas quickly. To minimize the impact on production, product quality, and by extension, plant economics, operating practices are necessary to combat plant disturbances or failures. These 'recipes' involve the efficient use of the buffer capacities located throughout the plant. In the best case, these buffer capacities will allow some departments to operate normally, or at least close to nominal operating levels, while others are in shutdown mode.

1.2 Main Contributions

The main contributions of this thesis are the following:

1. Literature sources, fundamental models, plant data, and industrial studies were used to develop a dynamic model of a multiple-unit process system, suitable for the determination of optimal operating policies via dynamic optimization.

2. A two-tiered optimization approach to address linear dependencies amongst decision variables was developed and applied. A secondary criterion is optimized in a manner that does not compromise the optimality of the primary objective.

3. A fundamental nonlinear dynamic model of an oxygen delignification reactor was developed. The simplified plant model utilizes data generated from this model.

4. Optimal plant trajectories under planned and unplanned shutdown conditions were computed, with economics as the prime objective. The two-tiered approach

was used to also maintain a smooth plant operation. Sensitivity analysis was performed to investigate the impact of parameters including shutdown length, preparation time, and restoration time. In addition, an introductory study on the impact of uncertain estimates on the shutdown length was illustrated.

5. Downtime frequency distributions were used to determine optimal tank levels during steady-state operation. This was extended to the formulation of a mixed-integer dynamic optimization problem which determines whether or not it is economically viable to add additional storage capacities.

1.3 Thesis Overview

Chapter 2 – Literature Review

Chapter 2 presents a review of the key fundamentals and approaches used in this work. An overview of the Kraft process is presented, followed by a review of some of the work done in the management of pulp mill production. Optimization areas that are pertinent to this work, including dynamic optimization and mixed-integer dynamic optimization, as well as methods to solve such problems, are reviewed. A brief review of maintenance scheduling is also provided.

Chapter 3 – Process and Model Description

This chapter provides an overview of the basic assumptions and models used in the study of the industrial application, the Kraft pulp mill. Using a combination of literature models and studies, as well as industrial data, a dynamic model using fundamental and empirical components is developed. The development of a fundamental, nonlinear dynamic model for the oxygen delignification reactor is presented. The use of this model as well as fundamental model of a continuous digester from the litera-

ture are used for identification of the nonlinear relationships between throughput and delignification.

Chapter 4 – Optimization of Plant Operation: Formulation

The computation of optimal operating policies for the plant in the face of unit shutdowns requires a careful formulation of the optimization problem. Chapter 4 presents the full formulation of the problem, including the form of the objective function and important system constraints. An introductory case study is presented, and the presence of non-unique solutions identified. A review of some of the main approaches to solve multi-criterion problems is presented, followed by the proposal of a two-tiered approach. This is then applied to the introductory case study.

Chapter 5 – Optimization of Plant Operation: Case Studies

Chapter 5 is the first of two case study chapters. Based on the formulation developed in Chapter 4, operability case studies involving planned and unplanned shutdowns are presented. In each case, the flexibility of the model and formulation is illustrated, where sensitivity to shutdown length, preparation time, and restoration time are studied. A small illustrative study of the effects of imperfect estimations of the downtime length is also presented. Alternative formulations for solving the multi-criterion problem are also investigated.

Chapter 6 – Optimization of Plant Design: Formulation and Solution

Utilizing the main formulation issues described in Chapter 4, this chapter extends the operability studies to include plant design decisions. Through the use of knowledge of key downtime scenarios and a parallel-model approach, two types of design studies are illustrated. The first involves establishing a new steady-state operating point by modifying the steady-state buffer tank levels. The second involves a change to the plant flowsheet through buffer tank capacity addition. Additional formulation

issues including capital cost estimation and the treatment of integer variables are also presented.

Chapter 7 – Conclusions and Recommendations

A summary of this thesis is presented, highlighting the key findings obtained from the application of the optimization formulations to the case study scenarios. Key directions for future enhancements are identified.

Chapter 2

Literature Review

2.1 Introduction

In this chapter, a brief overview of the application is first presented. This is followed by a review of some of the work done in pulp mill production management. Optimization areas that are pertinent to this work are also reviewed, including dynamic optimization and mixed-integer dynamic optimization. The chapter concludes with a brief review of maintenance scheduling.

2.2 Process Description

As stated previously, the Kraft Pulping Process is a complex network of production departments, which are separated and buffered by intermediate storage capacities.

On the periphery of Kraft Mill are the wood chip receiving and preparation facilities. Some chips are brought in by truck, but chips can also be produced at some mills from logs. The logs are also brought in on truck, and are debarked and then chipped

and screened. To maintain a consistent and stable process, only chips of a certain size are processed. Also on the periphery of the mill are waste water treatment facilities and the chemical plant.

At the heart of Kraft process is the continuous pulp digester. The chips and white liquor are charged to the top of the digester. White liquor is a concentrated solution of sodium sulphide and sodium hydroxide. In the digester, the chips are cooked and the organic components are reacted and partially separated from the cellulose fibres. The major organic component, lignin, is essentially the 'glue' that bonds the cellulose fibres together when in wood form. By the end of the digester residence time, the chips become fibrous. However, there is still a significant amount of bonded lignin. The partially-removed lignin is first removed in a series of washing steps. The pulp stream is then passed through a set of screening processes to remove knots and other undigested pieces of wood. Simultaneously, the liquor, which is blackened during the digester process, is withdrawn from the digester for reprocessing.

At this point, the pulp is still dark in colour because of the lignin that remains with the cellulose fibres. The plant studied includes an oxygen delignification department to reduce the use of bleaching chemicals, and therefore reduce the amount of chlorine-containing emissions. In the oxygen delignification process, the pulp stream is first dewatered to raise the consistency, and is then combined with steam and caustic solution at desired dosages. Oxygen is fed counter-currently through a reaction vessel. While the lignin reacts with the oxygen and caustic in the desired reaction, an undesired side-reaction occurs in which the cellulose fibres are degraded, resulting in a decrease in viscosity. Therefore, in the O_2 delignification step, as well as in subsequent bleaching steps, it is critical that the processing conditions are balanced to maximize delignification, while maintaining pulp integrity.

Further whitening of the pulp is accomplished in the bleach plant. At the plant studied, a five-step bleaching process is employed, involving alternating steps of oxidation

and extraction. In the first bleaching stage, chlorine dioxide is used as the oxidant. The second stage is the first extraction stage, where caustic, peroxide and oxygen are reacted with the pulp. Chlorine dioxide is once again used in the third and fifth stages, while peroxide and caustic are once again used in the fourth stage.

Following storage in the high-density storage capacity, the pulp passes through the final cleaning stages where the finest particles are removed. The pulp feed then enters the header to the sheet-forming machine. The pulp flows from the header and is formed into a sheet along a wire-mesh. Water is removed from the pulp, increasing the consistency from 10% to 50%. The sheet then enters a dryer that is heated by steam, and the moisture content is further reduced to the final product requirement of 10%. The pulp is then cut, baled, and shipped.

The black liquor that is drawn from the digester and from the brownstock washers is first stored in storage vessels as weak black liquor. It is still valuable on two fronts – the organic component retained from the delignification reactions makes it a candidate fuel source, and its residual sodium content makes it valuable for reuse at the digester. Therefore, the liquor is then split and concentrated in two parallel multiple-effect evaporation units. The resulting concentrated stream of organic chemicals is then combusted in recovery boilers to produce steam for use in different areas of the plant. The concentrated liquor stream is reduced to a sodium smelt on the floor of the boilers. This smelt is dissolved to produce green liquor, indicating the presence of a high amount of iron sulphide. Through lime addition, reaction, and subsequent clarification, white liquor is regenerated for use in the continuous digester. In the associated lime cycle, the lime mud taken from the above clarification stage is calcined, and regenerated as burnt lime for use in the recausticizing steps.

2.3 Pulp Mill Optimization

In a capital-intensive industry such as pulp and paper, maximum utilisation of assets is essential. For this reason, many researchers have been investigating the optimal design, control, and operation of pulp mills. Some have looked at individual units, versus the plant as a whole. This includes extensive work on the continuous digesters (Wisnewski and Doyle [2001] and Wisnewski and Doyle [1998]), the bleach plant [Wang *et al.*, 2003], and vacuum drum washing systems [Kempe, 1995]. In addition, Soliman *et al.* [2004] present a rigorous fundamental model of the oxygen delignification unit, and apply a predictive-control scheme using a known disturbance set. Other researchers have focused on the energy system, in which optimal steam and electricity practices are studied (Snow and Realff [1998], Nilsson and Söderström [1992], and Fauconnier [1993]).

Allison [2004] reviews an area on the control of surge tanks in series. As described in Section 2.2, the Kraft Mill can be viewed as system of surge tanks in series, where the linkages between the surge tanks are the processing units themselves. Allison [2004] presents an optimization-free method for co-ordinating the loads on a set of surge tanks during a transient event. The scheme strives to relieve the impact of a surge on any single tank, and rather distributes the load across the plant to avoid upper and lower volume constraints on the surge tanks. Work by Pulkkinen [2004] focused also on the dynamic optimization of a small set of steady-state on/off processes with inventory dynamics. Their work was geared at developing optimal operating policies in off-line mode, and stressed the importance of end-point objectives, similar to the work of Allison [2004]. Both research groups recount that while the optimal solution to such problems over a fixed horizon is to drive storage vessels empty, this is not true in a continuous, rolling horizon scenario. Practical decision intervals of 1 hour over a time horizon of 1-2 operating days are used, with end-points set to match initial conditions.

There has been some work from a plant-wide perspective as well. Most of the pioneering work was done by research groups in Europe, primarily in Scandinavia. In the 1960s, Pettersson [1969] worked on a multi-product mill, in which a sulfate pulp mill, a kraft paper mill, and multiple paper machines were coordinated during planned maintenance shutdowns. A state-space formulation of the model was presented, accounting for dynamics in the buffer tank levels. The assumed control variables $\mathbf{u}$ were the production rates of the various plant processes. While up to twenty buffer tanks were available in the plant, reduction was realized by combining adjacent tanks and neglecting small tanks. A system involving three paper machines, nine processing units, and ten buffer tanks was considered for optimization [Pettersson, 1970]. Multiple shutdowns are considered along a time horizon spanning 24-48 hours, in which the system is not required to return to the nominal operating point. Optimization studies were based on minimizing variation of the production rates through various pieces of equipment, as the author assumes that the most economic way of running a mill is to maintain a high and uniform production rate through all processes. Leiviskä *et al.* [1979] and Leiviskä *et al.* [1980] discuss the advantages of production control systems for sulphate pulp mills.

The work by Uronen *et al.* [1984] discusses the economic justification for such systems. Motivation of such systems is presented, including discussion pertaining to increased throughput, reduction in raw materials and utilities, and decreased emissions and losses. Two simple case studies are presented, illustrating the benefit of buffer storage capacities around failure-prone equipment. However, once again, a return to the nominal state is not strictly enforced. Ruiz *et al.* [1990] introduces an automated system called Optimill, developed in France. Simple models involving yield equations for the main processing units are included. The user can configure the overall topology of the plant, and then through data acquisition, the system gains are identified (either automatically, or manually). A simulation mode is available to compute the impact of chosen input profiles, and simple linear programming approaches are used for

optimization.

More recently, Kayihan [1997] discusses rigorous optimization approaches to process systems management in the pulp and paper industry at various levels, including company-side, mill-wide, and process optimization. Lasslett [2000] uses flow-sheeting packages for production planning. Issues such as optimal storage levels based on the probability of shutdowns upstream and downstream of each storage are discussed. The implied approach in the work is to run the production departments at the maximum allowable rate until the storage capacities force shutdowns. Not considered explicitly is the importance of returning the mill operating point to the nominal point, including the stock levels. Dube [2000] looks at only the operational problem where the impact planned and unplanned shutdowns of operating areas is minimized using a production-based objective. The models assumed pseudo-steady state operation in the processing areas, and considered dynamics only in the inventories. Optimal use of the buffer capacities are illustrated for two scenarios. Production control systems have been shown to provide increases in mill production of 3-5%, and provide less tangible benefits such as reduce labor. Payback times of such systems can be as little as two years Uronen *et al.* [1984].

2.4 Dynamic Optimization

For applications such as the foregoing, where assumed steady-state operating facilities and dynamic inventories interact, a model of the system is described by a differential algebraic equation (DAE) system. Computation of optimal operating policies and plant designs therefore lead to dynamic optimization. Dynamic optimization problems are those involving models that include, as part of their equation set, differential equations to describe the dynamic behaviour of the system. The differential equations can describe time-dependent trajectories such as tank levels, or space-dependent

trajectories such as concentration profiles through a plug-flow reactor. In this work, the differential states will include the time-varying hold-ups within buffer capacities. Algebraic equations are used for, among other things, thermodynamic relationships or any physical phenomenon that is naturally algebraic.

Dynamic optimization problems are given by the general formulation [Cervantes and Biegler, 2001],

$$\min_{\mathbf{x}(t),\mathbf{y}(t),\mathbf{u}(t),t_f,\mathbf{p},\mathbf{d}} \phi(\mathbf{x}(t),\mathbf{y}(t),\mathbf{u}(t),t_f,\mathbf{p},\mathbf{d}) \tag{2.1}$$

subject to:

$$\dot{\mathbf{x}}(t) = \mathbf{f}(\mathbf{x}(t),\mathbf{u}(t),\mathbf{y}(t),\mathbf{p},\mathbf{d},t) \tag{2.2}$$

$$\mathbf{0} = \mathbf{h}[\mathbf{x}(t),\mathbf{u}(t),\mathbf{y}(t),\mathbf{p},\mathbf{d},t] \tag{2.3}$$

$$\mathbf{0} \leq \mathbf{g}[\mathbf{x}(t),\mathbf{u}(t),\mathbf{y}(t),\mathbf{p},\mathbf{d},t] \tag{2.4}$$

$$\mathbf{x_0} = \mathbf{x}(0) \tag{2.5}$$

$\mathbf{x}(t)$ is the vector of differential variables

$\mathbf{y}(t)$ is the vector of algebraic variables

$\mathbf{u}(t)$ is the vector of input variables

$\mathbf{f}$ is the vector of differential equations

$\mathbf{h}$ is the vector of equality constraints

$\mathbf{g}$ is the vector of inequality constraints

$\mathbf{d}$ time-invariant decision variables

$\mathbf{p}$ time-invariant parameters

t time

2.4.1 Methods of Dynamic Optimization

Since the early 1990s, the study of processes using dynamic simulation and optimization has grown significantly. Chemical processes are modelled dynamically using differential-algebraic equations (DAEs). The differential equations describe the time-dependent behaviour of the system, while the algebraic equations can describe other physical, chemical, or thermodynamic relationships. To use DAE systems in an optimization framework using an NLP approach, two major classes of dynamic optimization approaches have been applied to process problems. These are the (i) simultaneous approach and (ii) the sequential approach [Cervantes and Biegler, 2001].

The sequential approach is based on only discretizing the control variables (Control Vector Parametrization) into time-invariant parameters. This method is used in the software package, gPROMS/gOPT. First, initial conditions and a set of control parameters must be assumed and specified. The control variables may, for example, be represented as piecewise polynomials, with the decision variables in the optimization problem being the polynomial coefficients. The process model is then integrated with a DAE solver at each optimization iteration and values for the objective function and constraint equations are computed. The NLP solver then uses this information to find the optimal polynomial coefficient values in the control parameterization. A major advantage of the sequential approach is that it is a feasible path method. Therefore, intermediate solutions are still useful Biegler *et al.* [2002].

The second dynamic optimization approach is the simultaneous method which is applied in this research. Using this method, complete discretization converts a dynamic optimization problem involving differential equations into a finite-dimensional nonlinear programming problem. This avoids the computationally intensive integration step that is required in the sequential approach. An advantage of the simultaneous method is that the dynamic model and optimizer constraints are simultaneously con-

verged. Also, in a control problem, path constraints on the manipulated and state variables are handled easily. However, a major disadvantage is the large number of variables that result from the discretization. Another difficulty using the simultaneous approach is the challenge in initializing the system. Since the entire system has been discretized, each variable needs to be initialized at each time-point.

One possible method for discretization is orthogonal collocation on finite elements [Cervantes and Biegler, 2001]. Other methods that are suitable for discretization are the lower-order implicit Runge Kutta methods, such as the implicit Euler (backward-difference method). Explicit methods have associated stability issues, especially with stiff systems [Chapra and Canale, 1998].

2.4.2 Application Areas

Georgiadis *et al.* [2002] present a case study on a reactive distillation system which involves a rigorous dynamic model. The dynamic model relaxes many of the traditional assumptions used in a distillation study, and therefore, full dynamic characteristics are modelled. An economic objective function is employed to minimize the design cost. The decision variables in this study include the column diameter, and the condenser and reboiler surface areas. The sequential method of dynamic optimization is applied in the gPROMS environment. The design using a dynamic model is shown to be superior to that using a steady-state model, which produced potential operability bottlenecks. Additional dynamic optimization studies have been performed in area of design and control, including those by Pistikopoulos and Sakizlis [2001], Schweiger and Floudas [1998], and Ross *et al.* [2001]. This work is geared at simultaneously computing the physical design of a process system, as well as the control system that is to regulate it.

Dynamic models are critical in studying process systems under non-normal operating

conditions. This is the basis for this research, where the non-normal events are plant failures. These can also include planned maintenance shutdowns, the start-ups from these shutdowns, or potentially the commissioning of new processing units. The start-up or shutdown of units/plants, or the transition from one steady-state to another, can have a major impact on the overall economics of a process operation. Gani and Grancharova [1997] study the start-up of a methyl-tertiary-butyl ether (MTBE) production process including a mixing tank, a continuously-stirred tank reactor (CSTR) and a distillation column. They use the software package DYNSIM in the study with a modification to handle dynamic optimization problems. The objective function was to minimize the integral-squared deviation of the process variables (distillation column product flowrates and temperatures) from the required values. The decision variables were the control variable trajectories, namely the flowrate between the mixer and CSTR, the flowrate between the CSTR and the distillation column, and the reflux and boil-up ratios in the distillation column. It is shown that a dynamic optimization approach is by far superior to the steady-state approach.

2.5 Mixed-Integer Dynamic Optimization

Integer variables in a design problem are typically used to specify equipment selection, or the existence/non-existence of units. The simultaneous consideration of plant design and control, involving dynamic models of the system and integer decisions results in a Mixed-Integer Dynamic Optimization (MIDO) problem. The objective function considered in these problems can be economics-based, possibly involving some profitability assessment (eg., ROI, payback-time, etc.). It can also be a production objective such as throughput, purity, yield, etc. Constraints pertaining to material balances, energy balances, safety considerations, supply and demand, etc. are included in the formulation. Being 'dynamic', the equation set also includes

differential equations.

Grossman and Morari [1983] suggest that an economic objective function is best for design and control problems. This is appropriate since design decisions are determined in industry by some type of profitability analysis. Therefore, the economic objective function can be calculated as being the total profit for some predetermined amount of time (for example, the total annualized cost), or some profitability assessment such as those mentioned above. While safety and operational objectives are important as well, they can be handled in the set of constraint equations.

2.5.1 Application Areas

The optimal design of a binary distillation column, using an economic objective function and including effects of closed-loop dynamics is presented by Bansal *et al.* [2002]. A MIDO formulation is used, including time-varying trajectories of the operating variables, and discrete decisions for the number of trays, entry points for feed and reflux, and the control-loop pairing.

Pistikopoulos and Sakizlis [2001] illustrate a MIDO problem in a process control, design and operability problem. Two systems are discussed - a separation system, and a reaction/separation system. Discrete decisions are used to determine the number of trays in the distillation column and the pairing of manipulated and controlled variables. Continuous decisions present in the formulation represent the physical design characteristics and the tuning parameters for the determined control structure. The objective function is economics-based, minimizing the total annualized cost, including the capital expenditures and the utility costs. The authors consider the effect of time-varying disturbances and time-invariant uncertainty.

As mentioned above, these problems can involve uncertainty, as discussed by Mo-

hideen *et al.* [1996]. In this formulation, optimal plant and control design that deals with disturbances and parametric uncertainty is determined by the solution of a mixed-integer dynamic/stochastic problem. They describe an iterative decomposition algorithm strategy that determines the optimal design capable of handling a pre-specified uncertainty/disturbance set. The basic algorithm involves the following three steps:

1. An initial set of scenarios for the uncertain parameters is chosen.
2. For this set, the optimal process and control design is determined.
3. If the 'optimal' design is feasible over the whole range of the uncertain parameters, then the true optimal design has been found. If not, the critical scenarios are updated, and Steps 2 and 3 are repeated.

The above algorithm assumes that the uncertainty is uniformly distributed across the range of possible values, and therefore the solution must be feasible for the full range of the uncertain parameters.

2.6 Mixed-Integer Nonlinear Programming

The inclusion of a nonlinear process model along with integer decision variables leads to a mixed-integer non-linear programming formulation, which can be stated as Equation 2.6.

$$\begin{aligned} &\min_{\mathbf{x},\mathbf{y}} f(\mathbf{x},\mathbf{y}) \\ &\text{subject to } \mathbf{h}(\mathbf{x},\mathbf{y}) = \mathbf{0} \\ &\qquad\qquad \mathbf{g}(\mathbf{x},\mathbf{y}) \leq \mathbf{0} \\ &\qquad\qquad \mathbf{x} \in X \subseteq \mathbb{R}^n \\ &\qquad\qquad \mathbf{y} \in Y \text{ integer} \end{aligned} \tag{2.6}$$

In this case, $\mathbf{y}$ can take any integer values. Floudas [1995] illustrates that this formulation can be modified, whereby all integer variables are represented by binary variables, $\{0,1\}^q$.

Due to the nonlinearities, the MINLP problems are in general non-convex, and therefore it is possible that multiple local solutions exist. To find the global optimum, a global optimization technique must be applied.

2.6.1 Outer Approximation / DICOPT

DICOPT stands for 'DIscrete and Continuous OPTimizer'. The DICOPT solver is based on the ideas of Outer Approximation, Equality Relaxation and Augmented Penalty, and was developed by Viswanathan and Grossman [1990]. In the GAMS implementation, the DICOPT iterates between a primal integer problem and the relaxed master problem. Essentially, this is iteration between an NLP solver and an MIP solver. Since the iterations involve the solution of an NLP, the location of the global optimum is not guaranteed. As stated above, a global optimization technique would be required.

During the iterations, the primal problems generate a sequence of non-increasing upper bounds, while the master problems generate a sequence of non-decreasing lower

bounds. When these bounds are within some pre-specified tolerance, the algorithm terminates. Consider:

$$\begin{aligned} &\min_{\mathbf{x},\mathbf{y}} \ \mathbf{c}^T\mathbf{y} + f(\mathbf{x}) \\ \text{subject to: } &\mathbf{g}(\mathbf{x}) + \mathbf{B}\mathbf{y} \leq \mathbf{0} \\ &\mathbf{x} \ \epsilon \ \mathbf{X} \subseteq \mathbb{R}^n \\ &\mathbf{y} \ \epsilon \ \mathbf{Y}(0,1)^q \end{aligned}$$

Assume $\mathbf{f}(\mathbf{x})$ and $\mathbf{g}(\mathbf{x})$ are convex and continuously differentiable. Linearization of these functions underestimates the objective function and overestimates the feasible region. The basic algorithm involves the following steps:

1. Solve the primal problem for a fixed set of discrete variables, $\mathbf{y}^k$.
2. Update the upper bound (B_U) as being the minimum of the present upper bound and the solution of the primal problem in Step 1.
3. Solve the relaxed master problem, with linearized constraints.
4. Update the lower bound (B_L) as being the maximum of either the present lower bound or the solution of the master problem in Step 3.
5. If ($B_U - B_L$) is less than some pre-specified epsilon, then the algorithm stops. However, if the test criteria is greater than the pre-specified epsilon, y^{k+1} is set to be the discrete set found in the master problem, and the algorithm is repeated.

2.6.2 Simple Branch & Bound / SBB

The SBB acronym stands for Simple Branch and Bound. This technique is completely analogous to the Branch and Bound technique used in mixed-integer linear programming (MILP). In this case, the relaxed problems are solved by an NLP-algorithm. The general B&B technique involves a tree search in the integer space, solving relaxed NLPs at each node. A node is terminated when its relaxed solution (a) exceeds the current upper bound, (b) is found to be infeasible, or (c) yields discrete values for the integer variables. Once again, global optimality is not guaranteed since an NLP is being solved at each node.

The basic algorithm involves the following steps:

1. Solve a relaxed NLP at the first node.
2. Partition and constrain problem into separate domains. Solve relaxed NLPs at the new nodes, or follow a depth-first approach following one branch first.
3. When an integer solution is found, it becomes the updated upper bound.
4. If any relaxed/integer solutions are found to be greater than this upper bound, they are discarded, and then node is terminated.
5. Infeasible nodes are also terminated.

Figure 2.1 illustrates a tree of nodes in the branch-and-bound search. There are three main alternative approaches for selecting nodes for which to solve the relaxed NLP problem. These are the (i) Last-In-First-Out (LIFO), or depth-first search with backtracking, (ii) the breadth-first search, and (iii) the best bound search. The depth-first search involves selecting one of the children nodes from the current node. Backtracking occurs when the current node is fathomed, and the algorithm must

ascend in the tree to find a child node that had not been considered. The breadth-first search implies that all nodes at a given level must be considered before proceeding to lower levels. Option (iii) specifies that the order of the search depends on bounds on the integer solutions [Floudas, 1995].

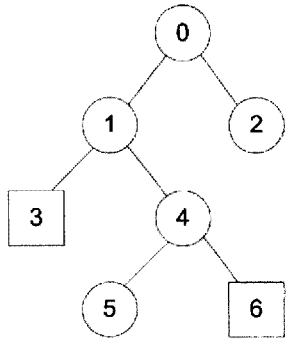

Figure 2.1: Branch and Bound

2.7 Maintenance Scheduling

Maintenance scheduling, or maintenance policy optimization, is concerned with determining when major plant equipment items must be taken off production for preventative maintenance. One of the first papers in this area was presented by Barlow and Hunter [1960], where they present two maintenance policies, corresponding to maximum and minimum required repair on single units. The former involves maintenance performed on a unit, such that it is returned to a condition where it is 'as good as new' (AGAN). The latter refers to the policy when the equipment experiences a failure, and it is returned to the state it was in just before the failure. This is referred to 'as good as old' (AGAO) condition [Barlow and Hunter, 1960]. These activities involve a long-term combined production/maintenance planning problem, since preventative maintenance activities are infrequent [Dedopoulos and Shah, 1996].

To fit this into the context of optimization under failure conditions, one must consider

two key points. First, optimal maintenance policies over a scale of months and years determine when equipment should be maintained, and lead to optimal operating policies during the maintenance shutdown computed in this thesis. Secondly, poor preventative maintenance policies lead to the failure of equipment, and consequently, optimal operating policies during equipment failure is necessary. Figure 2.2 describes the reliability of equipment without a maintenance schedule. The so-called 'bathtub curve' illustrates the susceptibility of equipment to failures at the beginning of its use, called the burn-in period. After some period of time, during normal operation, the rate of failure is constant with random cause. However, after this constant rate regime, the 'wear-out' phase brings a time of increasing failure-rate [Sanmarti *et al.*, 1997]. Equipment in the process industries are typically characterized by a relatively long period of increasing failure rate [Dedopoulos and Shah, 1996]. Other types of products may exhibit a true bathtub-shape, where the normal operation section is long and flat.

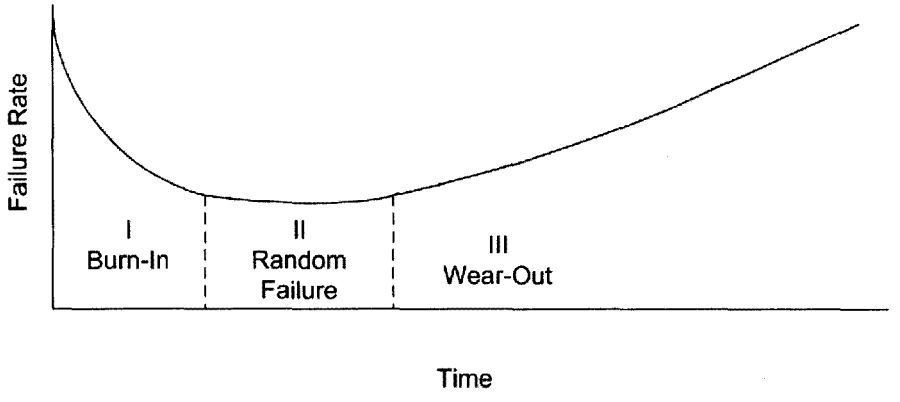

Figure 2.2: Bathtub or Weibull Curve

Pistikopoulos *et al.* [2000] have done work in the area of maintenance scheduling and process optimization, recognizing that system effectiveness and plant economics are a function of whether or not the process is available for operation. Using a mixed-

integer non-linear programming model, optimal maintenance policies for continuous operations are developed, and the impact of uncertainty on the maintenance schedules is addressed. The work considers primarily preventative maintenance of process equipment, using failure rate models. Vassiliadis and Pistikopoulos [2001] introduce the idea of availability threshold values. Equipment is given a failure rate profile that grows over time. When the profile hits the availability threshold, the processing unit must be taken out of service for maintenance for a pre-specified length of time. Using this model which predicts when maintenance is required, optimal maintenance policies are derived. The formulation can handle both LPs and NLPs for the process model, with the use of integer variables to model the availability/non-availability of processing. The sensitivity of the solution to uncertain parameters, maintenance task duration, and maintenance task cost are all addressed.

Key issues raised by Vassiliadis and Pistikopoulos [2001] are with respect to the objective function and the process model. The objective function is a balance between expected revenue and maintenance costs. The revenue will obviously be a function of the proportion of time the plant is available. In addition, if a failure occurs, the process model determining the operation must, in general, change. This will be in a manner the corresponds to specific piece of equipment that has failed. One example raised by the authors is the reduction of the number of equations necessary when a failure occurs in a reactor-sequencing example. Other possibilities are changes in the bounds on manipulated variables in the event of a unit failure.

2.8 Chapter Summary

This chapter has presented some of the key application and optimization areas pertinent to the work that follows. Building on the process knowledge and previous control/optimization studies that have been performed on the Kraft Mill process, a

model and optimization formulation are presented in the next two chapters.

Chapter 3

Process and Model Description

3.1 Introduction

3.1.1 Overview

While the techniques and approaches used in this work can be extended to other processes, the focus here is on the Kraft Pulping Process. Therefore, the purpose of this section is to provide a brief qualitative description of the process, followed by an overview of some of the main units and modeling approaches used in this study. Figure 3.1 presents the full plant layout. Many of the modeling details can be reviewed in Appendix A. The approach was to keep the models as simple as possible due to the problem size. Although compromising some model accuracy, computational benefits would be realized, especially during the design study phase. Also, an effort has been made to have a uniform level of complexity across the entire plant model.

The plant models have been developed based on various literature and industrial sources. While the style of the modelling was inspired by the work of Dube [2000],

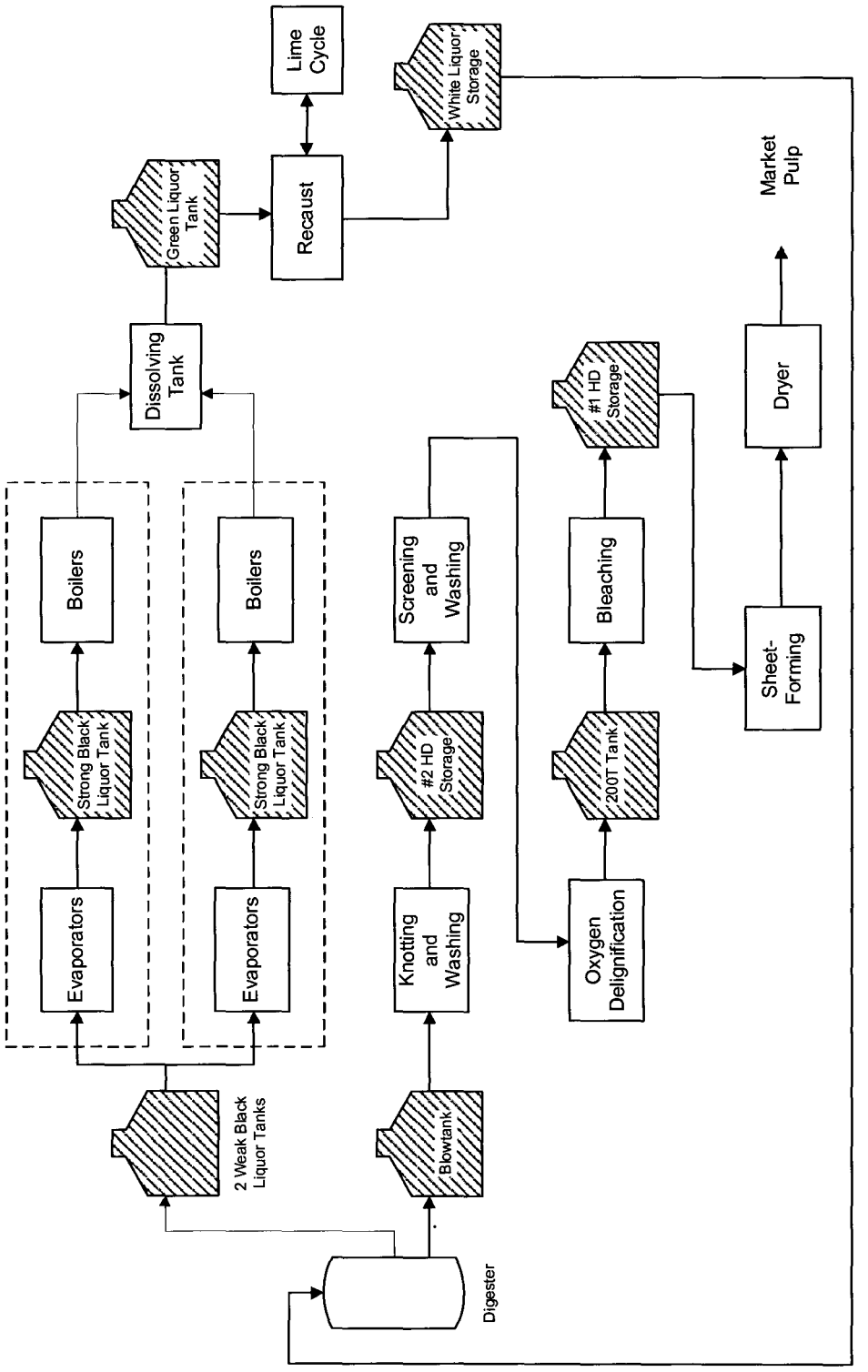

Figure 3.1: Basic Kraft Mill Layout

the overall plant flowsheet and equipment sizes are much different. Moreover, some process model enhancements have been made, including the inclusion of an oxygen delignification department. In addition, the division of process streams into various components was simplified in this work. The major assumption made during the modelling is that all process units apart from buffer capacities are modelled as pseudo-steady-state operations. The justification for this assumption is that the plant being modelled operates well beyond its design capacity. Therefore, the process fluids/materials spend very little time within the units, and steady-state assumption is approximately valid. Moreover, the control interval used was 1 hour, and therefore, it can be assumed that a perturbed production department will have reached steady-state in 1 hour.

The only dynamics assumed in the system are within the intermediate storage capacities. The storage capacities are modelled assuming perfect mixing in the radial and axial directions. The tanks are modelled using a set of differential equations - one to capture the dynamic behaviour of the stock level, and the rest to capture the dynamic response of the outlet concentrations to changes in flow and composition of the inlet and outlet streams. As explained in Appendix A, the engineering units for the flowrates through the plant model were mass units (tonnes/hr). This convention was chosen because the results could then be readily viewed in relation to the hourly production rate.

3.2 Model Overview

3.2.1 Overview

The Kraft models that follow are based on the plant being studied. While they do not exactly represent the true design of the plant, a reasonable amount of detail

has been included to ensure that meaningful exploratory optimization case studies were possible. The dynamic model that follows is based on fundamental concepts, previous research studies, literature sources, as well as plant and experimental data. For reasons of confidentiality, all critical operating data that are included in the models have been removed. The empirical information such as split fractions, chemical dosages, and pulp shrinkage factors have been taken from the published literature sources that describe similar processes.

3.2.2 Nomenclature

Table 3.1 outlines the nomenclature to be used in this thesis. Each stream is described using a subscripted stream number. The superscripted index refers to the component. For example, the statement,

$$F_i^j = F_{50}^P \tag{3.1}$$

with i=50 and j=P refers to the flow of pulp (in tonnes per hour) in stream 50. There are three main components considered in the model, namely pulp, dissolved solids and water. The liquor is composed of organic and inorganic dissolved solids and water. The pulp includes cellulose and bound lignin, as well as knots and shives that are rejected in screening units. The bound lignin is material that binds the cellulose fibres together. The Kappa Number, a term commonly used in the pulp and paper industry, is a measure of the residual bound-lignin content in the pulp. Knots are the large dense components that are difficult to break-down in the digester. For this reason, they are recycled back to the digester, with partial purging after the knotting department. Shives are undigested wood pieces that are not not classified as knots. Both knots and shives are assumed to be rejected using an empirical rejection coefficient, which is explained in the knotting and screening sections of the steady-

Table 3.1: Nomenclature

Symbol	Definition
P	Pulp
DS	Dissolved Solids
W	Water

state model. The term 'consistency' refers to the mass fraction of pulp fibres in a process stream (mass of fibres/total mass). The dissolved solids contains both organic and inorganic components. The organic components are combusted in the boilers, while the inorganic components are either removed from the system (purged) or used in the recausticizing section to regenerate white liquor.

The next sections describe the important production departments in the Kraft mill investigated. These include: Digester, Knotting/Washing, Screening/Washing, Oxygen Delignification, Bleaching, Drying, Evaporators, Boilers/Steam System, Liquor Regeneration. Each department is broken down into a number of sections that is appropriate for the process. Wherever possible, similar units are shown only once for clarity.

3.2.3 General Approach

The Kraft Mill models that follow are all steady-state mass balances, with the exception of the intermediate storage capacities. The goal of this research is to compute optimal trajectories for an integrated process. The optimal use of these inventories is the primary interest, and therefore, these are permitted to vary over the time trajectory.

Chemical processing units essentially accept a feed (or, a combination of feed stocks) and convert that feed into one or more outlet streams. For example, a pulp-drying unit

takes low-consistency pulp as the feed, and through a series of dewatering processes, outputs a water stream and a pulp stream. It is therefore convenient to express the flow of any component in an outlet stream as a fraction of the flow of that component in the inlet stream. A common approach to developing simple material and energy balances for a complex flowsheet of units is to use the split-fraction concept used and described by Sinnott [1993]. Figure 3.2 illustrates a single unit with one inlet stream and two outlet streams. The parameter, α_1, is the split-fraction coefficient, and specifies the linear proportion of component k in stream F_0 that flows into stream F_1. It will be described later this split-fraction factor can itself be a function of other operating variables. The outlet streams, F_1 and F_2, can either be channelled to downstream units, or recycled back to upstream processing units.

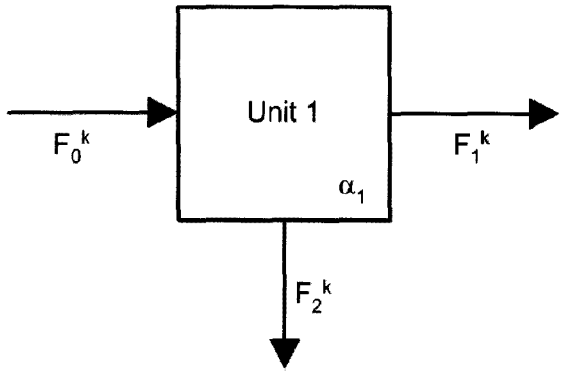

Figure 3.2: Flowsheet Modelling

3.3 Buffer Capacities

Figure 3.3 illustrates an example tank model. In this model, there is a tank with an allowable variance in stock level (maximum and minimum constraints on stock level), and one manipulable inlet stream (m_0), and one manipulable outlet stream (m_1). Each stream is comprised of three components, each with density ρ_i. In the pulp model, these components may relate to pulp (cellulose and bound lignin), dissolved

solids (inorganic and organic components, such as lignin leached from the pulp), and water.

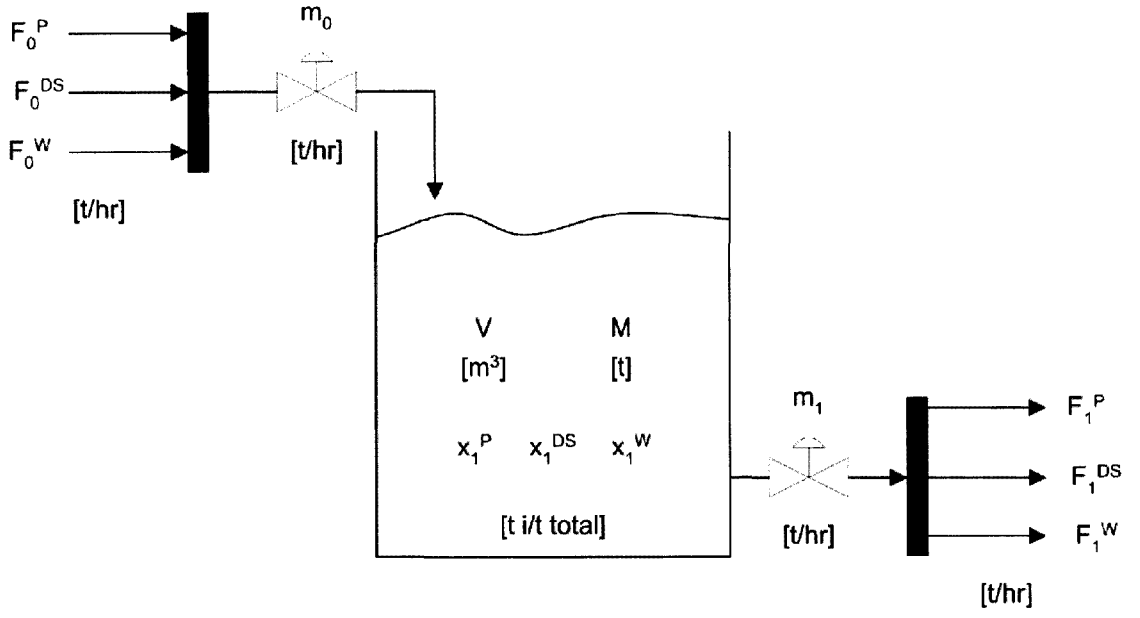

Figure 3.3: Intermediate Storage Tanks

The dynamic model of the tank system is as follows:

$$\frac{dM}{dt} = \dot{m}_0 - \dot{m}_1 \tag{3.2}$$

$$\frac{dx_1^P}{dt} = \frac{\dot{m}_0}{M}\left(x_0^P - x_1^P\right) \tag{3.3}$$

$$\frac{dx_1^{DS}}{dt} = \frac{\dot{m}_0}{M}\left(x_0^{DS} - x_1^{DS}\right) \tag{3.4}$$

$$\frac{dx_1^W}{dt} = \frac{\dot{m}_0}{M}\left(x_0^W - x_1^W\right) \tag{3.5}$$

$$x_j^i = \frac{F_j^i}{\dot{m}_j} \qquad \text{where i=P,DS,W and j=0,1} \tag{3.6}$$

$$V = M\left[\frac{x_1^P}{\rho^P} + \frac{x_1^{DS}}{\rho^{DS}} + \frac{x_1^W}{\rho^W}\right] \tag{3.7}$$

Equations 3.2-3.5 are the total mass and component balances, where 3.3-3.5 are de-

rived below. Equations 3.6 is the definition of the mass fraction and equation 3.7 is a conversion from mass to volume.

The basic balance for a component, i, is given by (3.8),

$$\frac{d}{dt}(Mx_1^i) = \dot{m}_0 x_0^i - \dot{m}_1 x_1^i, \tag{3.8}$$

which is differentiated via the chain rule to yield,

$$M\frac{dx_1^i}{dt} + x_1^i\frac{dM}{dt} = \dot{m}_0 x_0^i - \dot{m}_1 x_1^i. \tag{3.9}$$

Rearranging 3.9 and substituting 3.2 in for the dM/dt term yields

$$M\frac{dx_1^i}{dt} = \dot{m}_0 x_0^i - \dot{m}_1 x_1^i - x_1^i(\dot{m}_0 - \dot{m}_1), \tag{3.10}$$

which is then simplified to yield 3.11,

$$\frac{dx_1^i}{dt} = \frac{\dot{m}_0}{M}(x_0^i - x_1^i). \tag{3.11}$$

The above model assumes that there is only one stage in the storage tank, implying perfect mixing throughout, in both the radial and axial directions.

3.3.1 Volumes

A typical Kraft pulping mill has several storage volumes available. However, a subset of these will be considered as potential sites for disturbance rejection, for the following reasons:

Table 3.2: Available Storage Volumes - Pulp Cycle, m^3

Tembec Name	Size (m^3)	Location
Blowtank [300T]	2050	After Digester
2HD Storage	620	After Knotting/Washing
200T Tank	1780	After Screening/Washing
1HD Storage	1780	After Bleach Plant

(a) Some of the tanks throughout the plant are much smaller than others, and therefore can be assumed to operate at pseudo-steady-state. Essentially, the merit in using these tanks for buffering is negligible.

(b) Some tanks were combined if they were adjacent to each other in the true plant. For example, there physically exists 3 white liquor storage tanks between the Recovery Section and the Recycle Stream to the Digester. These three tanks were combined and considered as one common buffer capacity.

Tables 3.2 and 3.3 state the volumes that were deemed available for disturbance rejection. Also stated in the tables are the design capacities and location of each tank. It was assumed that the minimum level allowed was 10% of the capacity, and the maximum level allowed is 90% of the capacity. The nominal levels were assumed to be at 50% for all tanks. This follows the work of Dube [2000] and Pettersson [1969], as well as operational practices as discussed with plant operators.

Table 3.3: Available Storage Volumes - Liquor Cycle, m^3

Tembec Name	Size (m^3)	Location
Weak Black Liquor Tanks (2)	635	After Digester
Strong Black Liquor Tanks (2)	635	After Evaporators
Green Liquor Storage	620	After Dissolving Tank
White Liquor Storage	1780	After Recausticizing

3.4 Kraft Digester

3.4.1 Steady-state Mass Balances

The digester model is comprised of two steady-state sections, as illustrated in Figure 3.4. The first steady-state tank section is required to combine the wood and liquor and to vent steam. The second section is required for the extraction of black liquor which is sent to the recovery section (evaporators and recovery boilers). The final section is also used to send the material to the blowtank.

The wood charge is assumed to be 80 tonnes per hour at steady-state, which represents the mill production rate (average daily production rate) plus a tolerance for pulp lost in the form of knots, shives, and loss to the liquor cycle (not modelled). The inlet composition of the wood is stated in Table 3.4. The pulp contribution actually includes a lignin component of 27-30% [Grace *et al.*, 1989].

3.4.2 Nonlinear Delignification

The level of complexity of individual models for processing units was kept simple, and in many cases linear. The linear models often used constant factors to describe,

Table 3.4: Mass Fraction Composition of Softwood (Grace *et al.* [1989])

Component	Symbol	Value
Pulp	x_1^P	0.43
Dissolved Solids	x_1^{DS}	0.04
Water	x_1^W	0.53

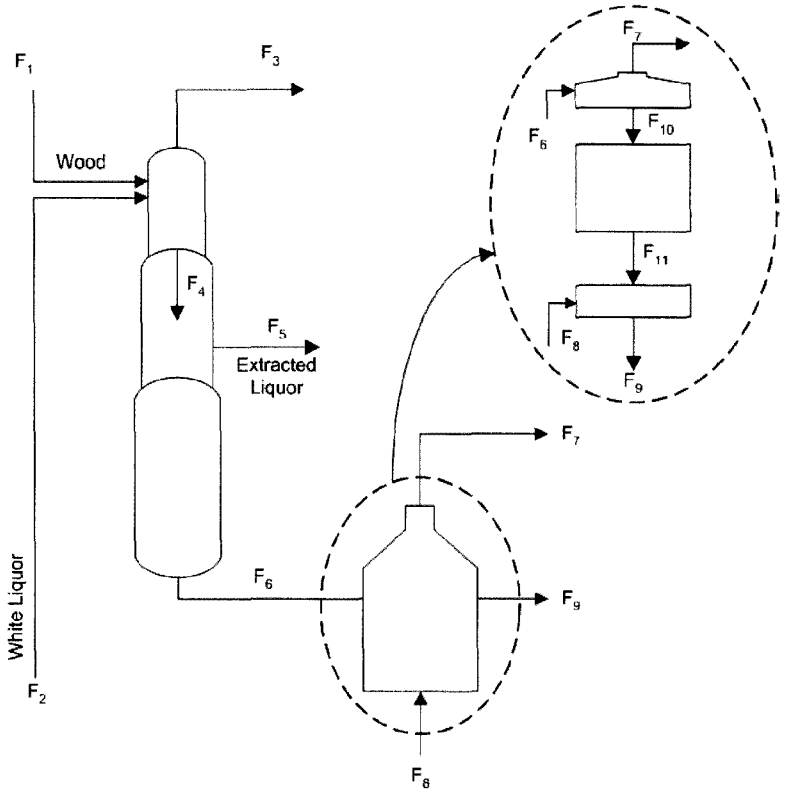

Figure 3.4: Digester and Blowtank

for example, steam economies, reaction rates, or splitter proportions. In two areas of the plant, this was improved through studies using nonlinear dynamic models. Such models were either developed or available for the oxygen delignification reactor and continuous pulp digester, respectively. From a process point-of-view, in these areas, lignin is removed from the cellulose fibres and therefore the amount of fibre decreases (pulp shrinkage). While the style of the models can be maintained, an inherently nonlinear relationship between the production rate and pulp shrinkage was sought. Pulp shrinkage is defined as the loss of pulp due to delignification, because the lignin is initially considered part of the pulp. Through analysis of a nonlinear model, one can uncover this relationship.

The steady-state relationships that are assumed for the digester are based on work done using a nonlinear dynamic model used by Wisnewski and Doyle [1998] and Wisnewski and Doyle [2001]. Due to a lack of Kappa number measurements and full understanding of the complexities within the digester, a common practice in industry is to maintain liquor flows to the digester in ratio to the chip load [Grace *et al.*, 1989]. While this ratio is maintained, variation in production rates impact the degree of delignification achieved due to the corresponding variation in residence time.

Approach

The goal of this section is to develop a relationship between the production rate and the pulp shrinkage factor. The shrinkage factor is defined as the proportion of the incoming pulp feed (to the particular unit, not to the plant) that is lost to delignification.

The fundamental, nonlinear dynamic digester model was treated mainly as a black-box, with only superficial knowledge of its operation necessary for the scope of this work. First, it is important to understand how the system works at the nominal

operating point. It is convenient to introduce the production factor, ζ, which is the ratio between the production rate at any given control interval and the nominal production rate. This is given by

$$\zeta = \frac{\text{Production Rate}}{\text{Nominal Production Rate}}, \tag{3.12}$$

where ζ=1 occurs when the production rate is equal to the nominal production rate. The development of nonlinear correlation models to describe the relationship between delignification extent and ζ is shown below. Of course, an alternative approach would be to develop a correlation in terms of the production rate directly. However, it was desirable to develop a model that would be independent of the engineering units used. As stated above, for the studies, all liquor flows were kept in ratio to the chip feed rate.

The study was accomplished using the continuous digester benchmark model developed by Kayihan *et al.* [1996], and used in studies by Wisnewski and Doyle [1998] and Wisnewski and Doyle [2001]. The production level was varied from 0.5 to 2.0 times the nominal operating rate. White liquor flowrates and extraction flowrates were manipulated to match the production rates, while digester temperature profiles were maintained as constant. Two Kappa numbers were recorded - one at the extraction point, and one at the blowline (digester outlet). Liquor densities were also recorded at these points. The results from the simulations are shown in Figure 3.5, where the independent variable is the production factor, ζ. The results for the blowline data illustrate that at the nominal operating point, the Kappa number is 30 (indication of bound lignin content), which will later be shown to be the inlet Kappa number to the next delignification step (oxygen delignification reactor).

The Kappa number data can be translated to pulp shrinkage factors, by using the well-established empirical relationship between the lignin concentration in the fibre

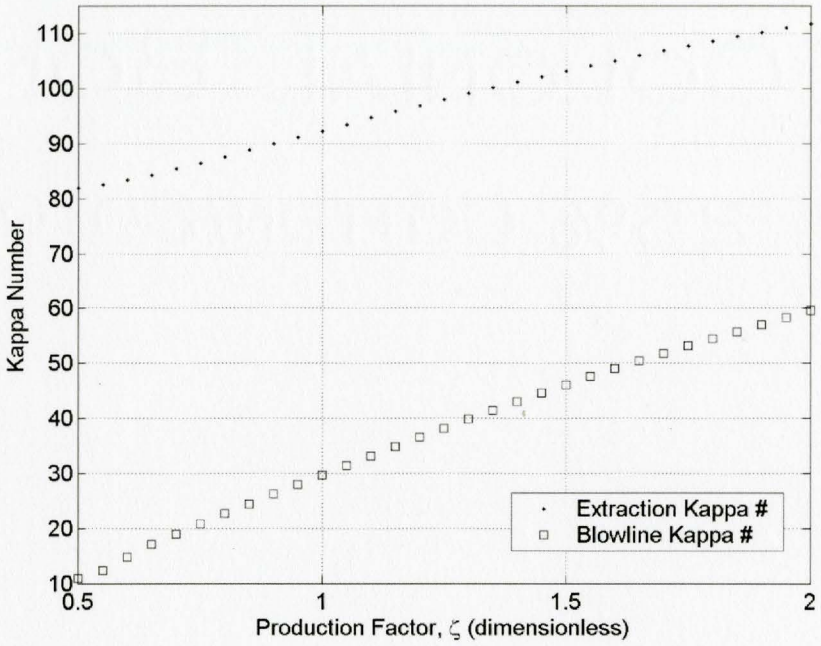

Figure 3.5: Extraction and Blowline Kappa Numbers versus Production Factor

and the Kappa number [Myers and Edwards, 1989], given by

$$[L] = 0.147K \tag{3.13}$$

where [L] is the concentration of lignin in the fibre in units of mass percent (%), and K is the dimensionless Kappa number.

Using Equation 3.13, the data collected is translated to pulp shrinkage factors, assuming an initial Kappa number equal to 165 [Grace *et al.*, 1989]. The data was found to be nonlinear. A quadratic model was fit to the extraction zone data (Equation 3.14), while a cubic model was fit to the blowline data (Equation 3.15). These are given by

$$\alpha_{shrink,1} = 0.3512\zeta^2 - 3.9384\zeta + 14.2390, \tag{3.14}$$

$$\alpha_{shrink,2} = -0.5588\zeta^3 + 2.5357\zeta^2 - 5.2384\zeta + 12.444. \tag{3.15}$$

where $\alpha_{shrink,i}$ has units of mass percent, %. To review, the shrinkage factor represents the reduction in pulp due to delignification, in units of mass percent. The data and models for the shrinkage factors are shown in Figure 3.6.

Equations 3.16-3.18 are component mass balances around the top of the digester, before liquor extraction. This is essentially the combination of the wood and liquor streams, and accounts for the steam vented from the digester during the cooking process. The constants x_1^i, as stated in Table 3.4, describe the proportion of the wood-chips that end up in each stream. Naturally, the sum of these constants equals 1.00. The balances in the top of the digester are

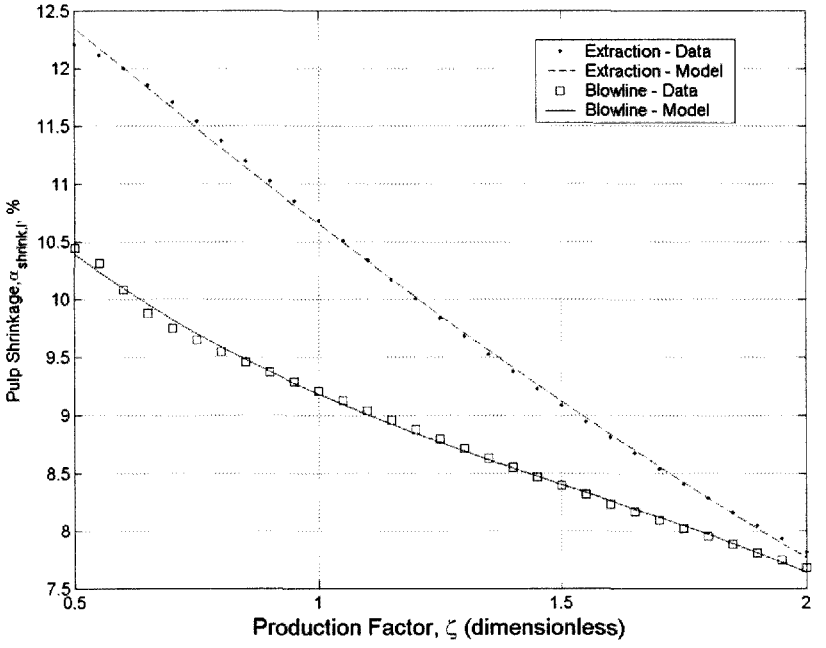

Figure 3.6: Digester Shrinkage Factor Models

$$F_4^P = (1 - \alpha_{shrink,1}/100)F_1 x_1^P, \tag{3.16}$$

$$F_4^{DS} = F_1 x_1^{DS} + F_2^{DS} + (\alpha_{shrink,1}/100)F_1 x_1^P, \tag{3.17}$$

$$F_4^W = F_1 x_1^W + F_2^W - F_3^{ST}, \tag{3.18}$$

$$F_3^{ST} = \alpha_{ST}(F_1^W + F_2^W), \tag{3.19}$$

where α_{ST}=0.04, which represents an approximation of the amount of steam vented from the digester and is assumed to be proportional to the inlet water flow [Dube, 2000]. The shrinkage factor, $\alpha_{shrink,1}$, is computed using the regression model discussed in Section 3.4.2. Also, the overall liquor-to-wood ratio is assumed to be 3.6 by mass (Dube [2000] and Grace *et al.* [1989]). This coincides with the liquor rate used in the studies by Kayihan *et al.* [1996].

Typical compositions of white liquor for use in batch digesters are approximately 1.0M in sodium hydroxide and 0.8M in sodium sulphide/sulphates [Grace *et al.*, 1989]. Using molar masses of NaOH and Na_2S, mass fractions can be calculated and are stated in Table 3.5. Therefore, the proportion of dissolved solids in the white liquor stream, F_2 is given by the sum of the salt mass fractions. The liquor flows are therefore related by

$$F_2^W = 0.788(F_2^W + F_2^{DS}), \tag{3.20}$$

$$F_2^{DS} = 0.212(F_2^W + F_2^{DS}). \tag{3.21}$$

The bottom section of the digester is modelled as a splitter, where black liquor is extracted half-way down the digester, and the pulp and remaining black liquor exits to the blowtank. It is assumed that no pulp is lost in the liquor extraction, and therefore, balances are

Table 3.5: Composition of White Liquor (Grace *et al.* [1989])

Component	Molarity	Molar Mass (g/mol)	Mass Fraction
Sodium Hydroxide	2.0	40	0.080
Sodium Sulphide	1.5	88	0.132
Water	—	18	0.788

$$F_6^P = (1 - \alpha_{shrink,2}/100)F_4^P, \tag{3.22}$$

$$F_6^{DS} = F_4^{DS} + (\alpha_{shrink,2}/100)F_4^P - F_5^{DS}, \tag{3.23}$$

$$F_6^W = F_4^W - F_5^W, \tag{3.24}$$

$$F_6^W = 0.62F_4^W, \tag{3.25}$$

$$\frac{F_5^{DS}}{F_6^{DS}} = \frac{F_5^W}{F_6^W}, \tag{3.26}$$

where the splitting of the liquor phase is based on industrial data. The shrinkage factor, $\alpha_{shrink,2}$, is computed using the regression model discussed in Section 3.4.2.

3.5 Knotting, Washing, and Screening

The knotting, washing, and screening departments all serve similar functions – that is, the removal of unwanted material from the process stream. Wash and dilution liquor is fed from downstream processes. In the event of a shutdown downstream, make-up water is used to prevent upstream shutdowns due to liquor shortage.

3.5.1 Knotting Process Description

The knotting department is a coarse-screening department in which wood knots and large undigested pieces of lumber chips are removed. In this section, the knotters are modelled using steady-state mass balances. The function of the knotters is to remove large undigested pieces of wood. These are then collected and recycled to the digester with the chip load (not modelled).

Figure 3.7 illustrates the knotting department, comprised of a Hi-Q knotter and a Jonsson knotter. The pulp stream first enters the Hi-Q knotter, where it is combined with wash liquor from downstream processes (wash liquor is fed counter-currently starting at the far end of the bleach plant). Accepted pulp is sent to a set of brown-stock washers, while the rejects are sent to the Jonsson knotter. In the Jonsson knotter, rejects from the primary Hi-Q knotter are further screened to remove knots.

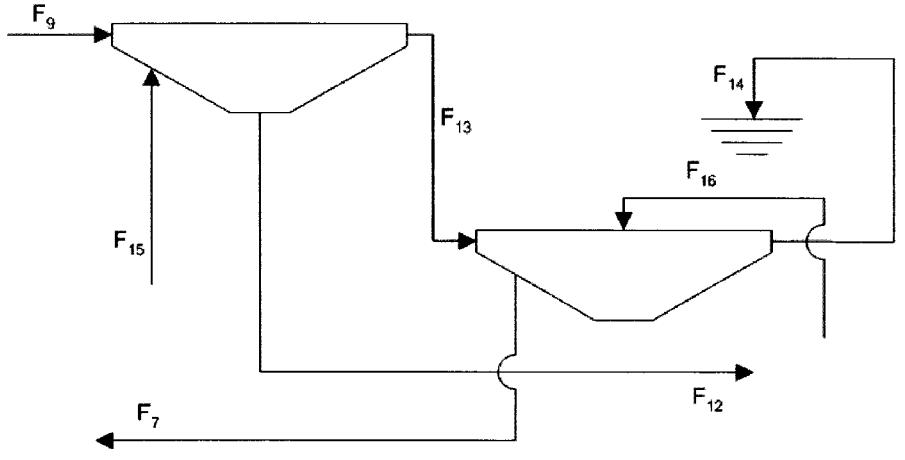

Figure 3.7: Hi-Q and Jonsson Knotters

The governing equations for these processes are mass balances, presented in Appendix A.

3.5.2 Washing Process Description

Figure 3.8 illustrates a set of vacuum drum washing units in series. Each unit consists of a header, a vacuum drum and a seal tank. The liquor used to shower the series of units flows counter-current to the pulp flow. A small storage tank is available at the outlet of the last washer. The outflow from each seal tank is split into two portions, to shower the previous stage and dilute the header box.

First, it is assumed that no pulp is lost in the filtrate stream from the vacuum drum washing unit. A set-point in the outlet consistency specifies the mass ratio of pulp to liquor that exits from the washing units. This set-point is achieved by manipulating the vacuum in the washer drum. Perfect control is assumed. The ratio of dissolved solids and water exiting with the pulp is not the same as that exiting as filtrate. The efficiency of the vacuum washing units in this section of the plant is assumed to be 90% – that is, 90% of the incoming dissolved solids are removed in the filtrate stream.

The governing equations for these processes are mass balances, presented in Appendix A.

3.5.3 Screening Process Description

A simplified pressure screen model is implemented here. There are four screens in the plant - two primary screens, one secondary screen and one tertiary screen. For simplicity, the two primary screens are combined into one stage. This is reasonable as the inlet streams originate from the same upstream location (brownstock washing department), and the outlet streams are mixed.

The job of the pressure screens is to remove 'shives' from the process stream. Shives are a wood species that is larger then processable pulp, but much smaller than knots. These particles do not bleach well, and ultimately lead to deformities in the the

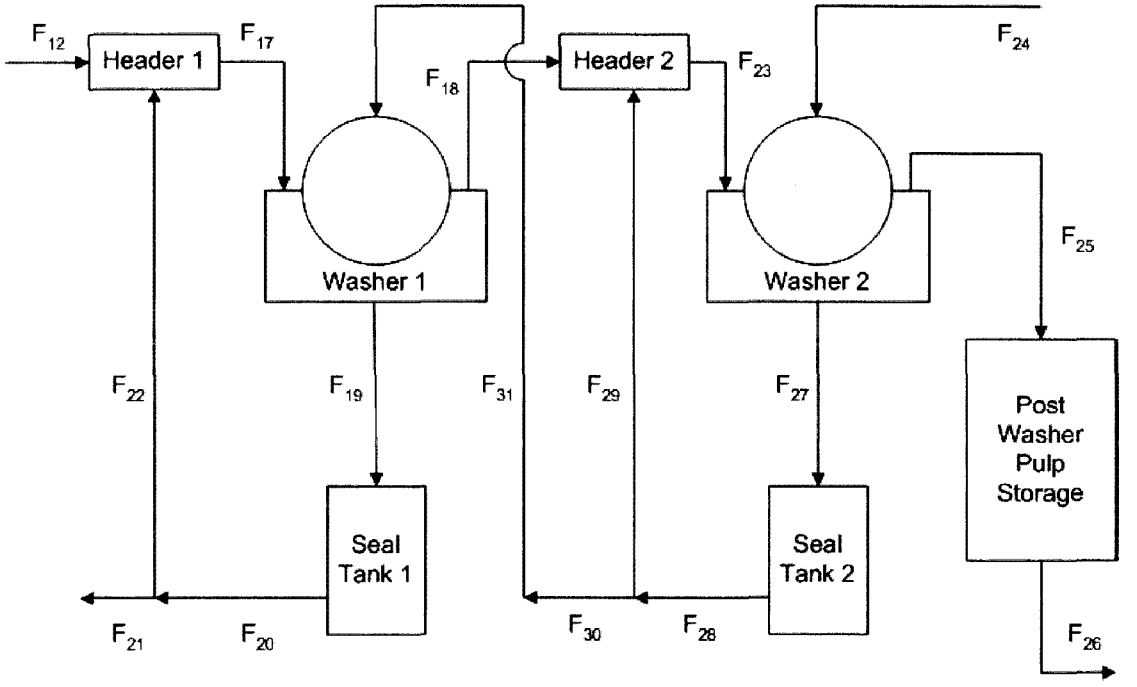

Figure 3.8: Brownstock Washers

formed sheets. Therefore, the three step screening process is used to remove the shives. Figure 3.9 illustrates the simplified set-up as described in Grace *et al.* [1989].

At the screening mix chest, dilution liquor dilutes the pulp stream prior to screening. The stream from the brownstock washers is at approximately 10% consistency. This must be diluted to 3% consistency before processing in the screening department, where the consistency values are based on typical industrial processes [Grace *et al.*, 1989]. The governing equations for these processes are mass balances, presented in Appendix A.

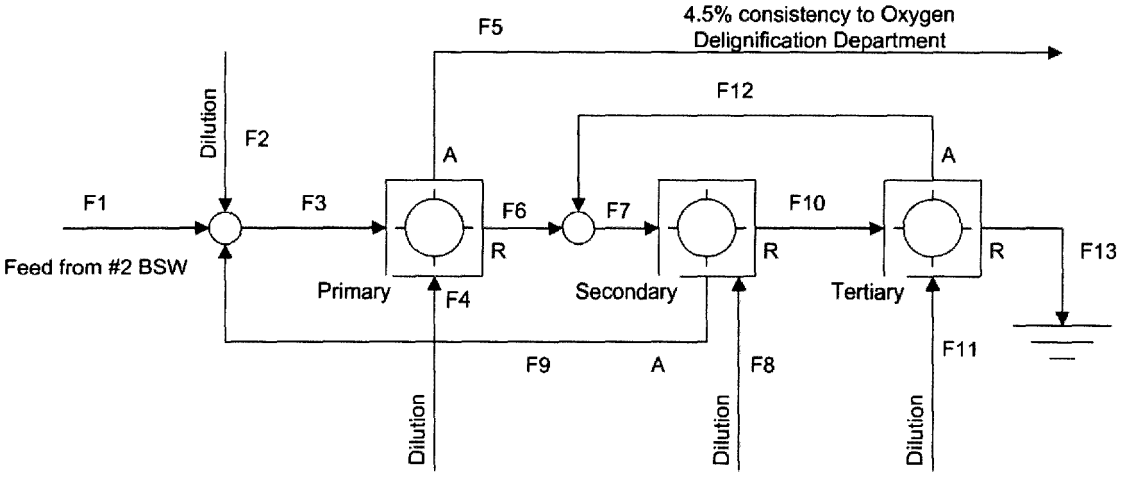

Figure 3.9: Screening Department

3.6 Oxygen Delignification

3.6.1 Overview

Due to environmental regulations on the use of chlorine in pulp whitening, many plants have built oxygen deligification facilities to reduce chlorine usage and emissions from bleaching departments. While effective in delignification, the process has the undesired side reaction of pulp degradation, which is exhibited as a drop in pulp viscosity. Therefore, the delignification is carried out as far as possible, while obeying a lower constraint on viscosity. The oxygen delignification department is shown in Figure 3.10. The stream from screen room is first reduced in water content in the feed press, and the resulting pulp stream at 30% consistency enters the mixer, where steam and chemicals are added. Chemical usage is related to the values given in Table 3.6. Steam is added to maintain the set-point reactor temperature (in this case, assumed to be the inlet temperature), which is usually around 100-120°C. Delignification reactions are carried out, and pulp is washed in a post-oxygen washer before storage prior to the bleach plant.

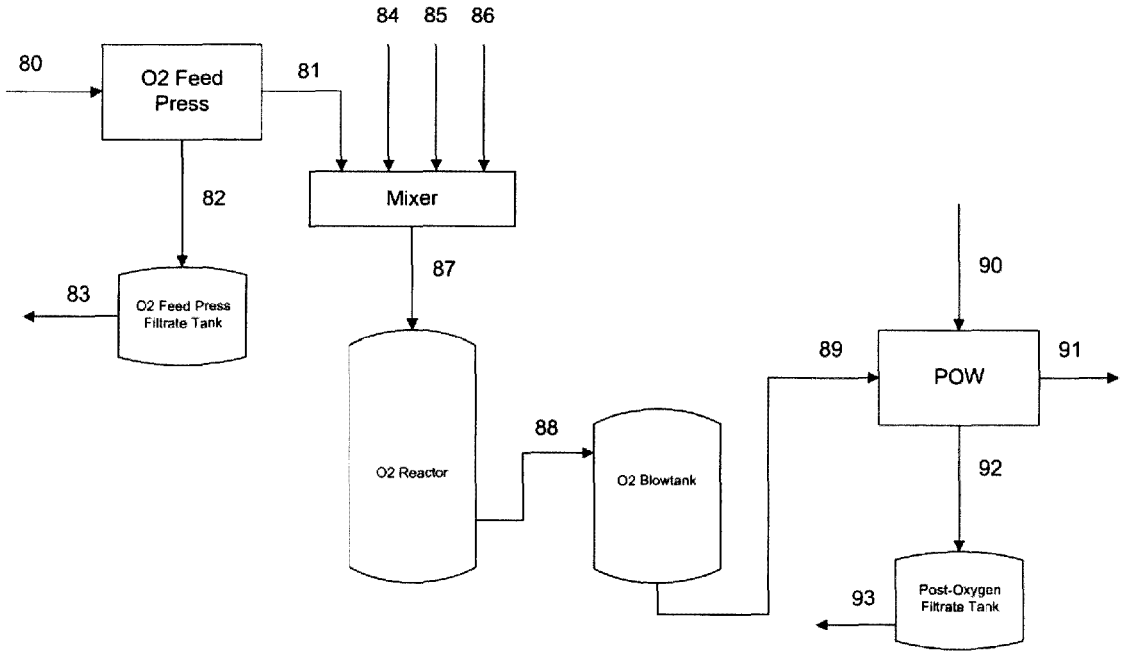

Figure 3.10: Oxygen Delignification Department

Table 3.6: Required Data for Oxygen Delignification Section [Grace *et al.*, 1989]

Data Item	Value	Engineering Units
Oxygen Applied	15	kg/t pulp
Sodium Hydroxide Applied	20	kg/t pulp
Magnesium Sulphate Applied	2	kg/t pulp

This section of the plant model presents a special case of the modelling work, in which a fundamental model was first developed, and subsequently used for identification. A fundamental model of the oxygen delignification process was developed by Soliman *et al.* [2004] and used here for identification. Figure 3.11 presents the basic structure of the model developed. The model is based on fundamental mass and energy balances, and consists of a mixer section and a reactor section. The mixer is assumed operate at pseudo-steady-state, and is the location at which the pulp, chemicals, and steam enter. Perfect mixing is assumed within the mixing process. The reactor exhibits both temporal and spatial variation. Instead of modelling the process using a PDE formulation, the reactor is rather modelled as a series of CSTRs, a common approach when modelling behaviour approaching plug flow. Literature-based models for lignin content, NaOH consumption, as well as a simple energy balance are used in the model. Note that this approach differs from the previous sections of the model, and therefore a balance must be met to match the complexities in the different areas of the plant.

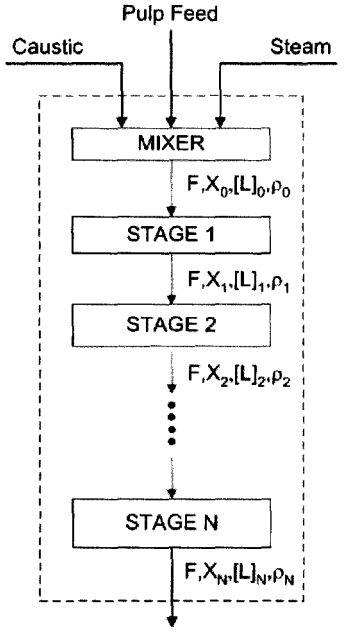

Figure 3.11: Oxygen Delignification - Mixer and Reactor

3.6.2 Mixer

The oxygen delignification mixer is modelled as a steady-state mixing point. Entering the mixer are the pulp stream from the upstream washing and screening department as well as fresh caustic and steam from the utilities cycle. The dilution of the pulp stream due to the steam and caustic additions effectively decreases the consistency entering the reactor section of the model. The steam and caustic flowrates are determined from the desired dosages given in Table 3.6. The inlet temperature of the reactor can be specified, and the steam flow into the mixer is thereby back-calculated. This essentially models a temperature control system, that operates perfectly with no dynamics.

The energy balance within the mixer requires an estimated heat capacity for the inlet pulp mixture. The heat capacity of pulp mixtures assumed to be a weighted average between the individual specific heat capacities of water (4.18 J/g.K) and paper (1.34 J/g.K), using a 1 g basis (Data from Incropera and DeWitt [1996]). The weights are X and 1-X, where X is the consistency. For further detail, see Soliman *et al.* [2004]. The main pulp equations are given by (see Figure 3.11 for notation).

$$F = F^P + F^{OH} + F^{Steam}, \tag{3.27}$$

$$X_0 = \frac{F^P}{F}, \tag{3.28}$$

$$c_{p,pulp} = c_{p,water}(1 - X_0) + c_{p,paper}X_0, \tag{3.29}$$

$$\rho_0 = \frac{1}{\frac{1 - X_0}{\rho_{liquor}} + \frac{X_0}{\rho_{pulp}}}. \tag{3.30}$$

3.6.3 Reactor

The reactor is based on a number of kinetic models found in the literature that were developed based on batch experiments. This includes work by Iribarne and Schroeder [1997], Myers and Edwards [1989], and Agarwal *et al.* [1998]. Below are some of the main equations with further detail given in Soliman *et al.* [2004].

First, the lignin content in the fibres is divided into portions that have fast reaction kinetics, slow reaction kinetics, and zero kinetics (L_f, L_s, and L_b). The latter implies bulk transport through the reactor. The initial lignin concentration, $[L]_0$ (in g lignin per g fibre), is calculated at the outlet of the mixer.

$$[L]_{fast} = 0.225 \times [L]_0 \tag{3.31}$$

$$[L]_{slow} = 0.675 \times [L]_0 \tag{3.32}$$

$$[L]_{bulk} = 0.100 \times [L]_0 \tag{3.33}$$

The reaction vessel is modelled as as a series of stirred-tank reactors, as shown in Figure 3.11. At each stage, there are material balance equations for pulp consistency, the three lignin phases, cellulose, and sodium hydroxide. The balances take the form similar to Equation 3.34 at each stage, which is a balance on fast-reacting lignin

$$\rho_n V \frac{d(X_n[L_f])}{dt} = F_{n-1}X_{n-1}[L_f]_{n-1} - F_n X_n [L_f]_n - \rho_n V X_n R_{f,n} \tag{3.34}$$

where X_n is the pulp consistency, L_f is the concentration of fast reacting lignin, and F is the pulp flow rate. The final dynamic balance at each stage is an energy balance, in which the heat of reaction is estimated from operating data given in Tatsuishi *et al.* [1987]. Further details of the model can be found in Soliman *et al.* [2004]. The

composite model comprised of the mixer module and reactor stages was coded in the MATLAB/Simulink environment, and is used in the next section.

3.6.4 Capturing Nonlinear Behaviour

The full nonlinear dynamic oxygen delignification model was used to develop a relationship between the production rate and pulp shrinkage, similar to that presented for the digester. For the analysis, it was assumed that chemical and steam additions are in linear ratio to the production rate. This is reasonable because literature sources typically give dosages relative to production rates (eg. kg NaOH per tonne of pulp) (Grace *et al.* [1989], Sakuma *et al.* [1987] and Tatsuishi *et al.* [1987]). Moreover, it is assumed that the inlet consistency is constant. This is reasonable, as perfect consistency control is assumed at the outlet of the oxygen feed press by manipulating the vacuum in the press (See Appendix A). In summary, the study focused on the univariate effect of the production rate on pulp shrinkage, measured by Kappa number in the nonlinear model.

A similar approach to the digester identification is employed here, using a production factor, ζ. When ζ=1, the production rate is equal to the nominal production rate. Using the nonlinear model, the production factor was varied from 0.3 to 2.0, and the drop in Kappa number was recorded. Chemical and steam dosages were controlled to maintain the prescribed dosage and reactor temperature, respectively. For example, the caustic dosage was kept in constant ratio with the pulp (i.e., kg NaOH per tonne of oven-dry pulp), which is a common standard industrial practice.

Figure 3.12 presents the results of the study, where the independent variable is the production factor, ζ and the measured variable is the outlet Kappa number. A lot of process information an be inferred from the univariate graph. First, as indicated in the figure, there is no relationship between the production rate and shrinkage when

$\zeta < 0.7$. At low flowrates, or high residence times, the chemical reactions taking place are able to go to completion (i.e., complete consumption of NaOH). Therefore, no matter how slow the flowrate, additional delignification does not occur. This is a key nonlinearity in the system that must be captured in a production rate study. Another important aspect of the process is that the nominal operating point is situated where the NaOH is slightly in excess, shown by the ability to achieve additional delignification by making a marginal decrease in throughput. This is characteristic of chemical processes that operate with critical reagents slightly in excess. This minimizes the wasted NaOH, without having it act as a limiting reagent. Finally, as throughput increases, the amount of delignification that occurs decreases nonlinearly. In summary, two key nonlinearities were noted in the process. These are the transition from a flat 'zero-relationship' at low production rates to a causal relationship at moderate and high production rates, and the nonlinear decrease in delignification at moderate and low production rates.

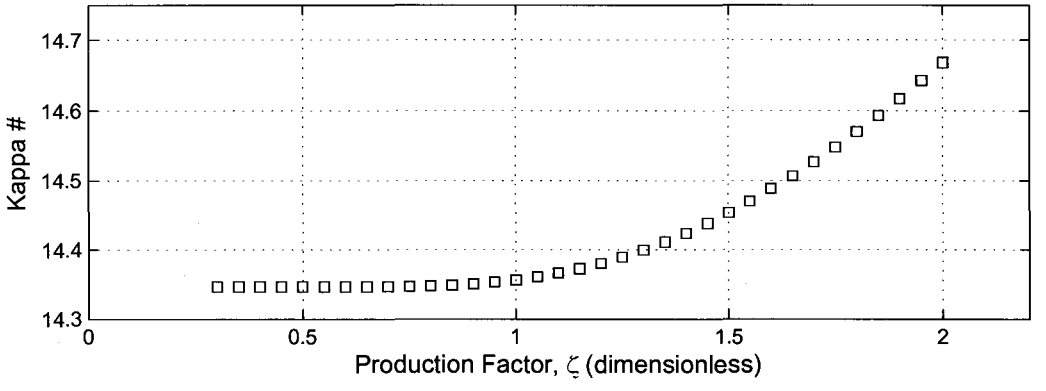

Figure 3.12: Results from Nonlinear Model for Oxygen Delignification

The Kappa number data can be translated to pulp shrinkage factors, by using the well-established empirical relationship between the lignin concentration in the fibre and the Kappa number [Myers and Edwards, 1989], given by

$$[L] = 0.147K \tag{3.35}$$

where [L] is the concentration of lignin in the fibre in units of mass percent (%), and K is the dimensionless Kappa number. The final step of the study was to develop a mathematical model to describe the relationship between the production factor (proportional to the production rate) and the shrinkage factor. This was achieved by performing fitting a polynomial to the data collected from the simulations. It was found that a cubic equation was the best fit, with the equation given by

$$\alpha_{O2} = -0.0113\zeta^3 + 0.0116\zeta^2 - 0.0022\zeta + 2.301 \tag{3.36}$$

where the intercept (b=2.301) was strictly enforced due to the process knowledge described above (no delignification when $\zeta \leq 0.7$). To review, the initial zone is constant due to the complete consumption of the hydroxyl groups. After this point, the shrinkage decreases with increasing production rate. Figure 3.13 illustrates the accuracy of the cubic model (R=0.9989), where the dependent variable is now the pulp shrinkage in mass percent (%). The points represent the data collected, and the solid line is the model.

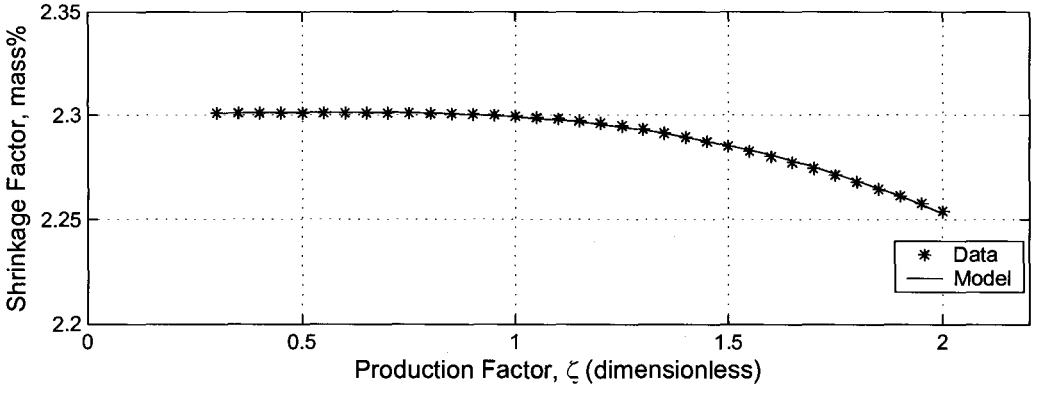

Figure 3.13: Shrinkage Factor versus Production Rate with Regression Model

Using this relationship, the steady state models described in Appendix A were developed.

3.7 Bleach Plant

In the bleach plant, final whitening of the pulp is accomplished by what is usually a 5-step process.

3.7.1 Model Description

Kinetic models are not applied for the delignification and extraction reactions. Instead, empirical consumption factors are used to identify the relationship between the pulp flow through the bleach plant and the chemicals consumed. The factors are based on drops in Kappa number, as found in the literature [Wang *et al.*, 2003]. There are five bleaching or extraction stages, with order being: D100, EOP, D1, EP, D2. The 'D' stages include the addition of chlorine dioxide (ClO_2) and chlorine (Cl_2).

A schematic of the bleaching department is given in Figure 3.14. A detailed graphic of a single stage is provided in Figure 3.15. Each stage consists of the following components: chemical mixer, reaction tower, washer header, drum washer, and seal tank.

The governing equations are simply mass balances, most of which are given in Appendix A. Table 3.7 presents the steam and chemical dosages used per oven-dry tonne of pulp at each bleaching stage. The corresponding drops in Kappa number are given in Table 3.8.

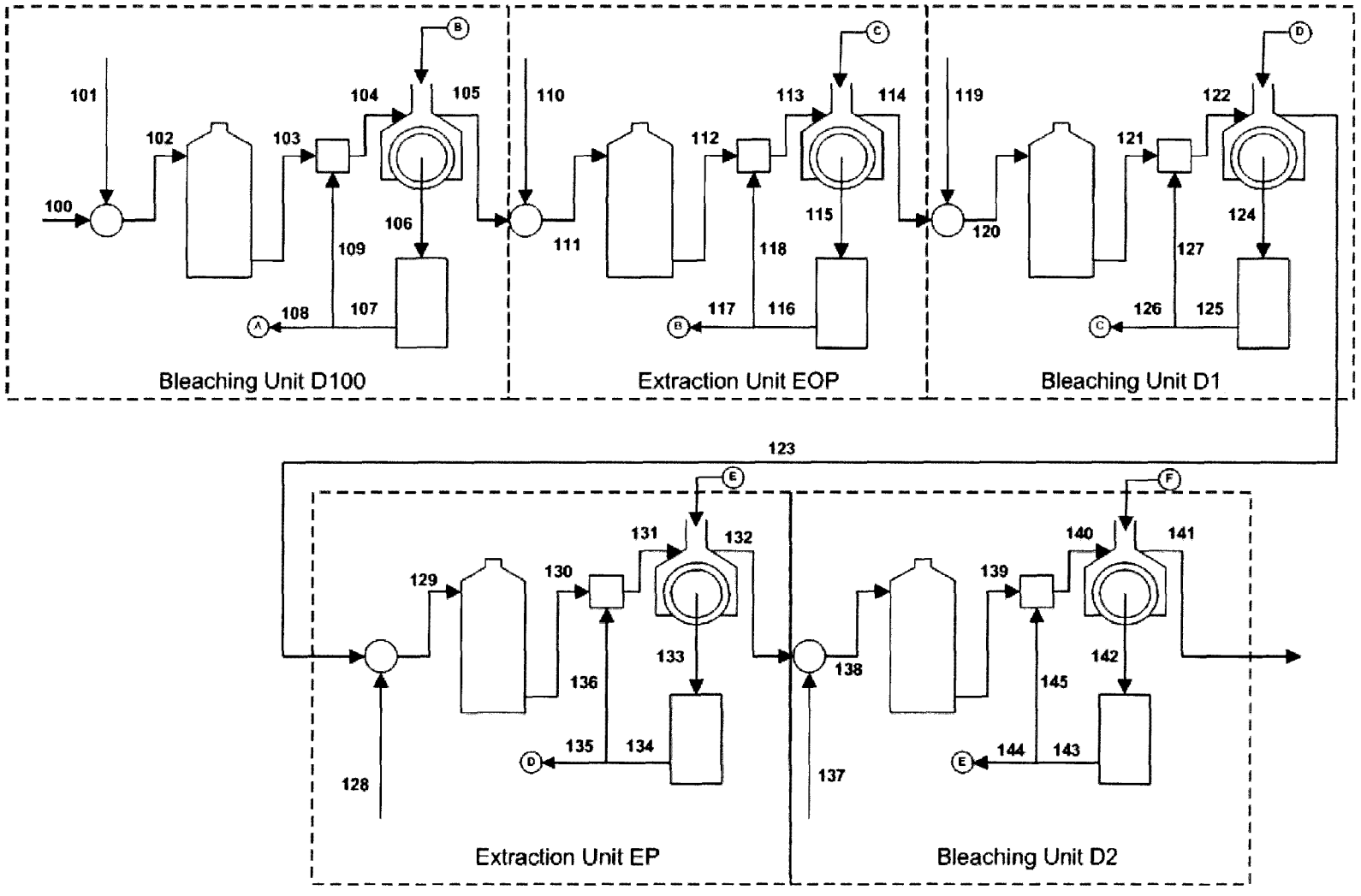

Figure 3.14: 5-Step Bleaching Department

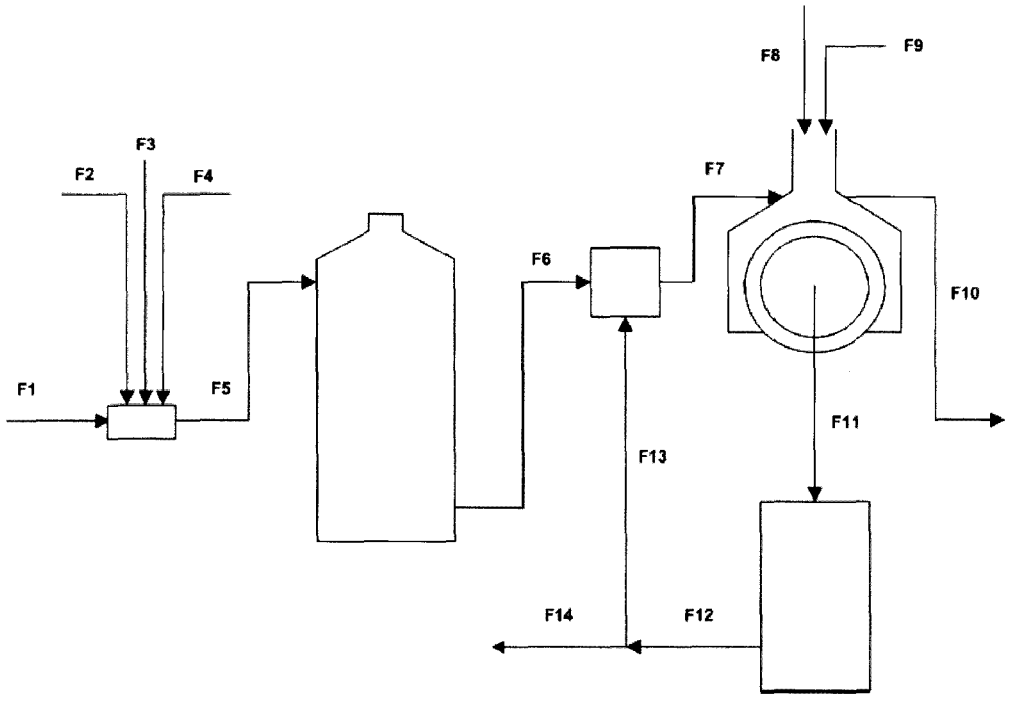

Figure 3.15: One Bleaching Stage

Table 3.7: Bleach Stage Chemical Additions

Stage	Cl_2 (kg/tonne)	ClO_2 (kg/tonne)	NaOH (kg/tonne)	MP Steam (kg/tonne)
1=D100	1.359	0.571	0	0
2=EOP	0	0	9.546	40.485
3=D1	0	1.812	1.533	40.485
4=EP	0	0	2.160	40.485
5=D2	0	0.906	0.209	40.485

Table 3.8: Assumed Bleach Stage Shrinkage Factors Dube [2000]

Stage	α	Drop in Kappa
1=D100	1.9	0.129
2=EOP	1.1	0.075
3=D1	0.6	0.041
4=EP	0.5	0.034
5=D2	0.4	0.027

3.8 Pulp Drying

Figure 3.16 presents the schematic representing the model used for the drying section. The dry end includes the headbox, the sheet-forming machine and pulp press, and the dryer. The outlet of the dryer represents the mill production. All units are modelled as steady state operations, with assumptions on consistencies at three points in the line. Table 3.9 presents the key empirical moisture constraints used in the model. The first three entries are the pulp consistency requirements for each of the three machine sections. The fourth entry, the dryer steam economy, specifies the quantity of medium-pressure steam required to evaporate one kilogram of water in the pulp stream.

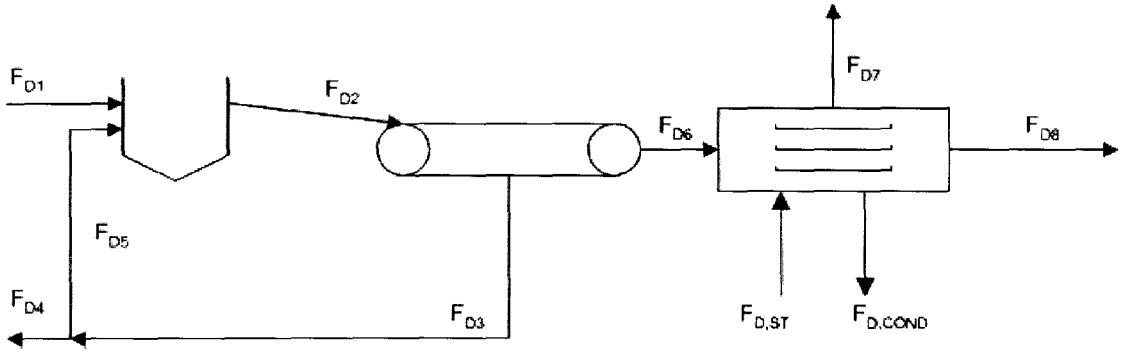

Figure 3.16: Dry End

Table 3.9: Required Data for Drying Section [Dube, 2000]

Data Item	Value	Engineering Units
Water content at Headbox Outlet, $x^W_{headbox}$	0.99	kg H_2O/kg
Water content at Dryer Inlet, x^W_{dryer}	0.45	kg H_2O/kg
Water content of Market Pulp, x^W_{market}	0.10	kg H_2O/kg
Dryer Steam Economy	2.00	kg MP steam/kg H_2O

3.9 Liquor Concentration

The black liquor extracted from the digester is split and sent to two weak black liquor tanks. These are both modelled dynamically, as discussed. The outlet of these tanks is the feed to the two multiple-effect evaporator systems, an example of which is illustrated in Figure 3.18. The systems are both backward-feed design. The important aspect in modelling the recovery section is to capture the relationship between the production rate and the steam consumption. The approach chosen is to utilize the well-established approximation for multiple effect evaporator system, where steam economy (equal to the mass of water evaporated per mass of steam input) is approximately equal to the number of effects (Geankoplis [2003] and Perry and Green [1997]). Many authors indicate that the steam economy will increase linearly (approximately) with the number of effects, but will be numerically less than the number of effects (Ray and Singh [2000] and Thamaraiselvan and Sivalingam [2003]). Smook [1992] illustrates a linear relationship between the number of effects in a multiple-effect evaporation system and the steam economy (Figure 3.17). Figure 3.18 shows the six effects present in each recovery line. However, using the steam economy approach, only the four streams indicated need to be considered. In the figure, F1 is the inlet weak black liquor stream and F2 is the the inlet medium pressure steam stream. F3 and F4 are the outlet streams for the concentrated black

liquor and condensate, respectively.

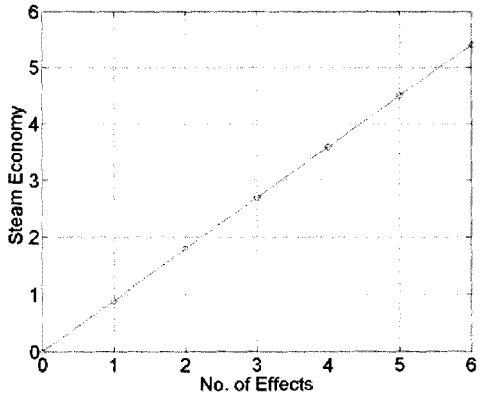

Figure 3.17: Evaporator Steam Economy [Smook, 1992]

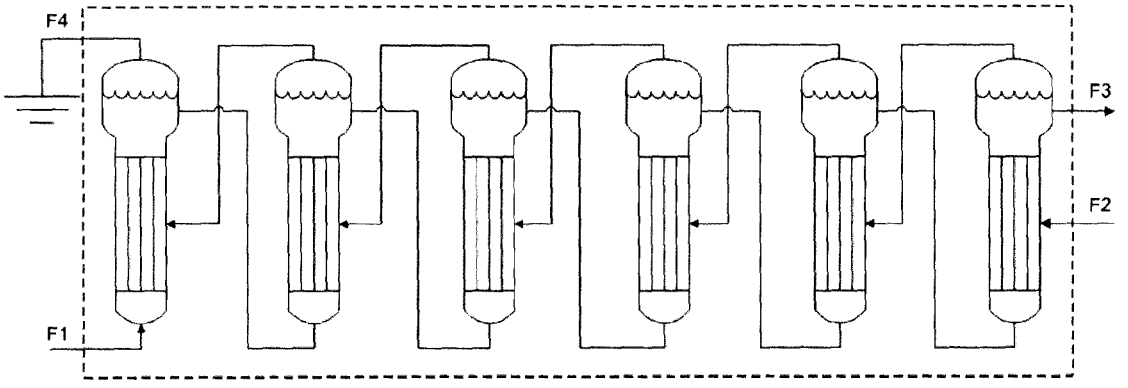

Figure 3.18: Typical Recovery Line

Therefore, assuming the above steam economy for a six-effect design, the mass balances are given by

$$F_1^W = F_3^W + F_4^W \tag{3.37}$$

$$F_1^{DS} = F_3^{DS} \tag{3.38}$$

$$F_4^W = 5.5 \times F_2^W \tag{3.39}$$

$$F_3^{DS} = x_{DS,i}(F_3^W + F_3^{DS}) \tag{3.40}$$

where Equations 3.37 and 3.38 are mass balances around the process stream, Equation 3.39 is the steam economy relationship that defines the amount of medium pressure steam required for the required heat duty, and Equation 3.40 is the required black liquor solids concentration at the outlet of the multiple-effect evaporation system. As stated, #1 recovery line produces 'strong' black liquor at 63% solids concentration, and #2 recovery line produces 'concentrated' black liquor at 70% solids concentration.

Downstream of the evaporators are the strong black liquor tank (for the evaporator bank with a nominal outlet concentration of 63% solids) and the concentrated black liquor tank (for the evaporator bank with a nominal outlet concentration of 70% solids). These are once again modelled dynamically, as discussed earlier.

3.10 Steam System

Figure 3.19 illustrates the boiler and steam system to be employed in this model. It is a steady-state model, that includes simple material and energy balances to determine the steam requirement for the plant.

3.10.1 Boilers

In each of the recovery boilers, it is possible to run on either black liquor solids, or natural gas. The refuse boilers require bark/wood, or natural gas. Table 3.10 illustrates the various data that is required for the boiler section. Many of the models that follow were inspired by Sarimveis *et al.* [2003].

The steam production in the recovery boilers is modelled as

$$F_{steam}(\hat{H}^{sat}_{hps} - \hat{H}^{sat}_{bfr}) = \eta_{BL}\Delta H^{c}_{BL}F_{DS} + \eta_{NG}\Delta H^{c}_{NG}F_{NG}, \tag{3.41}$$

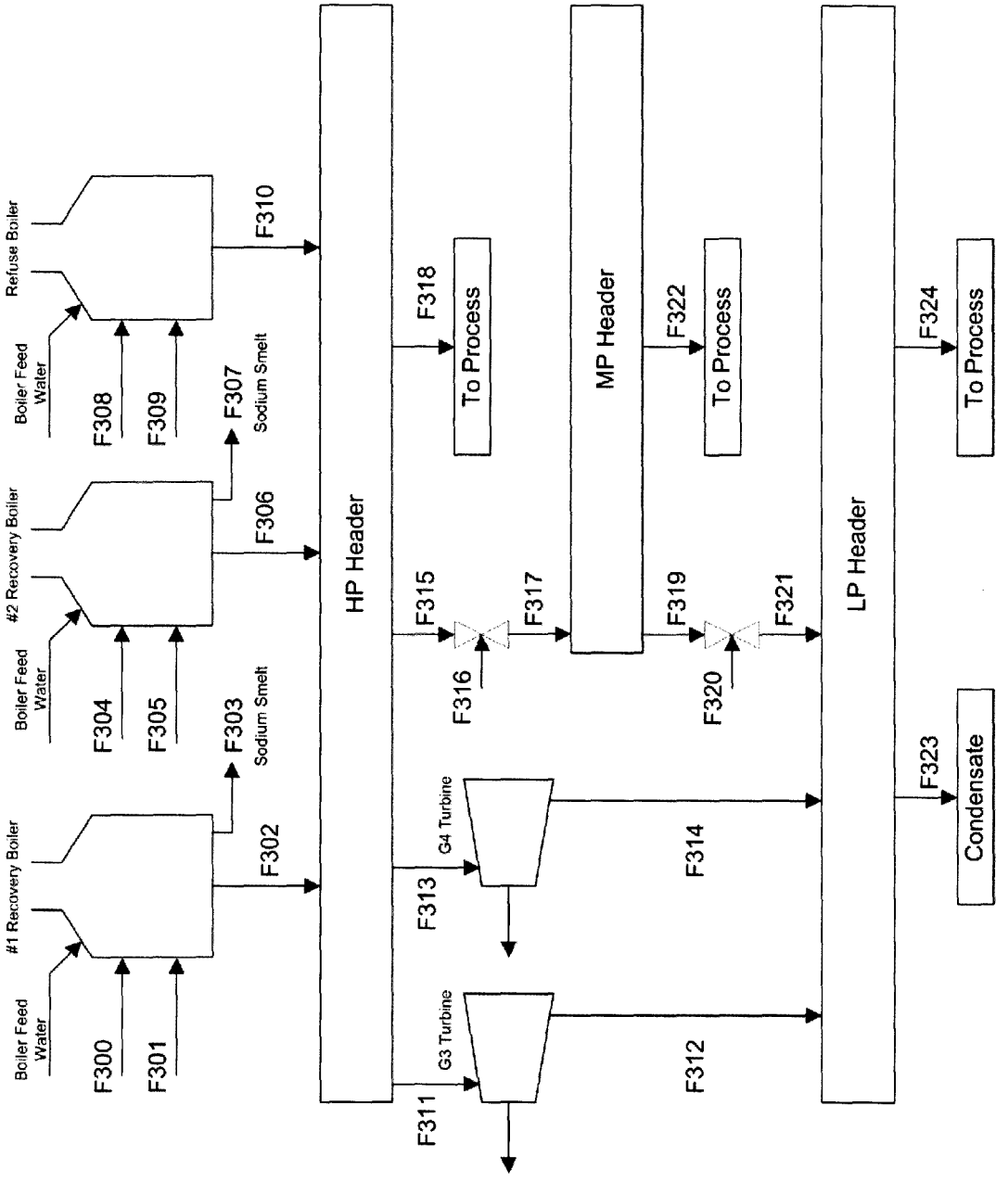

Figure 3.19: Boilers and Steam System

Table 3.10: Required Data for Boiler Section

Data Item	Value	Engineering Units
$\hat{H}^{sat}_{bfr}$ Boiler Feed Water Enthalpy	582	kJ/kg
$\hat{H}^{sat}_{hps}$ High Pressure Steam Enthalpy	3168	kJ/kg
$\hat{H}^{sat}_{mps}$ Medium Pressure Steam Enthalpy	2794	kJ/kg
$\hat{H}^{sat}_{lps}$ Low Pressure Steam Enthalpy	2756	kJ/kg
$\hat{H}^{sat}_{mpc}$ Medium Pressure Condensate Enthalpy	756	kJ/kg
$\hat{H}^{sat}_{lpc}$ Low Pressure Condensate Enthalpy	582	kJ/kg
η_{BL}, Efficiency on BLS	0.52	dimensionless
η_{WD}, Efficiency on Bark	0.65	dimensionless
η_{NG}, Efficiency on Natural Gas	variable	dimensionless
ΔH^{c}_{BL}, Heat of Combustion, Black Liquor	14,888	kJ/kg
ΔH^{c}_{WD}, Heat of Combustion, Wood	17,000	kJ/kg
ΔH^{c}_{NG}, Heat of Combustion, Natural Gas	54,000	kJ/kg

where the two sets of terms on the RHS correspond to the energy output for black liquor solids and natural gas. It is assumed that the steam production is the sum of that produced by the liquor and natural gas inputs. The natural gas efficiency is assumed to follow a nonlinear trend with steam demand to that found in Barroso *et al.* [2003]. Similarly, the steam production in the refuse boiler is modelled as

$$F_{steam}(\hat{H}^{sat}_{hps} - \hat{H}^{sat}_{bfr}) = \eta_{WD}\Delta H^{c}_{WD}F_{WD} + \eta_{NG}\Delta H^{c}_{NG}F_{NG}, \tag{3.42}$$

3.10.2 Turbines

The turbines are modelled using simple energy balances as well. Certain assumptions were made about the extraction pressures. For example, a dual-extraction turbine will require an enthalpy balance for each stage, multiplied by the respective efficiencies. This can be given by

$$Power = \eta_{mps}F_{mps}(\hat{H}_{hps} - \hat{H}_{mps}) + \eta_{lps}F_{lps}(\hat{H}_{hps} - \hat{H}_{lps}), \tag{3.43}$$

where the two sets of terms on the RHS corresponds to the sum of energy output of the two turbine stages.

3.10.3 Pressure-Reducing Valves

The purpose of pressure-reducing valves is provide pressure-control within the steam headers. Pressure reduction is achieved by de-superheating the higher pressure steam by spraying with boiler-quality water. For example, the mass and energy balances around a pressure-reducing valve (from HPS to MPS) is given by

$$F_{mps} = F_{hps} + F_{bfw}, \tag{3.44}$$

$$\hat{H}_{mps}F_{mps} = \hat{H}_{hps}F_{hps} + \hat{H}_{bfw}F_{bfw}. \tag{3.45}$$

3.10.4 Steam Headers

To maintain pressure in the three pressure levels, flows in and out of the headers must be balanced, as given by

$$\sum F_{hps,in} = \sum F_{hps,out}, \tag{3.46}$$

$$\sum F_{mps,in} = \sum F_{mps,out}, \tag{3.47}$$

$$\sum F_{lps,in} = \sum F_{lps,out}. \tag{3.48}$$

The main steam users in the plant considered in the model are the turbines, digester, bleach plant, oxygen delignification department, evaporators, and the pulp dryer. Following Equation 3.46, the high pressure suppliers are the boilers and the users are the turbines and pressure-reducing valves. There are assumed to be no high-pressure steam users in the processing units. Therefore, the mass balances is given by

$$F_{302}^{1RB} + F_{306}^{2RB} + F_{310}^{RB} = F_{311}^{1Turbine} + F_{313}^{2Turbine} + F_{315}^{PRV}, \tag{3.49}$$

where the requirements for the turbines and pressure-reducing valves are given by relationships in Equations 3.43–3.45. The medium pressure steam users are the digester, evaporators, and the pulp dryer. The mass balances are given by

$$F_{317}^{PRV} = F_{319}^{PRV} + F_{322}^{Process}, \tag{3.50}$$

$$F_{322}^{Process} = F_{ST}^{Digester} + F_{ST}^{Evaporators} + F_{ST}^{Dryer}, \tag{3.51}$$

where the requirements for the digester, evaporators, and pulp dryer are calculated through simple energy balances, or through steam economy relationships. The low pressure steam users are the bleach plant and oxygen delignification plants. Similar to the high and medium pressure header relationships, the mass balances are

$$F_{312}^{Exhaust} + F_{314}^{Exhaust} + F_{321}^{PRV} = F_{323}^{Condensate} + F_{324}^{Process}, \tag{3.52}$$

$$F_{324}^{Process} = F_{ST}^{O_2 Delig} + F_{ST}^{Bleach}. \tag{3.53}$$

3.11 Recausticizing

The recausticizing section is simplified for the purposes of this work, and the lime cycle is also not included in the model. Figure 3.20 illustrates the simplified liquor regeneration department. The smelt from the black liquor recover boilers is first dissolved using recycled water from the dregs filter and water from the lime cycle that is treated as make-up water in this model. Dregs, large fluffs of unburned carbon, are removed from the dissolving tank and are landfilled. The solution is then sent to the green liquor storage capacity that is modelled dynamically. In the lumped model for the slaker/causticizer, the green liquor is reacted with burned lime. Grits, large calcium-rich particles, are removed along with the lime mud. The resulting solution is sent to the white liquor storage tank for use in the digester. The governing equations are found in Appendix A.

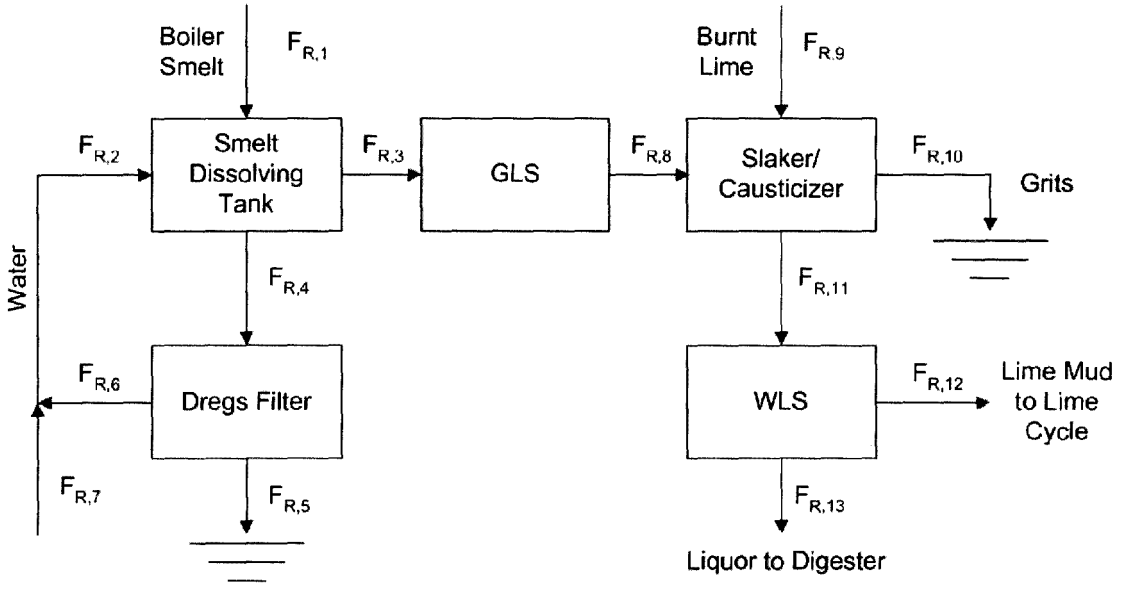

Figure 3.20: Liquor Regeneration

3.12 Chapter Summary

In this chapter, a simplified model of the Kraft mill process was presented. Encompassing the main process flows, this model will be utilized to develop optimal production rate trajectories through the departments in the face of plant disturbances such as scheduled maintenance shutdowns and unit failures. In Chapter 5, this will be extended to include design decisions.

Chapter 4

Optimization of Plant Operation: Formulation

This chapter will outline the overall formulation of the optimization problem and provide a brief description of some of the implementation issues tackled in the computational environment, GAMS.

4.1 Introduction

As reviewed in Chapter 2, the overall formulation of the dynamic optimization problem involves the formulation of a constraint set involving the process inputs and process outputs, path and end-point constraints on these inputs and outputs, as well as the formulation of a meaningful objective function over which the process system is to be optimized.

The overall formulation of the problem falls within the general formulation for dynamic optimization problems presented in Chapter 2 and takes the following form:

$$\max_{\mathbf{x}(t),\mathbf{u}(t)} \phi(\mathbf{x}(t), \mathbf{u}(t), \mathbf{z}(t), \mathbf{p}, t),$$

subject to

Model equations

$$\mathbf{0} = \mathbf{h}[\dot{\mathbf{x}}(t), \mathbf{x}(t), \mathbf{u}(t), \mathbf{z}(t), \mathbf{p}, t]$$

Path constraints

$$\mathbf{x}^{min} \leq \mathbf{x}(t) \leq \mathbf{x}^{max}$$

$$\mathbf{u}^{min} \leq \mathbf{u}(t) \leq \mathbf{u}^{max}$$

$$\mathbf{0} \leq \boldsymbol{\Delta}\mathbf{u}(t) \leq \boldsymbol{\Delta}\mathbf{u}^{max}$$

End-point Constraints

$$\mathbf{x}(t) = \mathbf{x}_0 \qquad \text{for } t > t_{end}$$

The development of the above components is described in the following sections. In the case of constraints on input usage, the two-tiered optimization approach described later in this chapter will be applied.

4.2 Formulation

For proper determination of 'optimal' designs or operating strategies when analyzing a physical system, it is necessary to work towards some objective. In the optimization of process systems, there are a few common types of objective functions employed. Production-focused objectives may be focused at maximizing throughput, minimizing impurities, or maximizing yield. Other possibilities include minimizing production time/schedules, or maximizing safety. A common shortcoming of these approaches is that is that the relationship to the economics of the process industry is indirect. While

issues such as safety and environment are paramount, objectives such as throughput-maximization may not necessarily be the strategy that maximizes the profit. One common scenario is that the fuel and energy costs associated with running an operation close to the design capacity are so large, that it is more economical to run below capacity and ultimately sell less product to the market. For these reasons, a common practice used in industry when comparing operating strategies and designs, is to base the comparison on economic information. Thus, an economic objective function will be applied in this study.

4.2.1 Objective Function

Previous research studies by Dube [2000] illustrated the use of a production-based objective function with penalties on deviations from buffer tank target levels. For example, this could be given by the general form,

$$\min_{F_i} \int_0^T \left(F_{pulp,sp} - F_{pulp}(t)\right)^2 dt + \sum_{j=1}^{n} \int_0^T P_j \left(h_{j,sp} - h_j(t)\right)^2 dt \tag{4.1}$$

where F_{pulp} is the flow of market pulp out of the system, F_i are manipulated plant inputs, j is the index corresponding to the set of buffer tanks in the system, and P_j is the penalty weight corresponding to tank j. The most important economic variable, pulp production, is considered in this formulation. However, the penalties on the buffer levels raise two key issues. First, the common issue when dealing with penalties in optimization problems is how to appropriately choose the parameters, P_i. Secondly, these penalties work to minimize the deviations from level set-points. The system, as modeled, is essentially a network of interacting level-controllers. Therefore, if these penalties are made large enough, aggressive control action results and the storage volumes would cease to function as buffer capacities. To allow the tanks to buffer the system from disturbances, namely equipment shutdowns, deviations from

level-setpoints are not included in the objective function. Instead, integral action is forced via end-point constraints as disussed by Allison [2004] and described later in this thesis. For these reasons, a purely economic objective function is used in the first tier of the formulation. The form of the profit-maximization objective function used in this study is given by

$$\max_{\mathbf{x}} \sum_{i=1}^{P} \mathbf{q}^T \mathbf{x}, \tag{4.2}$$

where $\mathbf{q}$ is the vector of economic weights associated with plant income and expenses (Table 4.1), and $\mathbf{x}$ represents the the operating variables considered, such as plant production, fuel usage, etc. These are summed over the time horizon from $i = 1$ to $t = P$. Note that the elements of $\mathbf{q}$ can be positive or negative, depending on whether the associated component of $\mathbf{x}$ represents an income-generating or expense-incurring variable. The elements of $\mathbf{x}$ will be strictly positive for this problem. The objective function is given by

$$\max_{\mathbf{x}} \sum_{i=1}^{P} [725F_{pulp,i} - 439.20F_{NG,i} - 1000F_{NaOH,i} - 1100F_{ClO2,i} - 100F_{Chips,i}] \tag{4.3}$$

where i is the time interval and all material flows, F_j, are on tonnes/hour.

4.2.2 Plant Operation

In general, two classes of scenarios are investigated – plant shutdowns that are planned and those that are unplanned. For planned plant shutdowns, there are three phases during which the operating point is moved about the operating window. These are the *preparation*, *shutdown*, and *restoration* phases [Dube, 2000]. During the preparation phase, the plant operators are able to prepare the plant for the maintenance

Table 4.1: Economic Factors

Item	Cost [$/unit]
Pulp production	$580 US/tonne
Pulp production	$725 CDN/tonne
Softwood Chips	$100 CDN/tonne
Natural Gas	$0.30 per Nm^3
Natural Gas	$439.20 per tonne
Chlorine Dioxide	$0.50 per lb.
Sodium Hydroxide	$1.00 per kg

shutdown. During the shutdown phase, there is no flow of process materials through the shutdown department. Alternatively, the flow may be reduced to a very small value, which mimics a radical plant slowdown. During the restoration phase, the plant is systematically returned to the steady-state operating point. Of course, during unplanned shutdowns or plant failures, only the shutdown and restoration phases are considered as these scenarios naturally provide no time in which to prepare the plant for the ensuing shutdown.

Depending on which of the two above scenarios is being considered, either two or three lengths of time are predefined in the problem, that correspond to the appropriate operation phases outlined above. For example, Figure 4.1 illustrates the generic case for each of the two classes of problems, where the variable F refers to the flow through the department that is shutdown. Figure 4.1(a) illustrates the case for a planned maintenance shutdown, in which the plant is at the nominal operating point from $t_0 - t_1$. Between $t_1 - t_2$, the plant is able to prepare for the impending outage which occurs between $t_2 - t_3$. This is followed by an available restoration time, $t_3 - t_4$, during which the plant is provided time to return to the nominal operating point which is

demanded at $t = t_4$. Figure 4.1(b) is the similar case for an unplanned shutdown, or unit failure. The difference is the lack of the initial preparation time. In this case, the plant is shutdown from $t_1 - t_2$, followed by a restoration period from $t_2 - t_3$.

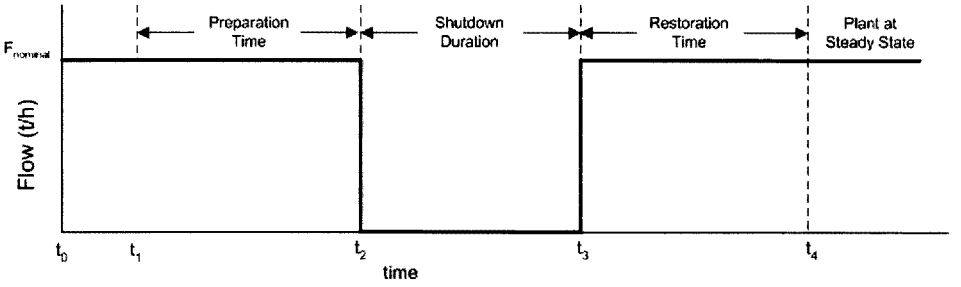

(a) Planned Maintenance Outage

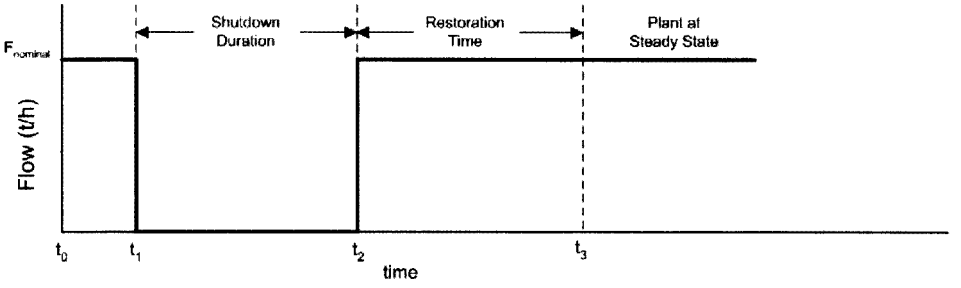

(b) Unexpected Unit Failure

Figure 4.1: Planned and Unplanned Shutdown Scenarios

Note that in both cases, the plant is held at the nominal operating point for the first time interval, $t_0 - t_1$ (scenario initialization). In addition, the shutdown phase is constrained to be $F = 0$. In all other time intervals, all variables are available for optimization. Therefore, during the preparation and restoration phases, the operation may be away from the nominal operating point, as opposed to the straight lines shown in Figure 4.1.

4.2.3 End-Point Constraints

Since it is difficult to characterize the economic penalty of having buffer capacity levels being away from their nominal state, the objective function cannot be used to push these levels back to their set-points. While a penalty on these would accomplish this, the objective function would no longer be purely economical. The formulation used in this work is to enforce the integral action through end-point constraints. The actual implementation involved enforcing the constraints for the last few time steps of the time horizon to ensure that system had returned to steady-state, and was not merely passing through the end-point during transient operation. The end-point constraints were implemented as

$$\begin{aligned} V(t) - V_0 + s_1 - s_2 &= 0, \\ s_1 + s_2 &\leq \epsilon, \\ s_1 &\geq 0 \\ s_2 &\geq 0 \\ t &\geq t_{end} \end{aligned} \tag{4.4}$$

where $V(t)$ is the volume accumulation in a tank for $t \geq t_{end}$, V_0 is the initial hold-up, and s_1 and s_2 are slack variables. The value chosen for ϵ was made as small as possible without hindering numerical performance. This was the motivation behind using the slack-variable formulation as opposed to a strict equality constraint, namely $V(t) = V_0$. For all cases, the value chosen was $\epsilon = 10^{-6}$. The choice of t_{end} is the end of the restoration period, and the sensitivity to this parameter is studied in Chapter 5. To review, V_0 was assumed to be 50% for all buffer capacities.

Without these end-point constraints, the solution to a given scenario may involve leaving the plant away from the steady-state operating level. This is not desirable

as it leaves the plant ill-prepared for a future disturbance, such as a shutdown. Of course, this assumes that the nominal operating point (in terms of buffer tank levels) is optimal for the disturbances of interest. This will be addressed in Chapter 6.

4.2.4 Path Constraints

The tank volumes are constrained at the end of the time horizon by the slack-variable formulation described above. In addition, the digester is required to return exactly to nominal operation for $t \geq t_{end}$. Implicit in these constraints is the requirement for all production levels to return to nominal values for $t \geq t_{end}$. However, during the preparation, shutdown, and restoration times, the production rates and buffer levels are free variables. These are manipulated appropriately to improve the objectives. However, due to plant design and process knowledge, path constraints must be enforced on these variables. These are given by

$$F_j^{min} \leq F_{ij}(t) \leq F_j^{max}, \tag{4.5}$$

$$V_k^{min} \leq V_{ik}(t) \leq V_k^{max}, \tag{4.6}$$

where i is the time interval, j is the set of processing units, and k is the set of buffer tanks. In most cases, to allow units to shutdown, the minimum flowrates through units is zero. The maximum production level through these units is arbitrarily set in some cases to be 20-30% above the nominal rate. The digester is assumed to operate at the bottle-neck point based on process knowledge. The storage capacities, as discussed, are permitted to fluctuate between approximately 10% and 90% of the design capacity.

4.3 GAMS Implementation

The modelling package being used for simulation and optimization is the General Algebraic Modeling System (GAMS), version 21.3. The use of a Matlab-GAMS interface is used for data manipulation and presentation of the results. Since a set of algebraic equations is necessary for use in GAMS, the state equations were discretized using a backward-difference approximation, as discussed in Section 4.3.1. MINOS (Modular In-core Nonlinear Optimization System) and CONOPT2 were used for the solution of the NLP problems, under default options. For the mixed-integer nonlinear programming (MINLP) problems presented in Chapter 6, the Simple Branch and Bound (SBB) solver was used, with the use of CONOPT or MINOS to solve the relaxed NLP at each node. The PC used for all cases was a Dell Pentium 4 2.53 GHz with 512 MB of RAM.

The following sections present some of the computational issues encountered during this study, including methods of initialization and problem solution.

4.3.1 Discretization of State Equations

The system investigated involved differential equations that were either linear, or mildly nonlinear due to bilinear terms. Initially, the equation system was discretized using orthogonal collocation on finite elements. However, this led to a system that was larger than necessary for the nature of the equation system. Therefore, the state equations were discretized using a low-order method capable of capturing mainly slow linear dynamics. While the explicit Euler Method is attractive because of its ease of implementation, slope inaccuracies and stability issues are inherent in the method, especially for stiff systems [Chapra and Canale, 1998]. For these reasons, the backward-difference (Implicit Euler) was applied for implementation of the state equations. This

is a commonly used method, used in studies by Armaou and Christofides [2002], and is stated mathematically below as given in Chapra and Canale [1998].

Consider

$$\dot{\mathbf{x}} = \mathbf{f}(\mathbf{x}, t)$$

This is approximated as

$$\frac{\mathbf{x}_k - \mathbf{x}_{k-1}}{\Delta t} = \mathbf{f}(\mathbf{x}_k, t_k)$$

where

$$\Delta t = t_k - t_{k-1}$$

4.3.2 Initialization and Solution Techniques

As discussed in Section 4.2.2, the disturbances (failures or scheduled shutdowns) are introduced into the system by fixing the appropriate flows to $F_j = 0$ for the desired time-period. For example, considering a 24-hour time period, the shutdown scenario may require an 8-hour shutdown in the middle of the overall horizon. Therefore, the flow through the department experiencing the shutdown would be fixed to zero for the middle 8-hour period, and remain at its nominal level for the remaining time intervals.

Considering this scenario and the aforementioned initialization technique, serious computational difficulties were encountered. The drastic disturbance introduced, forcing the production department from the nominal-state to zero-state, presented a situation in which the system of equations would not solve. Therefore, a homotopy-type technique was developed to slowly introduce the disturbance into the plant. This approach utilizes multiple-solve statements in the GAMS implementation, and solves the system successively as the disturbance is introduced.

Homotopy, first formulated by Poincaré around 1900, is the 'continuous transforma-

tion from one function to another'. For example, a function, namely $\mathbf{g}(\mathbf{x}, y)$ can be transformed from some state $\mathbf{f}(\mathbf{x})$ to another state $\mathbf{h}(\mathbf{x})$, through some y on the range [0,1]. This is accomplished such that $\mathbf{g}(\mathbf{x}, 0) = \mathbf{f}(\mathbf{x})$ and $\mathbf{g}(\mathbf{x}, 1) = \mathbf{h}(\mathbf{x})$. This approach is used in this study, considering the following functions for the desired production rates through a given department during a shutdown period, $t_1 - t_2$.

$$\mathbf{f}(x) = \mathbf{F}_{\mathbf{nominal}} \qquad t = [t_1, t_2] \tag{4.7}$$

$$\mathbf{h}(x) = \mathbf{F}_{\mathbf{min}} \qquad t = [t_1, t_2] \tag{4.8}$$

To overcome the computational obstacle, homotopy is applied to transform from $\mathbf{f}(\mathbf{x})$, the nominal operating-point, to $\mathbf{h}(\mathbf{x})$, the shutdown scenario. To apply the homotopy technique, $\mathbf{g}(\mathbf{x}, y)$ is first modified and becomes

$$\mathbf{g}(\mathbf{x}, \alpha_{failure}) = \alpha_{failure}\mathbf{F}_{\mathbf{nominal}} \qquad t = [t_1, t_2], \tag{4.9}$$

where $\alpha_{failure}$ is a parameter that is on the range [0,1]. In this case, however, $\alpha_{failure}$ is initialized at $\alpha_{failure}$=1. This initializes the full trajectory as $\mathbf{F}_{\mathbf{nominal}}$. Figure 4.2 presents the idea, that involves the following steps.

1. Beginning with Iteration 1, the system is first solved for the nominal operating point in which no disturbance is assumed ($\alpha_{failure}$=1).

2. Iterations 2 to N-1 are those involving $\alpha_{failure}$ between 1 and 0. These iterations gradually introduce the full failure, by transforming the forcing function trajectory from the nominal-input to the disturbance-input. At each iteration, the optimization problem is solved, and its solution is used as the initial guess

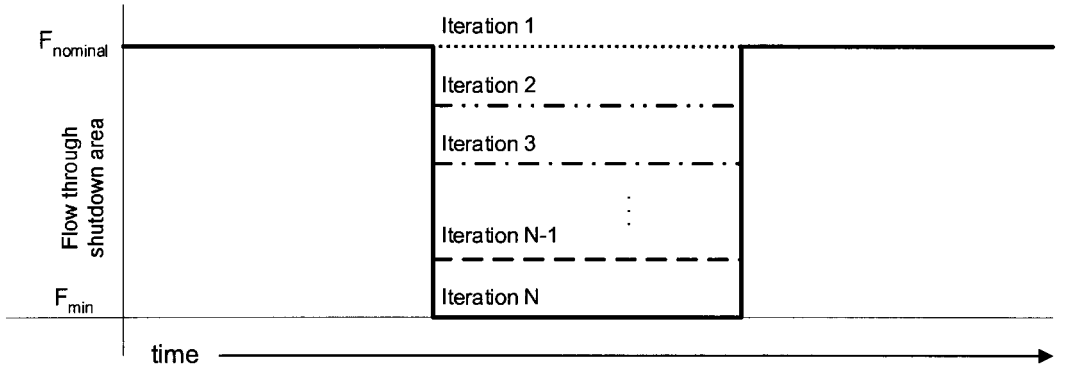

Figure 4.2: Homotopy Technique

for the next iteration. The values and step-size used (and number of iterations) is determined based on success in finding a solution. These choices will most likely vary from scenario-to-scenario, depending on how much the plant needs to be moved to reject the disturbance. For more complicated scenarios, small step-sizes and a greater number of iterations will be required. Note that with the exception of the the first time-step and the time-steps defining the end-point constraints, all other variables are free for optimization.

3. Iteration N is the final iteration, where the full disturbance is introduced by setting $\alpha_{failure}$=$\alpha_{failure,desired}$. This parameter can be decreased to some low value, with the physical significance being the drastic slow-down in production. In the possible case that $F_{min} = 0$, the parameter is decreased to $\alpha_{failure} = 0$.

Nonlinear programming problems are inherently non-convex. By solving the problem multiple times, this also essentially is giving the problem a variety of starting points. As long as the solutions go the same location using a variety of homotopy paths, it can be assumed that a 'good' local optimum has been found. Nevertheless, different starting points were used, especially for the design problems in Chapter 6. The location of a local optimum is all that is guaranteed by the MINOS and CONOPT2 nonlinear programming solvers used in this work.

4.4 Introductory Case Study

Using the model and problem formulation discussed above, we now present an introductory case study involving a planned maintenance shutdown at the bleach department. Table 4.2 outlines the scenario parameters, and Figures 4.3, 4.4, 4.5 illustrate some of the main process variables.

It is assumed at 4 hours of preparation time and a 6-hour restoration period are available for an 7-hour shutdown at the bleach plant. The economic objective achieved is \$178,522. Figure 4.4(b) illustrates the shutdown period at the bleach plant, indicated by the feed rate to this department being driven to zero for the 7-hour time interval. Because the scenario assumes a plant preparation time of 4hours, the bleach plant is permitted to maximize through-put for this period, thereby transferring upstream storage to the downstream buffer vessel. This transfer is indicated by the decrease in volume at the 200T tank (upstream, Figure 4.4(a)) and the increase in volume at the bleach tank (downstream, Figure 4.4(c)). Analysis of the production areas away from the bleach plant illustrates some interesting behaviour. Figure 4.3(a) illustrates the trajectory of the wood-chip feed to the digester, the measure of digester production rate. Although the shutdown begins at $t = 5h$, the digester is not impacted until much later along the time horizon. However, this results in a rapid and substantial decrease in the production rate at $t = 6h$ and $t = 10h$. This decrease in production occurs to balance the slowdown at the downstream knotting/washing department (Figure 4.3(c)), thereby meeting the end-point constraints on the final blowtank volume. The optimal solution determined exhibits erratic behaviour at the oxygen delignification and drying departments, as illustrated in Figures 4.3(e) and 4.4(d). In the case of the former, this results in fluctuations in the buffer volume, the 2HD tank, which is located upstream of the bleach plant. The action taken on the liquor cycle is illustrated in Figure 4.5(a)-(d). The weak black liquor tanks accumulate material since there is a reduction in use at the boilers, which are further

Table 4.2: Introductory Case Study: Bleach Plant Shutdown

Preparation Time	4 hours
Shutdown Duration	7 hours
Restoration Time	6 hours
Economic Objective Value	\$178,522
$\sum \Delta u^2$ (scaled)	1,989,580

downstream (Figure 4.5(a)-(b)). This downturn in use is related to the drop in steam usage at the oxygen delignification, bleaching, and drying departments. Irregular flow trajectories within the recausticizing areas leads to fluctuations in the downstream liquor storage vessels (green and white liquor storage vessels, Figure 4.5(c)-(d)).

Results involving erratic plant movement were observed for some scenarios studied by Dube [2000], primarily when a long time-horizon was used. This was deemed a requirement for the plant to remain feasible during long shutdowns. In this work, some trial-and-error case studies revealed that this erratic plant movement is not necessarily required to achieve the objective function value obtained. It was found that multiple solutions were possible for the maximum profit value. Therefore, it was desirable to locate the solution that minimized input usage. This is treated in the next section.

4.5 A Multi-criterion Approach to Handling Non-Uniqueness

In this section, various approaches to multi-criterion optimization problems are reviewed. These methods aid in overcoming the non-uniqueness shown in Section 4.4,

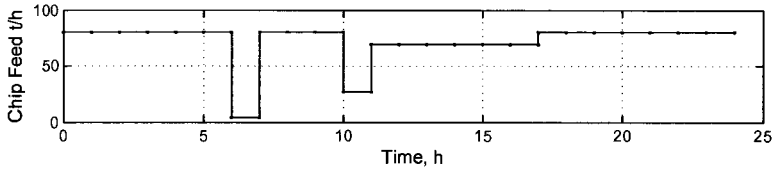

(a) Digester Feed

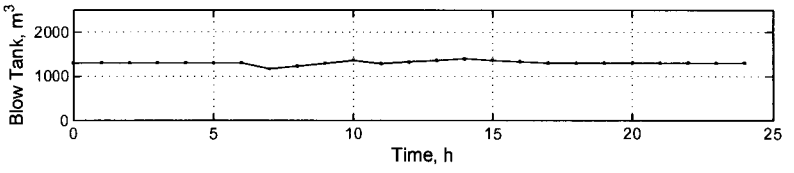

(b) Blowtank Volume

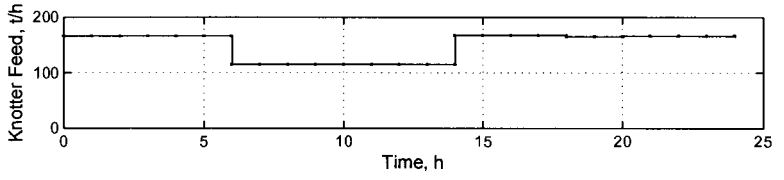

(c) Knotter Feed

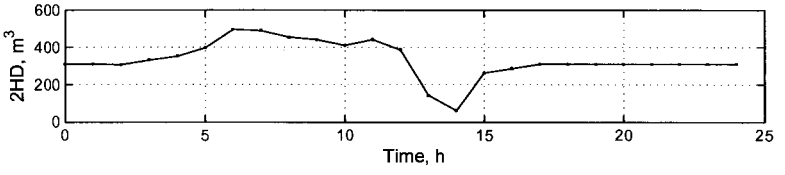

(d) 2HD volume

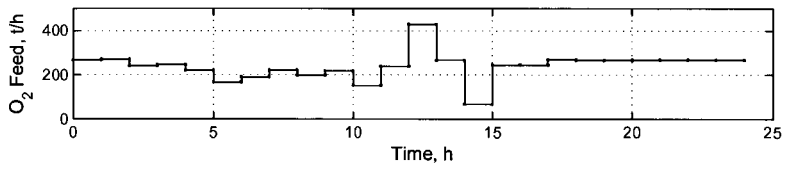

(e) O_2 Feed

Figure 4.3: Introductory Scenario: Variable Trajectories (only economics considered)

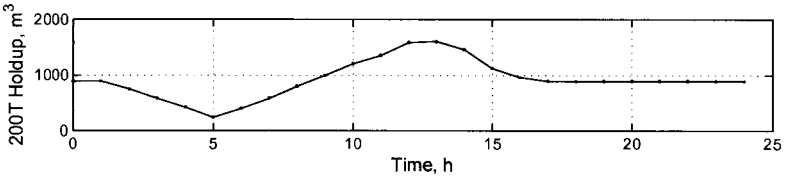

(a) 200T Volume

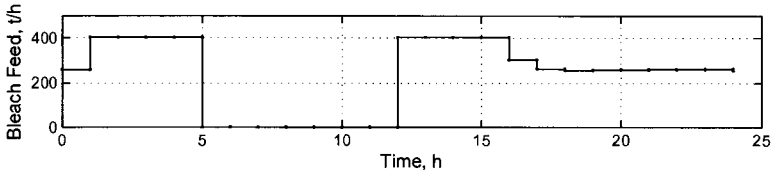

(b) Bleach Feed

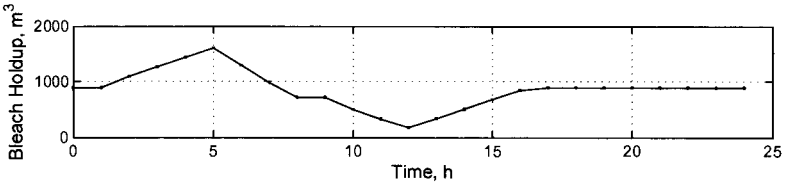

(c) Bleach Storage Volume

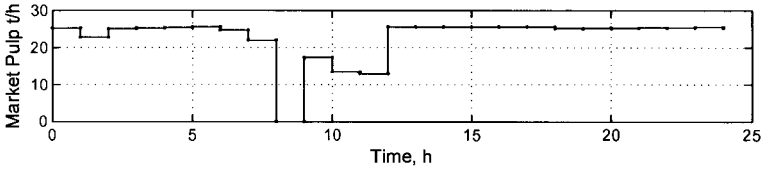

(d) Pulp Production

Figure 4.4: Introductory Scenario: Variable Trajectories (only economics considered, continued)

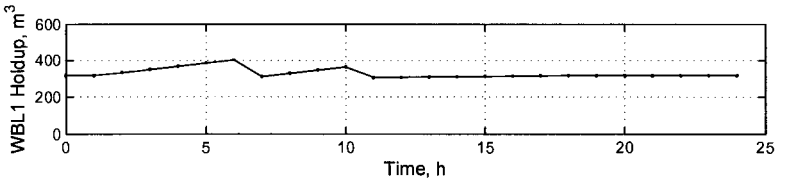

(a) Weak Black Liquor Storage

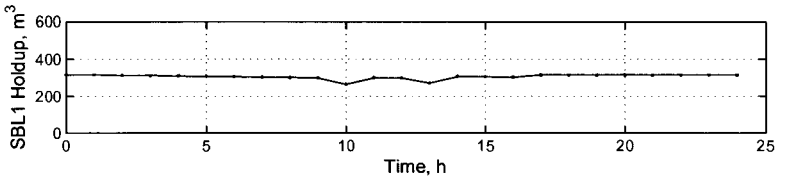

(b) Strong Black Liquor Storage

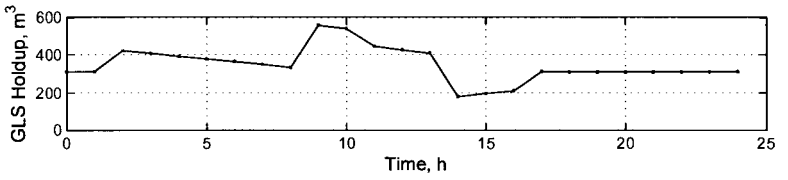

(c) Green Liquor Storage

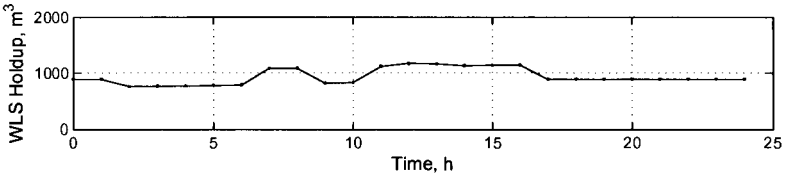

(d) White Liquor Storage

Figure 4.5: Introductory Scenario: Variable Trajectories (only economics considered, continued)

which is due to a large number of degrees of freedom, resulting in a poorly-conditioned variable matrix. In other words, linear dependencies between operating variables leads to a situation where there may be more than one solution in which the economic optimum is achieved, while still obeying all system constraints. Dube [2000] makes mention of this phenomenon, however, in that study, it was concluded that erratic plant movement was a result of longer shutdown times (i.e., rough operation required to maintain feasibility). In this work, we show that multiple solutions may exist for the economic objective, and therefore, effort will be focused on finding the solution that requires the least input usage.

In this section, four possible approaches are discussed to achieve 'unique' solutions to the problems described in this thesis. Three of these methods are then implemented and tested in this thesis. The problems discussed in this thesis involve a very large number of variables and constraints. The operation is assumed to be quite flexible, and mathematically, this means that there are many degrees of freedom. These degrees of freedom include the set of 'valves' available for manipulation, multiplied by the number of control intervals in which they can be manipulated. This results in non-unique optimal solutions, and can occur in the following situations:

1. Two or more variables have *equal weight* in the objective function.
2. Two or more variables have *no weight* in the objective function.
3. Two or more variables have unequal weights in the objective function, but there is an allowable *trade-off* between variables which yields no change in the objective.

There is an analogous phenomena when applying model predictive control (MPC) to ill-conditioned systems. Ill-conditioning of the variable matrix was discussed by Qin and Badgwell [2003], and a few remedies considered. Among these include singular value thresholding, controlled variable ranking and input move suppression.

Singular value thresholding (SVT) involves decomposing the process model using a singular value decomposition, and discarding values below a threshold. Input move suppression is analogous to the penalty-method discussed later in this section. This non-uniqueness of the solution to an optimization problem is easily seen in a function of two variables. Assume that the quadratic approximation to a plant's economic objective function is given by

$$f(\mathbf{u}) = (4 - u_1 u_2)^2, \tag{4.10}$$

where $\mathbf{u}$ is the vector of manipulated variables that are positively constrained. The resulting non-linear optimization problem is given by

$$\begin{aligned} &\min_{\mathbf{u}} (4 - u_1 u_2)^2 \\ &\text{subject to:} \\ &\qquad u_1 \geq 0 \\ &\qquad u_2 \geq 0 \\ &\qquad \mathbf{u}_0 = [0 \ 0]^T \end{aligned} \tag{4.11}$$

As stated in 4.11, the plant is assumed to be initially at the origin. The contour plot for the profit function is illustrated in Figure 4.6. Clearly, the minimum function value is non-unique, resulting in a line. The goal when considering problem 4.11 is to move the plant operating point to maximize profit, while minimizing input usage.

4.5.1 Augmented Penalty Function

One method to minimize the profit function and input usage simultaneously is to augment the profit function with terms that describe the movement of the operating

point. For example, this could be the sum of squared changes in the input variables. This effectively acts as a soft constraint, and is given by

$$\sum_{i}^{N} \Delta u_i^2 \tag{4.12}$$

where $\mathbf{u}$ is the set of manipulated plant inputs. Referring to the example problem given in 4.11, the augmented objective function would be given by

$$\min_{\mathbf{u}} (4 - u_1 u_2)^2 + \beta_1 \Delta u_1^2 + \beta_2 \Delta u_2^2 \tag{4.13}$$

where β_i are the penalty parameters that are set arbitrarily. Note that in this case, since the initial operating point is the origin, $\mathbf{\Delta u} = \mathbf{u}$. Figure 4.6(a) illustrates the original problem, and Figure 4.6(b) illustrates the problem involving the penalty function.

As illustrated, the augmented penalty function yields a unique minimum of ϕ=1.00 at $\mathbf{u} = [1.732 \ \ 1.732]^T$, assuming that $\beta_i = 1$. If this point were then evaluated using the true objective function, the objective value is ϕ=7.00. Based on Figure 4.6 and the known solution of ϕ=0.00, this is clearly suboptimal. This solution can be improved by modifying the penalty factors, β_i, and this will be investigated using the Kraft Mill model in Chapter 5.

Therefore, although this example of penalty function illustrates that the objective function can be altered such that a unique solution exists, there are two key issues that remain:

Sub-Optimal Solution When the solution to the problem involving the augmented penalty function is evaluated using the true economic objective, a sub-optimal profit is realized. This is because the shape of the response surface becomes

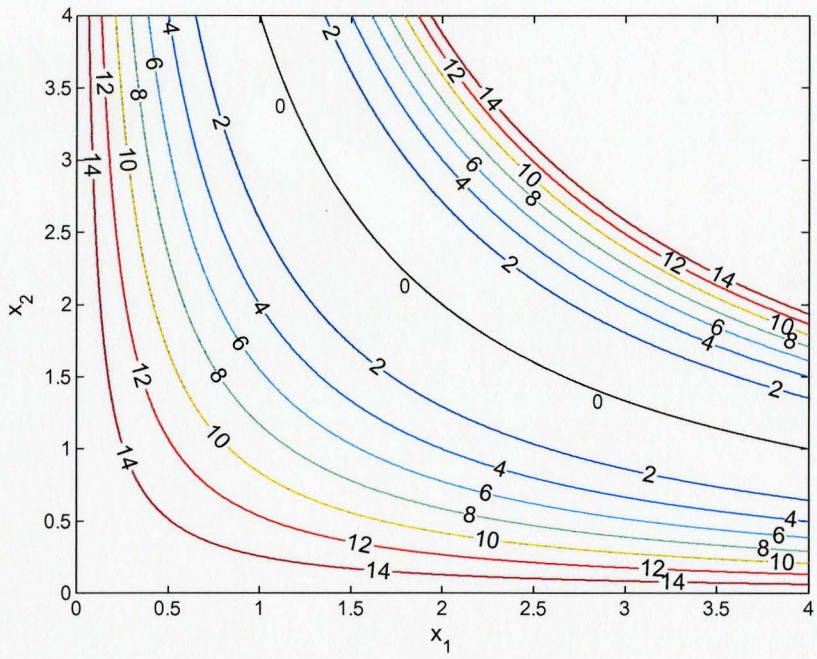

(a) Original Ridge Problem

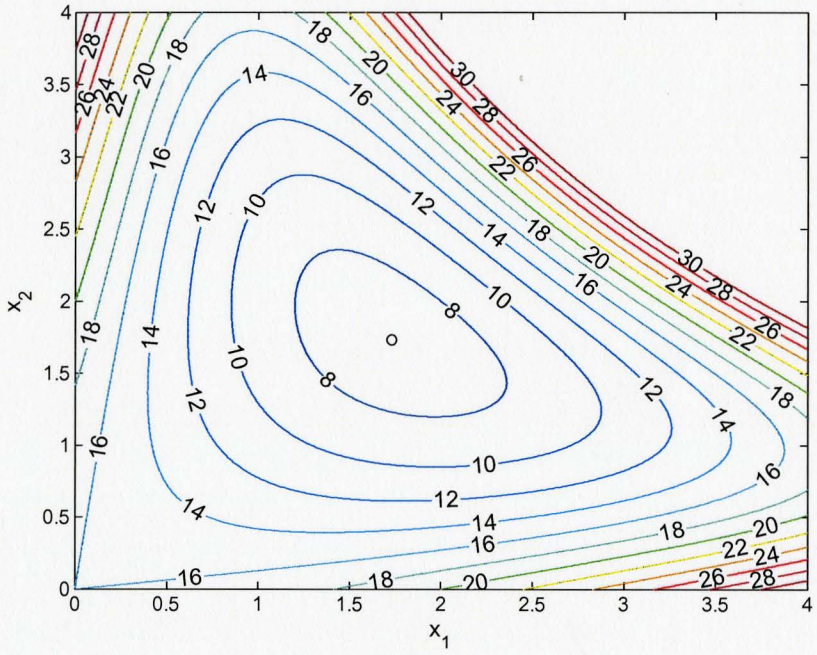

(b) Ridge Problem with Augmented Penalty

Figure 4.6: Ridge Example with and without Augmented Penalty

distorted. A related point is that when the penalty function is applied, the objective function becomes a combination of economic and operation objectives, which is not the preferred situation.

Penalty Factors The penalty factors, β_i, can be modified to find a better solution to the economic objective. However, there is no way of determining what the appropriate factors are. The penalty would have to be large enough (relative to the other objective costs) to have a 'suppression' effect, but small enough such that the true economics of the system are not affected to greatly. This becomes a limiting issue when the number of manipulated variables becomes large.

For the above reasons, this approach is abandoned for this research.

4.5.2 Constraint on Overall Manipulated Input Effort

The first of two *hard constraint* approaches to finding a unique solution and limiting input usage is discussed here. It involves placing an upper bound on the sum of squared changes in *all* plant inputs. In the above problem, this involves adding an inequality constraint into the formulation, namely

$$\sum_{i}^{N} \beta_i \Delta u_i^2 \leq \Psi. \tag{4.14}$$

where N is the number of input variables, β_i are optional weighting factors, and Ψ is the upper bound on the sum-of-squares. The key issues here are the choice of β_i and Ψ. While the weighting factors can be assumed to be unity, indicating that all inputs are of equal importance, the choice of Ψ is critical. If Ψ is too small, the problem is overly constrained, resulting in a sub-optimal solution. If Ψ is too large, non-uniqueness of solution will remain an issue. These are illustrated in Figure 4.7, based

on the above problem in Equation 4.11. The shape of the feasible region becomes one-quarter of a circle.

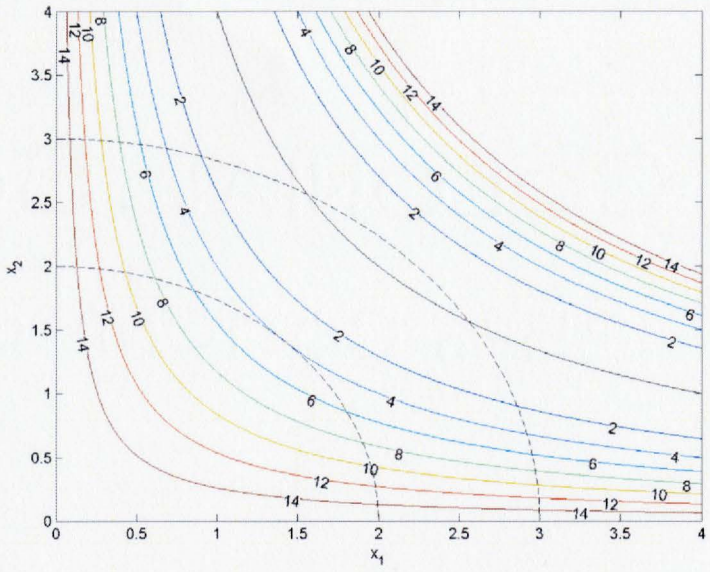

Figure 4.7: Hard Constraint on Plant

Two potential constraints are shown. The first, with radius, $\Psi = 2$, will yield a sub-optimal result as it does not include the minimum ridge in its feasible region. The second, with $\Psi = 3$ will include a subset of the ridge region, and therefore, non-unique solutions will result. Depending on the constraint set in larger problems, the choice of Ψ may also make the problem infeasible. Once again, arbitrary decisions must be made on the magnitude of the weighting and bounding factors. As shown, these decisions can yield sub-optimal solutions and can potentially provide optimal solutions that are non-unique. A unique optimal solution is possible, but it will require a precise value of Ψ a priori, which is highly unlikely. While these non-unique solutions may be an improvement over the base case problem, the forgoing issues make this an unattractive approach in this thesis. This will be illustrated in Chapter 5.

4.5.3 Rate-of-Change Constraints

A second hard-constraint approach is to introduce rate-of-change constraints into the problem. From an industrial perspective, these rate-of-change constraints can represent the reasonable rates at which operating point (i.e., production rates) can be moved during the time interval of interest. The rate-of-change constraint on the plant variables, stated simply, is

$$\| \Delta \mathbf{u} \|_\infty = \| \mathbf{u}_{i+1} - \mathbf{u}_i \|_\infty \leq \mathbf{b}_i \tag{4.15}$$

where the norm is taken component-wise, $\mathbf{u}$ is the vector of plant variables, $\mathbf{b}$ is the vector of scalar values that represent the maximum movement in a variable per time interval, and i is the index of discrete time intervals. The absolute value operation is non-differentiable, and therefore must be modified for use in the NLP problem. The implementation of these rate-of-change constraints was achieved using two slack variables for each plant variable. For example, if $\mathbf{u}$ is the vector of plant variables for which the rate of change is to be controlled, the formulation is

$$\mathbf{u}_{i+1} - \mathbf{u}_i + \mathbf{s}_{1,i} - \mathbf{s}_{2,i} = \mathbf{0} \tag{4.16}$$

$$\mathbf{s}_{j,i} \geq \mathbf{0} \tag{4.17}$$

$$\mathbf{s}_{j,i} \leq \mathbf{b}_i \tag{4.18}$$

$$i = 1, ..., P$$

$$j = 1, 2$$

where $\mathbf{s}_{j,i}$ are the vectors of non-negative slack variables that have an upper limit of $\mathbf{b}_i$, once again, representing the maximum movement in the plant variables per sampling interval. It should be noted here that the elements of $\mathbf{b}_i$ can be set inde-

pendently. However, depending on the lengths of the the shutdown and restoration being simulated, small values within $\mathbf{b}_i$ can lead to infeasible problems. Figure 4.8 illustrates a hypothetical case in which this can occur if the optimization problem is not formulated properly.

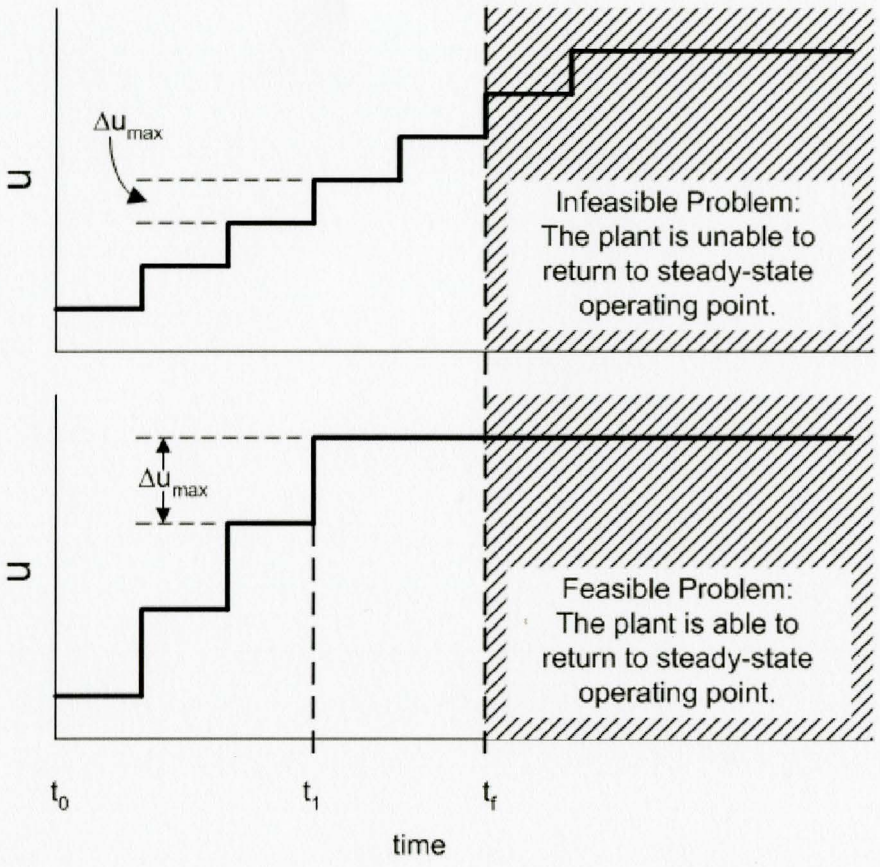

Figure 4.8: Rate of Change Illustration

This approach provides some realism to the problem, as long as the individual constraints are based on good engineering judgement. The issues of sub-optimality and infeasibility, as well as good choices for the upper bounds remain potential problems. Returning to the problem in 4.11, feasibility will not be an issue. However, depending on the values chosen for $\mathbf{b}$, sub-optimal and non-unique solutions will be possible.

4.5.4 Proposed Two-Tiered Approach

A two-tiered optimization approach is proposed as a preferred alternative. When it is known that a large number of degrees of freedom leads to non-unique solutions to the economic objective, this formulation can be used. It involves the following steps:

1. Choose an initial guess to the solution.
2. Solve the first tier, maximizing the economic objective function.
3. Transfer the economic objective function into the constraint set, and set it equal to the optimum value found in Step 2.
4. Solve the second tier, minimizing the input effort. Note that the initial guess to this tier is the solution of the first tier.

The feasible region for Tier 1 is the standard operating space, governed by the constraint set. The feasible region for Tier 2 is the intersection of the Tier 1 operating space with the hyperline defined by the economic optimum found in Tier 1. The solution found in Tier 2 is the overall solution to the problem considered.

This is now illustrated using the simple 2-variable problem described above. Mathematically, this method can be broken down into the *two tiers* as described above. The formulation of the first tier is the base case problem as shown in 4.11, where $F_{opt,t1}$ is the value at the optimum. The second tier requires the addition of the extra equality constraint to lock the economic objective at its optimum value. This second optimization problem is given by

$$\min_{\mathbf{\Delta u}} \sum_{i=1}^{2} \beta_i \Delta u_i^2$$

$$\begin{aligned} &\text{subject to:} \\ (4 - u_1 u_2)^2 - F_{opt,t1} &= 0 \\ u_1 &\geq 0 \\ u_2 &\geq 0 \\ \mathbf{u}_0 &= [u_{1,t1} \;\; u_{2,t1}]^T \end{aligned} \tag{4.19}$$

where β_i are optional weighting factors and $\mathbf{u}_{t1}$ is the location of the optimum achieved in Tier 1. Note that because the plant is assumed to be initially at the origin, $\mathbf{\Delta u} = \mathbf{u}$. Graphically, the two-tiered approach can be viewed as the scenario described in Figure 4.9. Based on an initial guess, the initial solution to Tier 1 might be $\mathbf{u} = [1\ 4]$, with $F_{opt,t1} = 0$. Tier 2 is essentially a search over the constraint defined by $F_{opt,t1} = 0$, to find the minimum input usage. Because it is assumed that $\beta_1 = \beta_2$, the optimum occurs when both inputs are used in equal amounts. Therefore, the optimum for the problem in Tier 2 is located at $\mathbf{u} = [2\ 2]$. Finally, the formulation of Tier 2 can be somewhat relaxed for computation benefit by introducing a tolerance, ϵ_{opt}, that allows some tradeoff between the two objectives. In this case, the strict equality constraint would be relaxed using slack variables, to become

$$\begin{aligned} (4 - u_1 u_2)^2 - F_{opt,t1} + s_1 - s_2 &= 0 \\ s_1 + s_2 &\leq \epsilon_{opt} \\ s_1 &\geq 0 \\ s_2 &\geq 0 \end{aligned}$$

This method is preferred, because it achieves minimum movement in the input variables in the region where the objective function is maintained at its optimum. Moreover, feasibility is not an issue in the two-tier approach. As long as Tier 1 is feasible,

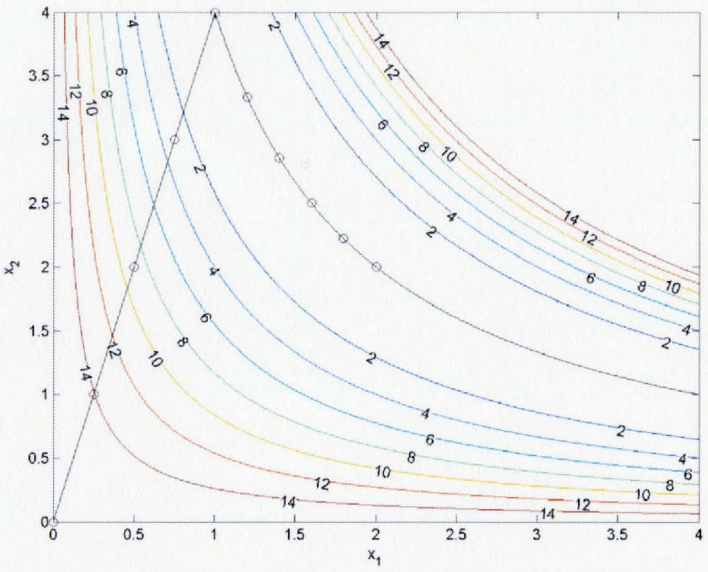

Figure 4.9: Two Tiered Approach to Ridge Problem

Tier 2 will be feasible – in the worst case, the location of the optimum in Tier 2 will be that of Tier 1.

4.5.5 Application of Two-Tiered Approach to Introductory Case Study

Returning to the study presented in Section 4.4, we apply the proposed two-tiered approach handle the non-uniqueness observed. Due to the size of the industrial problem, one modification to the approach is necessary that was not required in the two-variable problem outlined above. This change was to provide a small relaxation to the second tier, such that the profit was allowed to degrade 1.0% (from Tier 1) to improve numerical performance (i.e., convergence to a solution). Mathematically, this is stated as,

$$\Phi(\mathbf{u})_{tier2} \geq 0.99\Phi(\mathbf{u})_{tier1}, \tag{4.20}$$

where $\Phi(\mathbf{u})_{tier1}$ is the economic objective in Tier 1 and $\Phi(\mathbf{u})_{tier2}$ is the economic objective in Tier 2. The operational objective decreases to $\sum \Delta u^2 = 471,037$, compared to $\sum \Delta u^2 = 1,989,580$ found in the single-tier approach described in Section 4.4. A review and comparison of the Figures 4.10, 4.11, and 4.12 to the corresponding variables in Section 4.4 shows a much smoother operation that achieves essentially the same economic performance.

4.6 Chapter Summary

This chapter has presented the overall formulation to the optimization problem involving a multi-unit system under shutdown conditions. This included the the following issues.

- An economics-based objective function is necessary to characterize the optimal operation during a plant shutdown. Merely maximizing production may not necessarily lead to the most profitable outcome.
- Path and end-point constraints are necessary to ensure trajectories are within physically reasonable bounds, and to ensure that the plant returns to the nominal operation at the end of the time horizon.
- Due to a large number of degrees of freedom, the solution to the economics-based problem can be non-unique. This non-uniqueness can lead to rough plant movement that still obeys the constraint set. To maintain a smooth and economically favorable operation, an optimization problem involving two tiers was presented. A profit-maximization objective was applied as the first tier of the

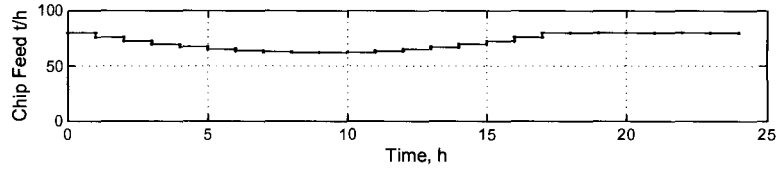

(a) Digester Feed

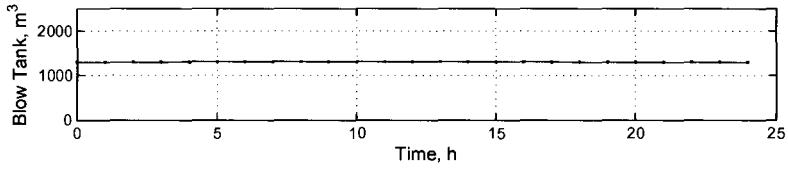

(b) Blowtank Volume

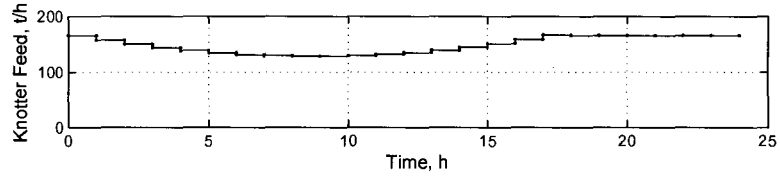

(c) Knotter Feed

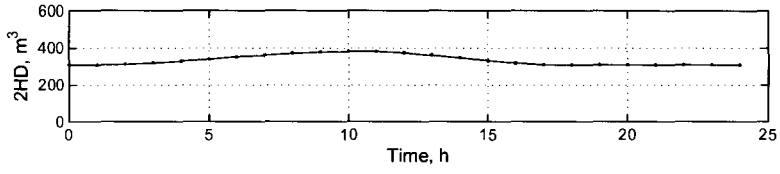

(d) 2HD volume

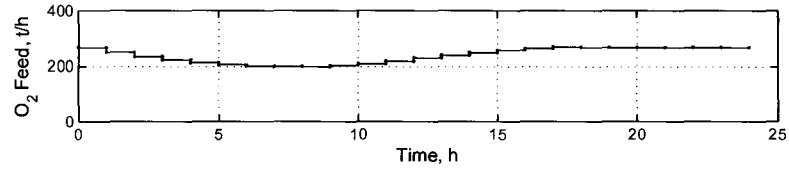

(e) O_2 Feed

Figure 4.10: Introductory Scenario: Variable Trajectories using two-tiered approach

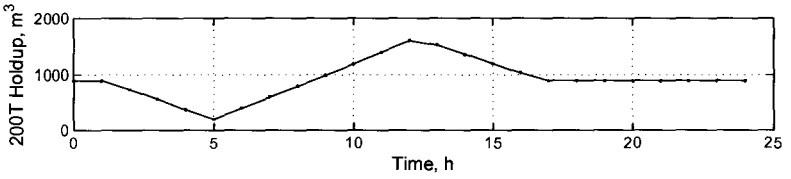

(a) 200T Volume

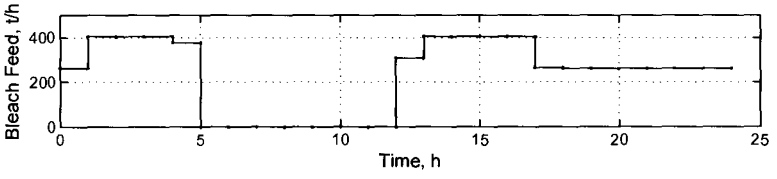

(b) Bleach Feed

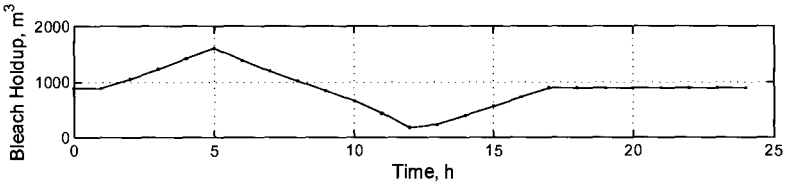

(c) Bleach Storage Volume

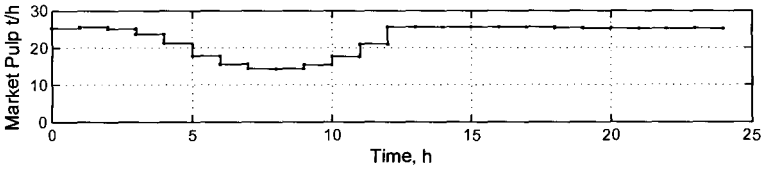

(d) Pulp Production

Figure 4.11: Introductory Scenario: Variable Trajectories using two-tiered approach (continued)

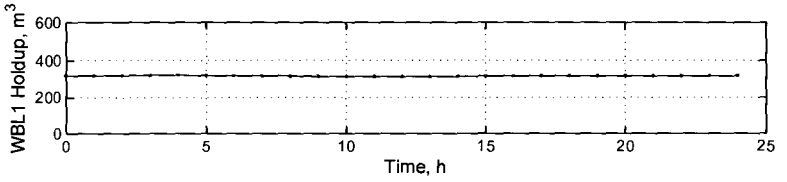

(a) Weak Black Liquor Storage

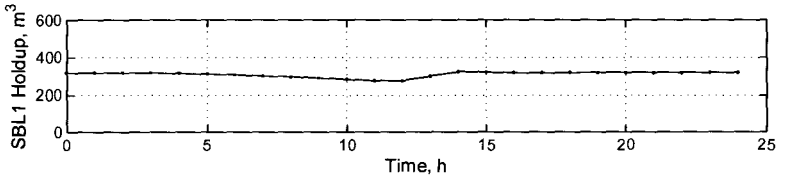

(b) Strong Black Liquor Storage

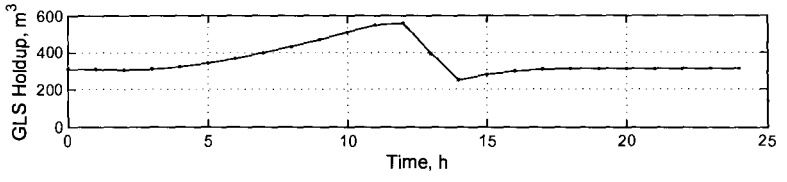

(c) Green Liquor Storage

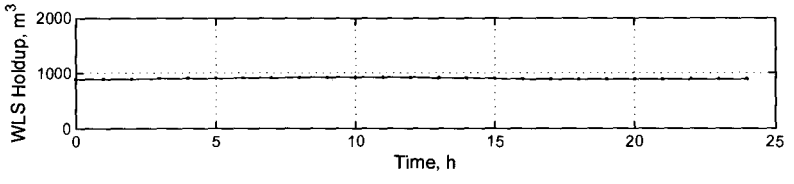

(d) White Liquor Storage

Figure 4.12: Introductory Scenario: Variable Trajectories using two-tiered approach (continued)

problem. The second tier involved moving along the hyperline that defined the maximum profit, to determine the minimum input usage. This was illustrated for an introductory case study.

Chapter 5

Optimization of Plant Operation: Case Studies

5.1 Introduction

Three sections of case studies are presented, along with extensions into sensitivity to selected parameters and constraints. Investigations into alternate formulations to handle the non-unique solutions are also studied.

5.2 Case Studies: Maintenance Shutdowns

In this section, scheduled shutdowns in the digester and bleaching areas are investigated and studied under different conditions. The benefit of preparation is illustrated through movement of the plant operating point to a more advantageous location in the operating window prior to the shutdown.

5.2.1 Digester Shutdown

It is often said that the Kamyr digester is the 'heart' of the pulp mill operation. In a study such as this one, the study of the plant's behaviour under failure conditions, this is easily illustrated. The digester is the location at which the main raw materials enter the process, namely the softwood chips and the recycled white liquor. The digester is also the site at which black liquor is produced and subsequently concentrated and combusted for steam production that is used throughout the plant. Consequently, when the digester is unavailable or operating at very low production rates for extended periods of time, the rest of the kraft mill is essentially crippled. Therefore, the first case study to be presented involves a shutdown at the digester. Optimal plant variable trajectories and resultant objective values are computed for a variety of studies.

Table 5.1 provides data for various preparation times and shutdown durations. The effect of restoration time is studied later, and therefore, it is kept constant in these studies. The cases have been chosen such that the benefit of preparation time and impact of the shutdown duration can be easily seen. The very poor operating profits are mainly due to the loss of production (zero digester feed), as well as the need to use natural gas due to the black liquor shortage.

Figures 5.1-5.2 illustrate the effect of preparation time through analysis of Cases 4 and 6 above. As the number of degrees of freedom increases (allowable preparation time), marginal increases in the economic objective are realized. Because the digester is so critical to the plant operation, improvement in the objective is hard to achieve with additional preparation time. This is true, especially since the digester is assumed to operate at the maximum possible level. The small improvements realized when the preparation time is increased is primarily due to the boilers being able to run at more efficient levels.

Figures 5.1(a) and 5.1(b) illustrate that the optimal solution involves filling the stor-

Table 5.1: Results for Scheduled Digester Shutdown

Case	Preparation Time (hrs)	Shutdown Time (hrs)	Restoration Time (hrs)	Profit ($/day)	$\Sigma\Delta u^2$ (scaled)	CPU Time (seconds)
1	4	7	5	106,420	260,528	48
2	4	9	5	77,374	264,717	47
3	6	7	5	108,621	188,119	63
4	6	9	5	78,485	208,067	126
5	8	7	5	109,755	218,829	44
6	8	9	5	79,620	190,980	210

age tanks adjacent to the digester during the preparation phase, and then drop in volume during the shutdown. This prevents the downstream knotting/washing department from having to shut down operations (Figure 5.2(a)). This department is required to shutdown during long digester outages because the lower constraint on the blowtank volume becomes active. Figure 5.1(d) shows the drop in market pulp production that is spread across the preparation, shutdown, and restoration periods (available degrees of freedom). This approach minimizes the variation of the throughput through the machine and dryer, and is a result of the two-tiered optimization approach.

Figure 5.1 shows that the added flexibility that Case 6 has because of the two additional hours of preparation time. In both scenarios, the blowtank is filled to the maximum allowable limit. However, the weak-black liquor tank is filled only in Case 6. In addition, the loss in market pulp production is divided across the two additional hours, thereby reducing the variation in throughput through this department. Because the digester is at the bottle-neck point, a relatively modest economic benefit is realized by the extra preparation time. As indicated by the values for the operability objective in Table 5.1, there is more plant movement in Case 6 because of the

increased degrees of freedom (i.e., two additional hours of plant movement). Note that the specified end-point constraints are obeyed for the last three time steps. Figure 5.2(d) illustrates the storage volumes in the recovery lines. These operations slow down during the preparation period to accumulate some material in upstream storage tanks, such that production levels can remain at moderate levels during the digester shutdown. These are more efficient than having to operate at lower levels during an unplanned outage. Note that because the evaporators and boilers run at proportional rates to one another, the strong black liquor tanks remain at a constant level. This is the case for some failures, in which manipulating selected buffer tank volumes yields no improvement in the objective. This was also observed by Pettersson [1969] and Dube [2000].

Some of the most influential constraints on the system being investigated are the end-point constraints that are specified from the end of the restoration period, and are enforced for the remainder of the 24-hour time horizon. These constraints are investigated in the next section.

Impact of Energy Cost

An issue facing industry in recent years is the rapid increase and frequent fluctuation of energy prices, specifically for commodities such as oil and gas. Figure 5.3 is a trend in the price of natural gas charged to commercial customers in Ontario since mid-1996. While the trend was increasing slowly and steadily prior to 2000, significant increases and fluctuations have been seen since. This includes an almost five-fold increase in 2001. Differences in the cost of the energy inputs will most definitely impact the optimal manner in which to operate a plant, especially during transient events such as equipment shutdowns.

Figure 5.4 illustrates this effect for an 8-hour planned maintenance shutdown at the

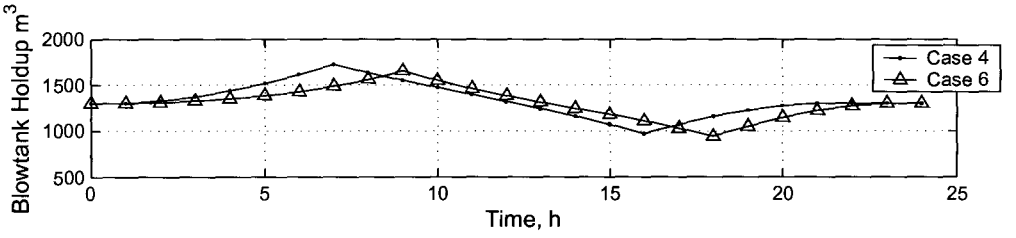

(a) Blowtank Holdup

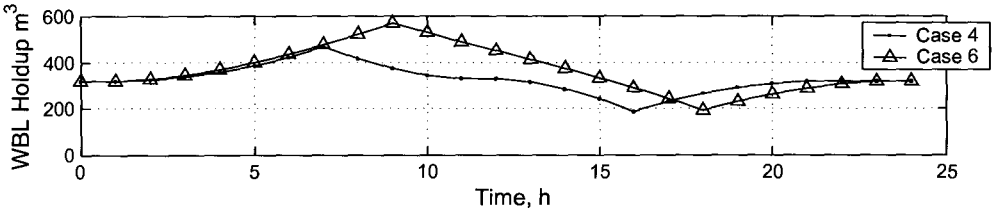

(b) Weak Black Liquor Holdup

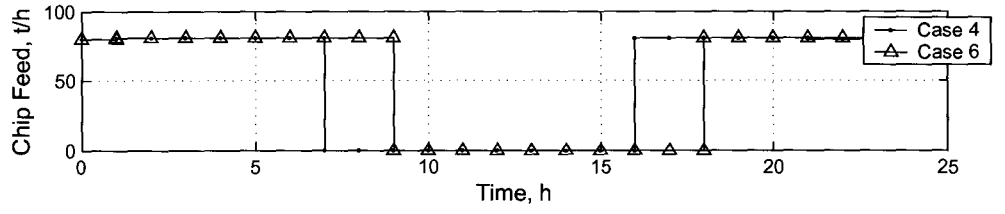

(c) Digester Production

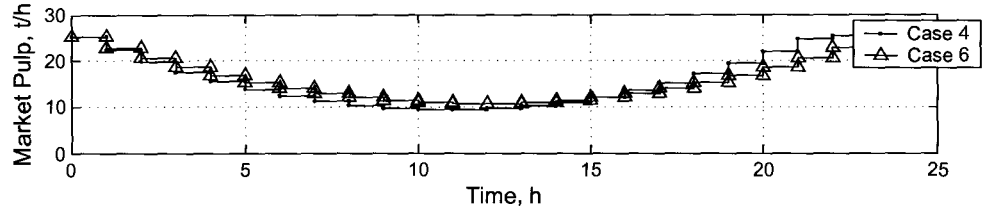

(d) Market Pulp Production

Figure 5.1: Response of Plant Variables to Digester Shutdowns (Cases 4 and 6)

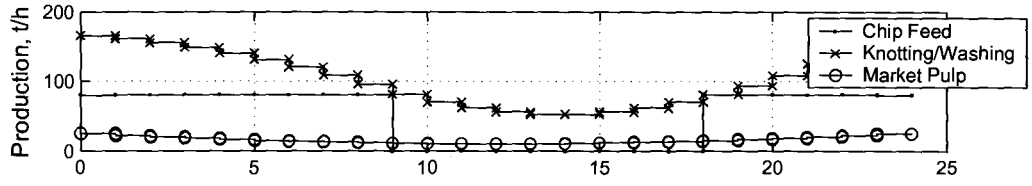

(a) Pulp Line Production

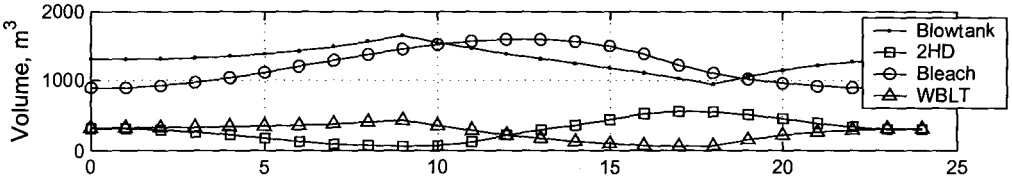

(b) Pulp Line Buffer Capacities

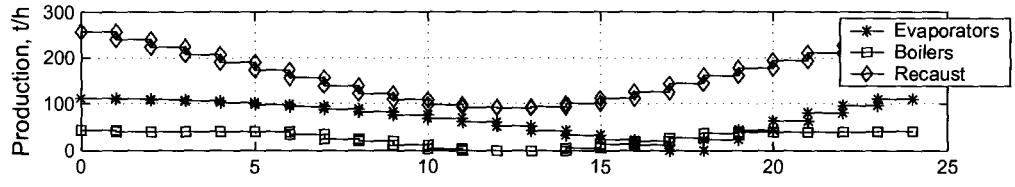

(c) Liquor Cycle Production

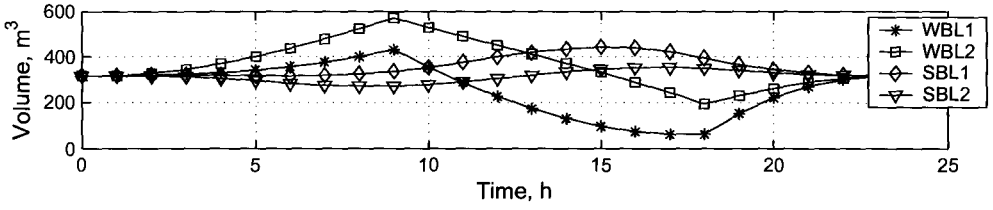

(d) Liquor Cycle Buffer Capacities

Figure 5.2: Response of Plant Variables to a Digester Shutdown (Case 6)

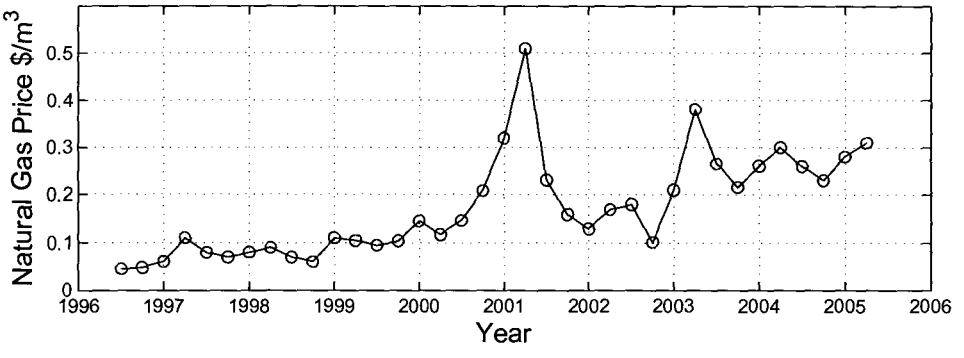

Figure 5.3: Natural Gas Price [http://www.energyshop.com]

digester. There are 3-hours of preparation time available, and a 3-hour restoration period. It is assumed that the steady-state production rate cannot change, and therefore, the digester feed rate is the same at the beginning and end of the time horizon. If the gas price were to double to just above the peak price from 2001, the optimal solution would involve slightly lower production during the transient. Of course, this means that the optimizer finds a trade-off between utilities conserved at the higher energy price, versus market pulp produced. This is an indication that perhaps the steady-state plant operation should change, even when shutdowns are not occurring. Of course, this assumes that the production rate can decrease (i.e., plant not constrained by market demand). Further study involving fluctuating energy or raw material costs can include optimal production rates. It is reasonable to postulate that the steady-state production rate can be chosen based on a trade-off between market-pulp produced versus utilities (for example, natural gas) consumed. This is not pursued in this thesis, and left for future study. Table 5.2 illustrates the impact on plant economics, where the decrease in profit is attributed both to decreased production, and increased operating costs throughout the plant.

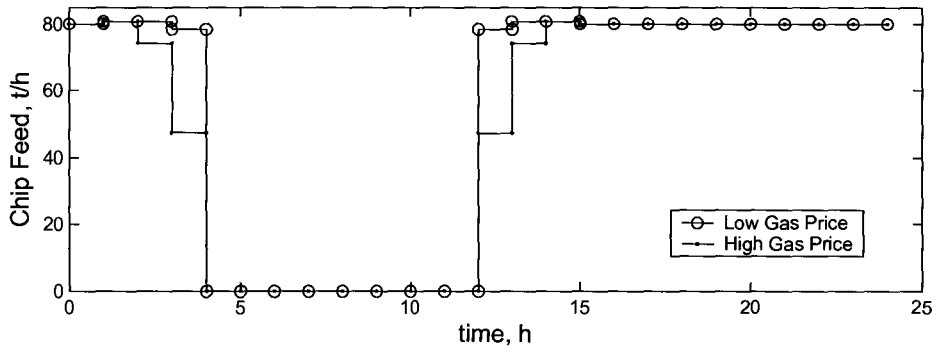

Figure 5.4: Digester Feed Rate and Gas Price

Table 5.2: Impact of Gas Price on Plant Economics

Case	Natural Gas Price ($/t)	Profit ($/day)	$\Sigma\Delta u^2$ (scaled)	CPU Time (seconds)
1	440	106,420	260,528	48
7	880	88,126	284,216	52

Relaxation of End-Point Constraints

The following study is based on Case 1 above, in which the buffer tank levels are required to return to their scaled nominal values, within $\epsilon = 10^{-3}$. The following analysis uncovers the economic benefits of relaxing this constraint, while still requiring the individual department production rates to return to nominal values. While economic benefits are realized for the finite time horizon, the assumption implicit in this formulation is that the plant does not need to be ready for any subsequent disturbances. However, the pure inventory cost is illustrated using the two-tiered optimization approach.

Table 5.3 and Figure 5.5 illustrate the trends of the objective function values with the value of epsilon. It is not surprising to see that as the value for ϵ is increased, the profit increases (Figure 5.5(a)). The profit is realized as the pulp tanks empty

Table 5.3: Relaxed End-Point Constraint Study

Epsilon, ϵ	Profit ($/day)	$\Sigma\Delta u^2$ (scaled)	CPU Time (seconds)
10^{-3}	106,420	260,528	72
0.05	121,400	241,687	107
0.10	135,590	201,475	92
0.4	191,417	186,214	68
0.7	240,454	164,473	83
0.8	258,368	161,762	96
0.9	260,960	159,541	34
1	264,160	156,343	57
2	271,041	152,497	49

pushing the production of pulp out of the system. Of course, this production is limited by the maximum production through the machine and dryer section. Coinciding with this trend is a decreasing trend in the operational objective, $\Sigma\Delta u^2$. As the end-point constraints are relaxed, the system is not required to work to return the buffer tank levels back to the nominal operating point. Figure 5.5(b) illustrates the well behaved curves for the buffer capacity located downstream of the oxygen delignification department as ϵ is increased. Of course, since it is a pulp tank, the optimizer finds that emptying it yields the maximum possible profit.

In practice, one would not allow the buffer tank levels to run dry during the recovery from a fault. This situation is undesirable from an operability point-of-view, especially with a system with poor reliability. Subsequent failures or maintenance shutdowns can cascade through the multi-unit system very quickly when surge tanks are allowed to empty. Re-optimization from an operating point other than the nominal operating point is discussed in Section 5.5.

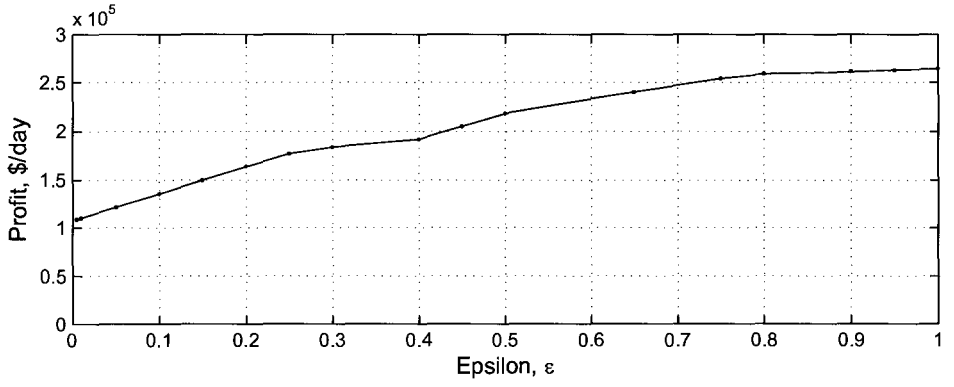

(a) Operating Profit vs. ϵ

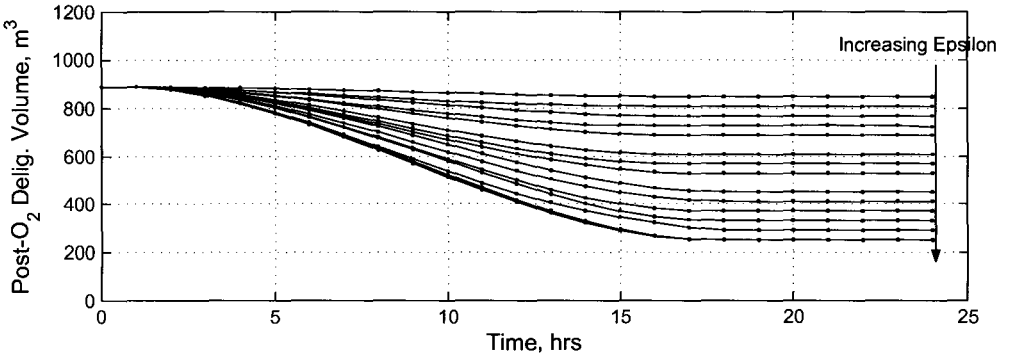

(b) 200T tank with increasing value of Epsilon

Figure 5.5: Impact of Endpoint Constraint Relaxation

Table 5.4: Results for Scheduled Digester Shutdown

Case	Preparation Time (hrs)	Shutdown Time (hrs)	Restoration Time (hrs)	Profit ($/day)	$\Sigma\Delta u^2$ (scaled)	CPU Time (seconds)
7	4	7	5	176,737	471,037	74
8	4	9	5	146,601	547,817	55
9	6	7	5	180,382	342,638	107
10	6	9	5	150,247	528,033	65
11	8	7	5	181,622	389,784	55
12	8	9	5	151,411	433,749	25

5.2.2 Bleach Plant Shutdown

A shutdown in the bleach department has a heavy impact the pulp mill, as no finished pulp can be sent to the sheet-forming machine and dryer sequence. The same pattern of preparation, shutdown, and restoration times has been used as in the digester shutdowns to provide a comparison for the relative impacts of the two departments shutting down. As Table 5.4 illustrates, for identical timing patterns, operating profits are superior in the event of a bleach-plant outage (See Table 5.1). This is because shutdowns in the digester department cascade through all three of the cycles (pulp, liquor, steam) considered in this work, essentially crippling the plant. Since the bleach plant is located far enough downstream, and separated from the digester by multiple storage vessels, the digester can be kept running and production is not impacted as severely. Table 5.4 also illustrates the expected increase in operating profit as more preparation time is made available.

The shutdown period for Case 7 and Case 11 from Table 5.4 is indicated in Figure 5.6. During the shutdown period, the upstream buffer capacity will fill, and the downstream buffer capacity will empty. This occurs because the adjacent and connected production areas attempt to continue some level of operation. Therefore, when the

outage is a planned maintenance shutdown, it is advisable that the upstream buffer capacity level is lowered and the downstream buffer capacity level is raised, prior the shutdown. As discussed previously, this is equivalent to moving the operating point to a location that is more economically favorable for the beginning of the outage. This is exactly what is illustrated in Figures 5.6(a) (upstream buffer tank) and 5.6(c) (downstream buffer tank) for two scenarios with equal shutdown durations and restoration times, but differing preparation times. In preparation for an outage in the entire bleaching plant, the upstream storage capacity is partially emptied, and the downstream storage capacity is partially filled. During the shutdown, the levels reverse to the maximum or minimum values at the end of the shutdown. During the restoration period, these levels are returned to the nominal state. For long shutdown scenarios such as these, it is not surprising that the optimal solution specifies the buffer tank levels approach maximum or minimum values to keep plant operations at the most efficient levels. For example, if the HD bleached pulp tank (downstream of bleach department) is filled prior to the outage, the machine/drying department can be run at a moderate level without having to stop the flow of market pulp. This is illustrated in Figure 5.6(d). In this particular case, this is a definite advantage. If the HD bleached pulp tank empties, the machine must be shutdown. Restarting the sheet-forming machine, and subsequently feeding the beginning of a pulp sheet to the dryer are two of the most difficult tasks facing Kraft mill engineers and operators. Therefore, a pulp shortage at the machine/drying sections must be avoided whenever possible. For other details pertaining to the impact of a bleach plant outage, the reader is referred to the introductory case study discussed in Sections 4.4 and 4.5.5.

The smooth profiles of many of the plant variables observed in Sections 5.2.1 and 5.2.2 are a result of the two-tiered formulation described. An alternate method reviewed in Section 4.5 is to place a constraint on the total plant movement across the time horizon. Schweiger and Floudas [1998] refer to this as the ϵ-constraint formulation. The application of this method is now discussed, using Case 12 above as the base

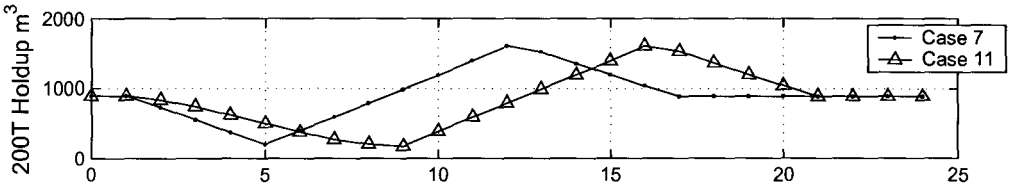

(a) 200T Holdup

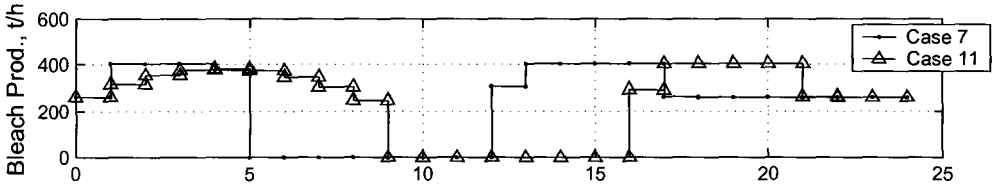

(b) Bleach Production

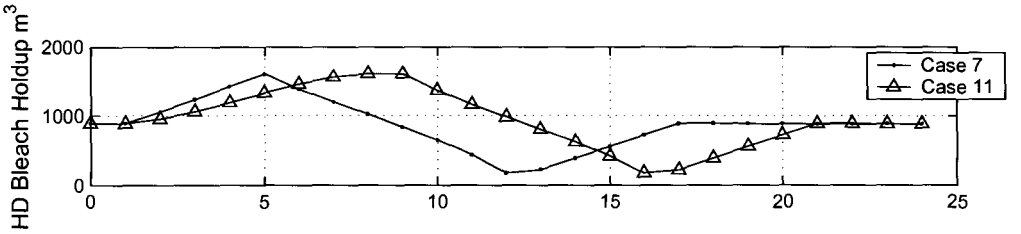

(c) HD Bleach Holdup

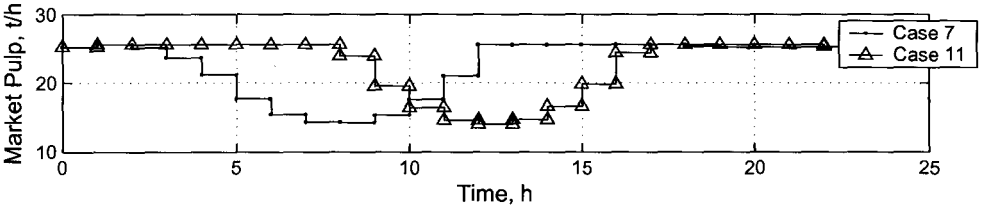

(d) Market Pulp Production

Figure 5.6: Response of Plant to a Shutdown at the Bleach Department

case scenario.

Impact of Hard-Constraint on Plant Movement

An interesting case from Table 5.4 is of course Case 12, where the preparation time and shutdown durations are the longest. It is therefore chosen to investigate the impact of a hard-constraint on the operability objective, given by

$$\sum_{i=1}^{M}\sum_{j=1}^{N}\Delta u_{i,j}^{2} \leq \Psi, \tag{5.1}$$

where i is the time interval, j is the set of plant inputs, and Ψ is the upper bound on the sum-of-squared input usage. This constraint is placed on the whole plant, and not on individual input variables. Note that this choice for Ψ is arbitrary, and is somewhat based on the scaling used in the problem. As illustrated in Section 4.5, the concern when utilizing this approach is that depending on the choice of the upper bound, Ψ, the true economic optimum may be limited because the Ψ-constraint is active. As the value for Ψ is made smaller, the economic optimum is expected to degrade. Another issue to be aware of involves the end-point constraints on the system that are non-negotiable. Since the scenarios require that the plant return to the nominal operating point by some pre-specified time along the horizon, there is inherently a *lower* bound on the operability objective. If the plant is moved too slowly, end-point constraints are not met, and the problem is deemed infeasible. This minimum amount of input usage corresponds to the movement required for the plant to remain feasible with production rates and surge tank levels within path constraints over the time horizon, but still meets end-point constraints. These issues further illustrate the benefit of the two-tiered approach utilized in this work. Our approach is, of course, applicable when a priority can be set on the different objectives sought. In other words, the primary objective (in this case, economics) is optimized first, and then the secondary

objective (in this case, input usage) is optimized without sacrificing the optimality of the primary objective. This is in contrast to the areas of bilevel, or multi-level optimization where competing objectives are optimized simultaneously. For details in this area, the reader is referred to Gümüş and Floudas [2001] and Vicente and Calamai [1994].

Figure 5.7 illustrates this trade-off curve between the value of Ψ and the economic objective. At very high values of the value of Ψ, there is no impact on the economic objective. This indicates that a critical value of Ψ has been passed. This critical value may be the upper bound on the $\sum \Delta u^2$ for a given value of the economic objective. In other words, as the bound on Ψ may become inactive after this critical value. Another possibility that the value represents the point at which a region including multiple solutions for the maximum profit is entered. As the value for Ψ is decreased, degradation of the objective value occurs as production areas are not permitted to move to more favorable regions. Perhaps the greatest impact at lower values of Ψ is during the preparation and restoration phases, where operating areas cannot reach higher throughput regions to increase production. This is seen in Figure 5.8 where the bleach plant and drying machine production rates are kept lower for $\Psi = 130,000$, than they are for $\Psi = 250,000$. Another consequence, as seen in Figure 5.9 is that buffer capacities are not used too extensively when the plant movement is constrained. The optimizer finds that minimum plant movement is achieved when production departments on either side of buffer capacities move with similar patterns over the time horizon. When this occurs, and the flows in and out of then tanks are equal, the levels are kept close to the nominal values. Except for the adjacent storage capacities, which move as described in the last section, the buffer capacities are not used as effectively for $\Psi = 130,000$.

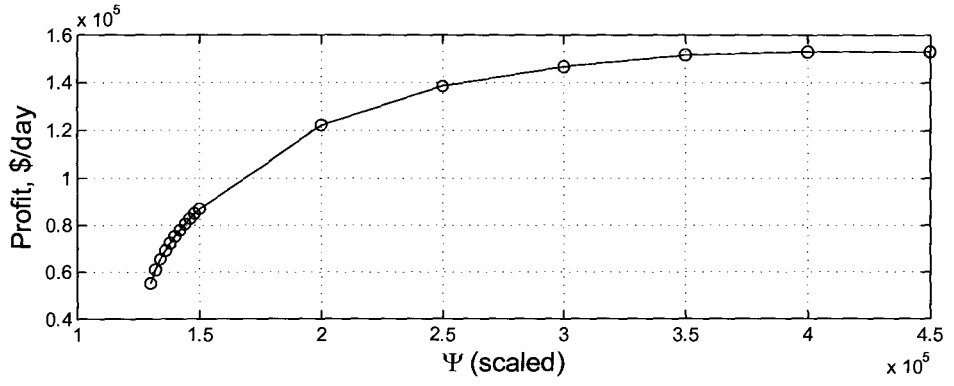

Figure 5.7: Trade-off curve between plant economics and the Ψ-constraint

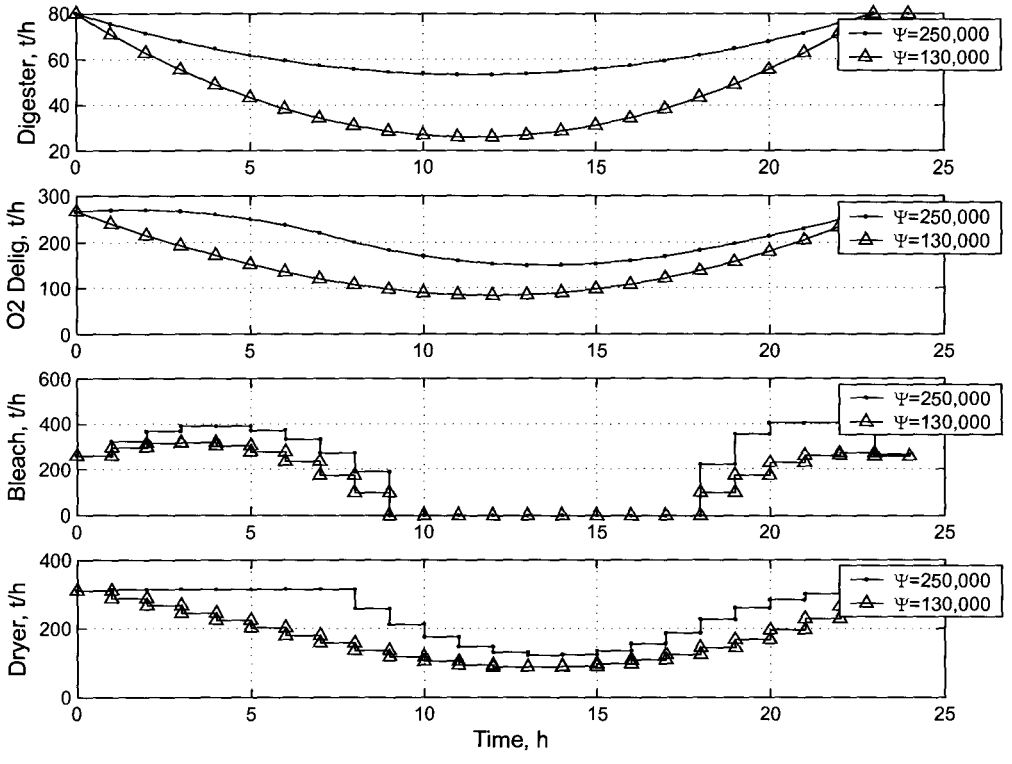

Figure 5.8: Trend in production rates for Ψ=130,000 and Ψ=250,000

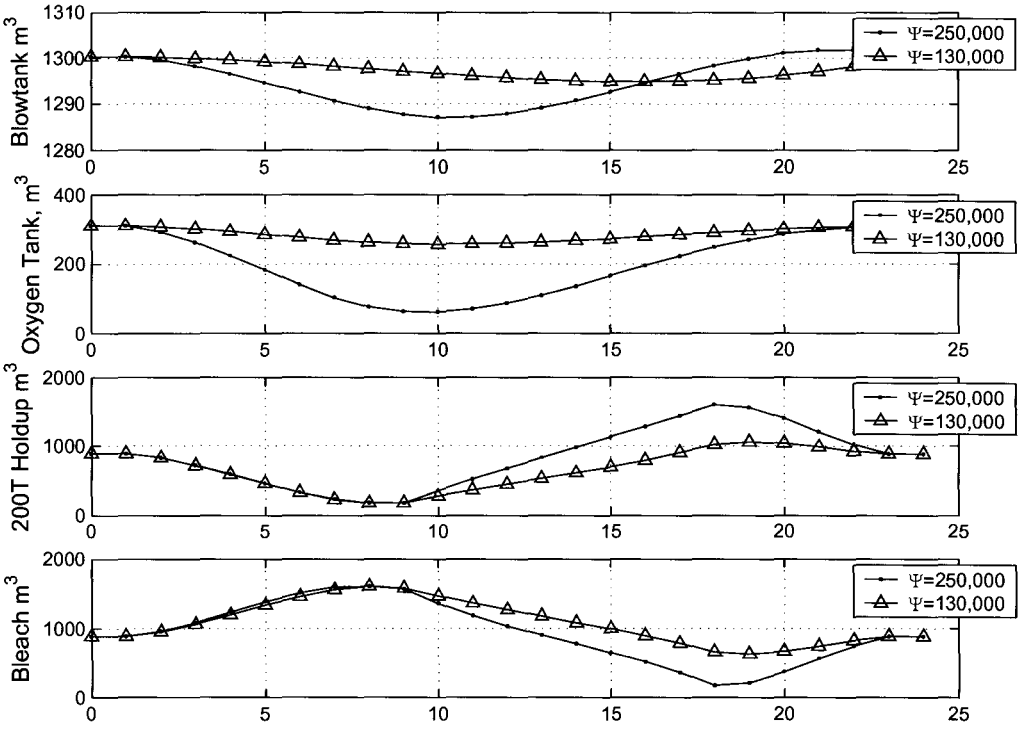

Figure 5.9: Trend in buffer capacities for Ψ=130,000 and Ψ=250,000

5.3 Case Studies: Unit Failures

In this section, unscheduled shutdowns are investigated. These are arguably the more interesting problems, as they have a much more severe impact on the plant and its economics, as well as more interaction with system constraints. Intuitively, unit failures pose a larger economic consequence than scheduled shutdowns of equivalent length because the plant operating point cannot be moved prior to the shutdown. Therefore, one would expect the economic objective to degrade further for a given shutdown scenario. Moreover, because these scenarios are *reactive*, the operability objective can be expected to increase, indicating a requirement of the plant to move more aggressively to remain feasible.

5.3.1 Oxygen Delignification Failure

The oxygen delignification department is situated between the washing/screening departments and the bleach plant. Failures in this department can be due to a variety of reasons. These include, but are not limited to, failure at the feed press, loss of oxygen feed, loss of steam line, and caustic shortage. Table 5.5 provides a summary of some of the key cases considered. In all cases, the failure is assumed to occur immediately after the first discrete time step. The shutdown duration and available restoration time are assumed to be known exactly for each of the cases considered.

Once again, the expected degradation in economics is seen as the downtime increases, assuming a fixed restoration time. Also, for a fixed shutdown duration, increases in restoration time allow the plant to operate at more efficient production levels, and the internal departments are permitted to catch up on lost production.

Figures 5.10-5.11 illustrate the effect of shutdown durations for Cases 13 and 16 above, for which the shutdown duration for Case 16 is 2 hours longer than for Case 13, but

Table 5.5: Results for Oxygen Delignification Department Failures

Case	Shutdown Duration (hrs)	Restoration Time (hrs)	Profit ($/day)	$\Sigma\Delta u^2$ (scaled)	CPU Time (seconds)
13	7	6	134,977	446,838	42
14	7	8	142,855	426,274	83
15	7	10	149,286	421,776	31
16	9	6	104,842	476,242	25
17	9	8	112,679	448,075	49
18	9	10	120,354	431,495	37

the restoration times are the same. Figure 5.10 shows that for each of the shutdowns, the 2HD stock tank (located directly upstream of the screening/oxygen delignification departments, See Figure 3.1) fills to the allowable capacity somewhere along the time horizon. As this constraint is approached, upstream production departments must also shutdown. Consequently, in both cases, the knotting/washing department must be shutdown so that this tank does not overflow. The induced knotting/washing shutdown can then impacts the upstream digester house, and cause slower operation there. The slower operation is seen in Figure 5.11(a), and since the production rate through the digester is slower than that of the knotting department, accumulation in the blowtank occurs (Figure 5.11(c)).

To achieve strong economic performance during the unscheduled shutdown of equipment, it is often necessary to bang the plant around within the operating window. While economically optimal, the objective of running a smooth operation during transient events is sacrificed. In this work, the two-tiered optimization approach is applied. An alternate method that is popular in optimization studies, in which economic and operability objectives are considered simultaneously, is to use a penalty function where the primary objective (plant economics) is penalized by the plant movement

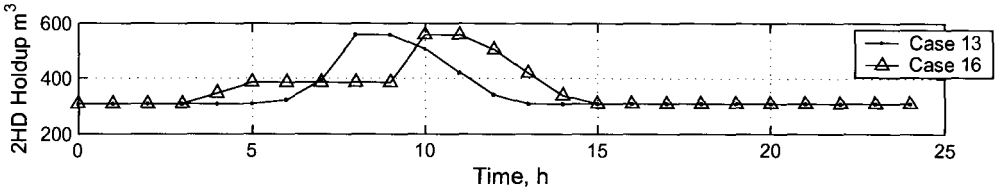

(a) 2HD Holdup

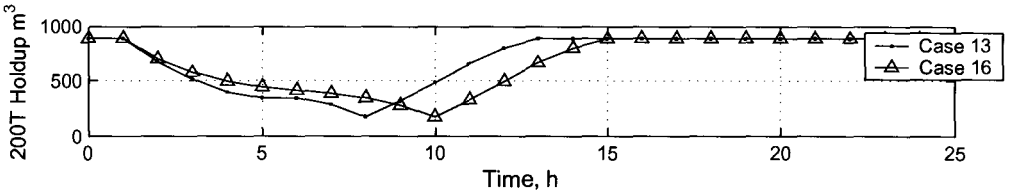

(b) 200T Holdup

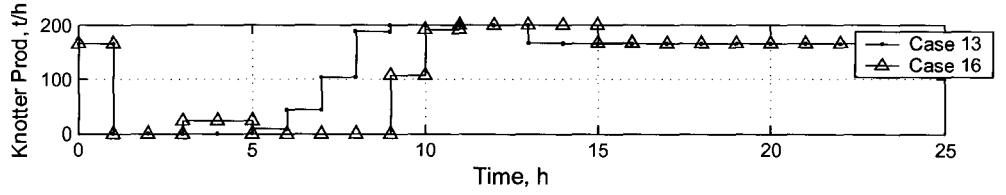

(c) Knotter Production

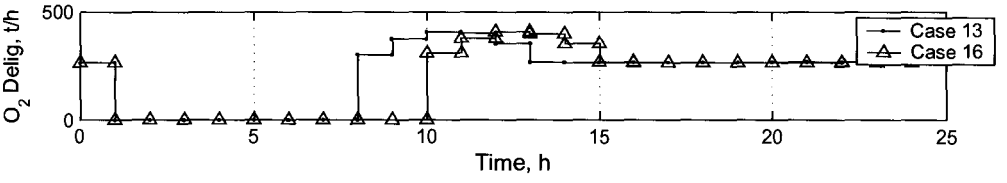

(d) Oxygen Delignification Production

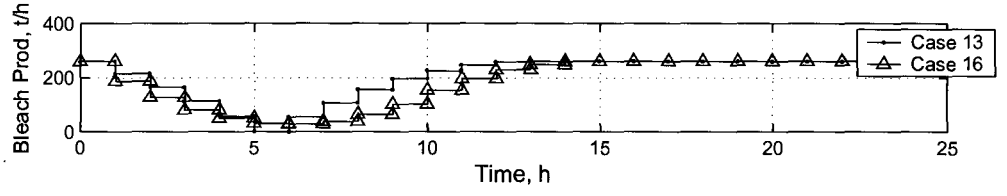

(e) Bleach Plant Production

Figure 5.10: Response of Plant Variables to a Oxygen Delignification Plant Failure

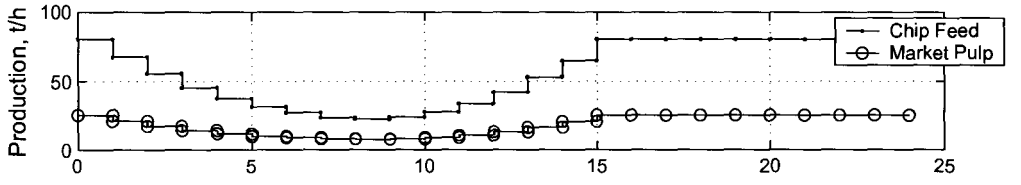

(a) Pulp Line Production

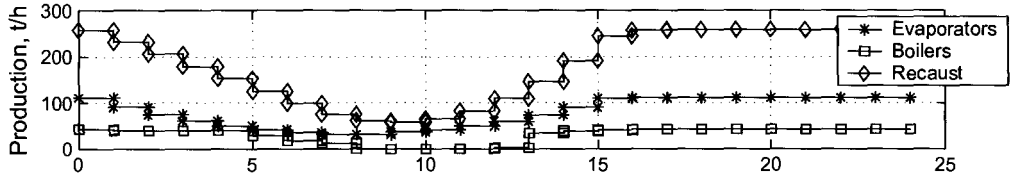

(b) Liquor Cycle Production

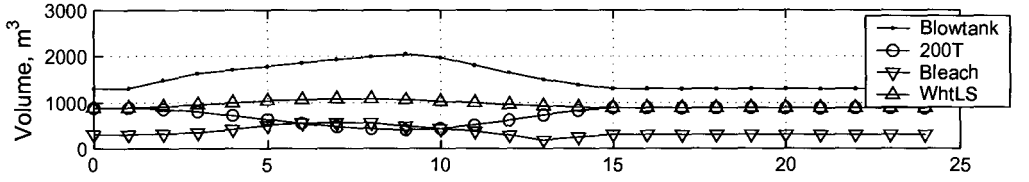

(c) Buffer Tank Holdups

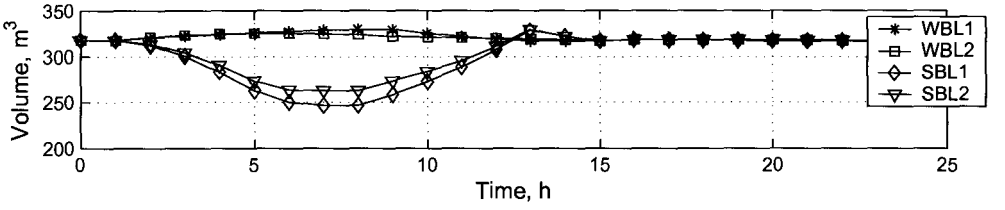

(d) Liquor Cycle Holdups

Figure 5.11: Response of Plant Variables to a Oxygen Delignification Plant Failure (Case 16)

objective through some constant set of weights, β. This method is investigated below.

Use of Penalty Function to Handle Non-Uniqueness

It is now convenient to illustrate another method used to achieve 'optimal' solutions to both the economic and operability objectives. To review, two objectives are of interest when analyzing systems under failure conditions. The first is the economics-based objective that we are trying to maximize, and the second is an operability-based objective that we are trying to minimize. Section 4.5 reviewed the various approaches considered for optimization of the multi-criterion scenarios pertinent to this thesis. The least attractive options are the ϵ-constraint and rate-of-change constraint formulations. These hard bounds can drive the solution to infeasibility, or to very poor (sub-optimal) solutions. In this section, the effect of the penalty method is presented. Based on one of the cases above (Case 18), a study was performed to determine the degree of sub-optimality yielded by the penalty-method, accompanied by a sensitivity analysis on the penalties, β_l. Once again, it is assumed that all β_l have the same value (i.e., all plant flows are equally suppressed). To review, the penalty formulation is given by

$$\Phi = \sum_{j=1}^{N} \sum_{k=1}^{t_f} c_j F_{j,k} - \sum_{l=1}^{P} \beta_l \sum_{k=2}^{t_f} (u_{l,k} - u_{l,k-1})^2 \tag{5.2}$$

where $F_{j,k}$ is the flow of stream j at time interval k with associated economic coefficient c_j, and $u_{l,k}$ is the production rate of department l at time interval k. Figure 5.12 illustrates the effect of the above formulation for the solution of a failure scenario. Case 18, which yielded an optimum operating profit of \$120,354, was used as the base case. This classic consequence of using penalty functions is discussed in Section 4.5. By augmenting the original economic objective function with the penalty term, the surface defined by the objective function and system constraints is changed. As the

figure illustrates, at very low values of the penalty, this effect is not too severe for the scenario. However, as the value of the penalty grows, the economic portion of the objective function degrades. Even at a penalty of $\beta = 10^{-3}$, the loss in profit is approximately \$20,000, which can accumulate quickly if the downtime scenario occurs frequently.

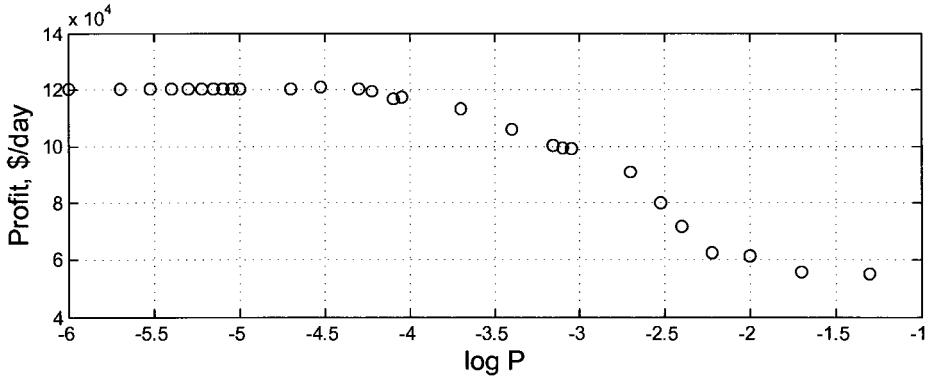

Figure 5.12: Degradation of Objective Value with Penalty

5.3.2 Dryer Shutdown

Perhaps the most common breakdown in the pulp and paper industry is a shutdown at the sheet-forming machine, which is directly linked with the pulp drying unit. This is, of course, detrimental to the profits realized for an operating period because no pulp is produced at all during the shutdown period.

Table 5.6 illustrates the dryer shutdowns considered. Figures 5.13 and 5.14 illustrate the importance of restoration time using Cases 19 and 21. These two cases have the same shutdown duration, but Case 21 has 6 additional hours of restoration time. When more restoration time is available (more degrees of freedom), the buffer capacities are better utilized to buffer the plant from the dryer failure. The adjacent bleach department is not required to shutdown in when eight hours of restoration time are

Table 5.6: Results for Machine/Dryer Department Failures

Case	Shutdown Duration (hrs)	Restoration Time (hrs)	Profit ($/day)	$\Sigma\Delta u^2$ (arbitrary)	CPU Time (seconds)
19	7	2	103,455	865,396	17
20	7	6	105,779	595,207	25
21	7	8	106,970	519,374	108
22	7	10	108,182	382,176	59
23	11	6	75,643	541,998	62
24	11	10	78,046	438,049	37

available, but must shutdown when two hours are specified. The reason for this is that at the end of the provided restoration period, the plant must be back to its initial state. When only two hours of restoration time are available, the Bleached Pulp Holdup cannot increase too far from its steady-state value, because it cannot return in time even if the dryer comes back online at its maximum production rate. Figure 5.13(c) illustrates this contrast where the bleached pulp buffer tank increases only slightly when the restoration period is only two hours long. Consequently, the bleach plant must be shutdown to maintain the constant level, as shown in Figure 5.13(b). Conversely, when eight hours of restoration time are available, the bleach tank can rise to its maximum level, and the bleach plant need not completely shutdown.

Figure 5.14 presents the response of several plant variables when very little restoration time is available, corresponding to Case 19. This situation probably would not arise in practice, where the plant has very little freedom to combat the failure. Since the preparation time is zero, and the restoration time is only two hours long, most of the operating departments must shutdown to ensure that the end-point constraints are met by the end of the restoration period. The outage in the drying department essentially specifies that all of the production departments will also slow down, and

subsequently shutdown. If the departments did not cease operation, the buffer levels would be left away from the nominal state since there is insufficient time to bring them back, even at maximum throughput rates.

5.4 Case Studies: Preemptive vs. Reactive

In Sections 5.2 and 5.3, scenarios involving planned maintenance shutdowns and unit failures were presented, respectively. In this section, we focus on an outage at the oxygen delignification department, and compare the preemptive (maintenance shutdown) and reactive (unit failure) scenarios. In both scenarios, we consider a seven-hour shutdown, followed by a three-hour restoration time. In the case of the planned maintenance shutdown, a five-hour preparation time is assumed. Figures 5.15, 5.16, and 5.17 illustrate the response of the plant to this type of shutdown. The shutdown at the O_2-delignification department is seen in Figure 5.15(e). During the unplanned shutdown sequence, the digester, bleaching, and drying departments must all drop production to low levels to ensure that buffer tanks do not empty, and that these tank volumes return to the steady-operating point by the end of the restoration time. This is seen in Figures 5.15(a), 5.16(b), and 5.16(d). The pre-emptive scenario, in contrast to the reactive scenario, also shows the expected trends in buffer capacities upstream and downstream of the O_2-delignification department. Intuitively, one would expect the upstream capacity to partially empty and the downstream capacity to partially fill. This is exactly what is observed in Figures 5.15(d) (upstream buffer tank) and 5.16(a) (downstream buffer tank). The evaporation and boiler systems are summarized in Figure 5.17. In both cases, the slow down at the various steam-consumption sites (digester, bleach plant, O_2 plant, and evaporators) requires a slow down in the boilers.

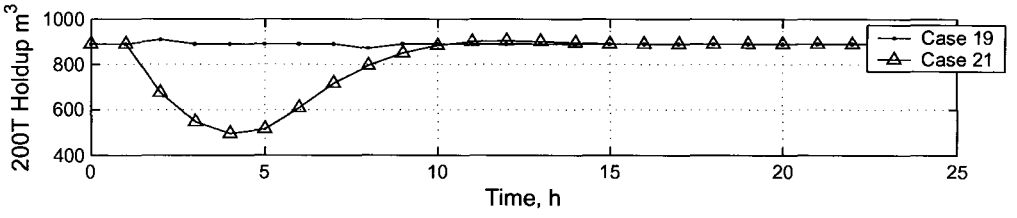

(a) 200T Holdup

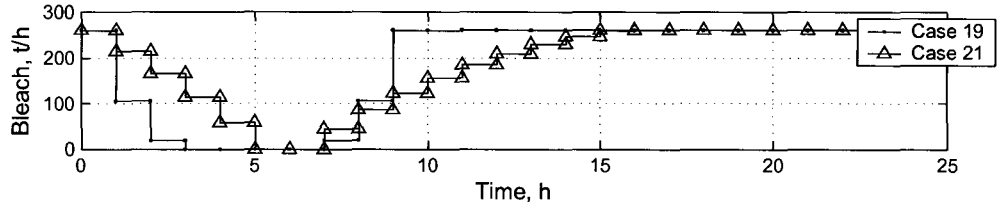

(b) Bleach Plant Production

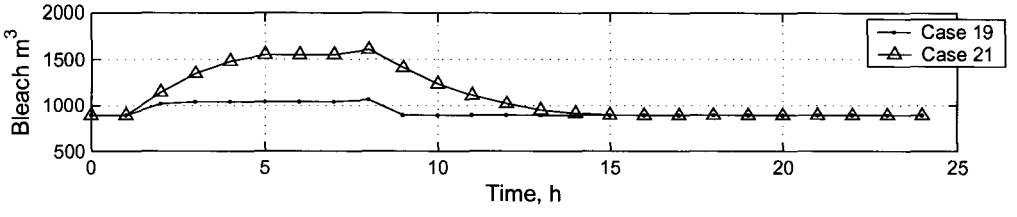

(c) Bleached Pulp Holdup

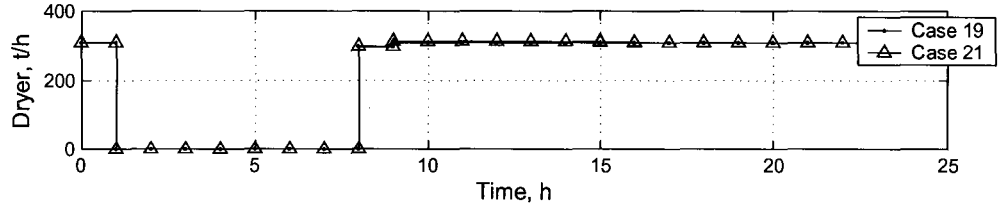

(d) Dryer Production

Figure 5.13: Response of Plant Variables to a Dryer Failure

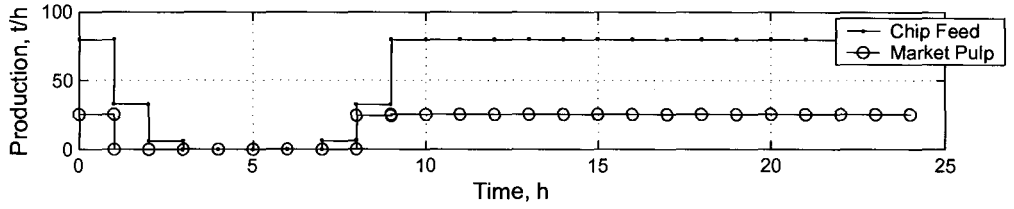

(a) Pulp Line Production

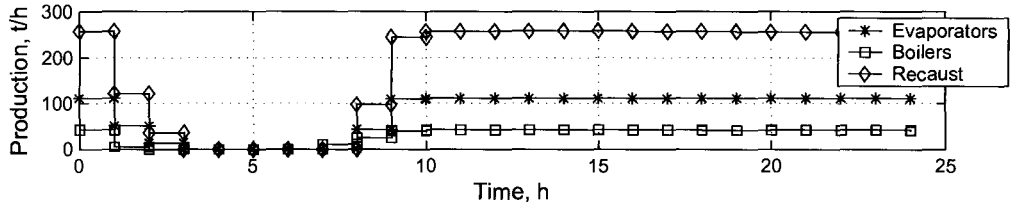

(b) Liquor Cycle Production

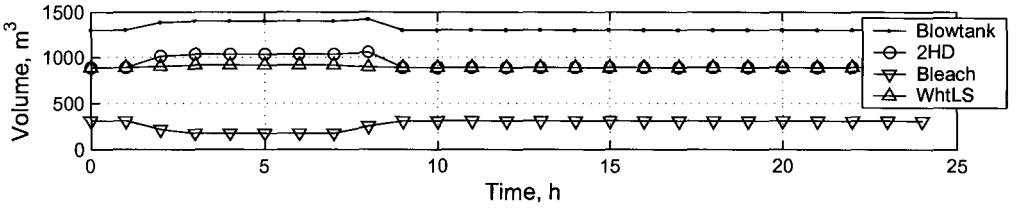

(c) Buffer Tank Holdups

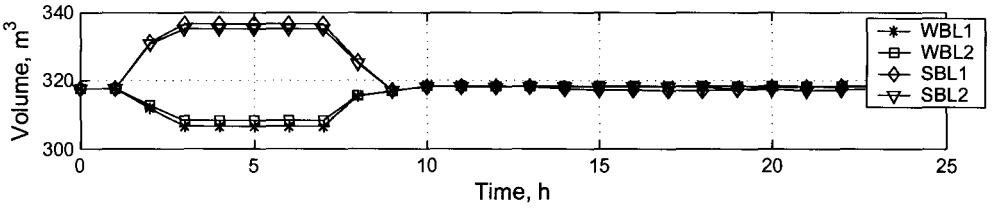

(d) Liquor Cycle Holdups

Figure 5.14: Response of Plant Variables to a Dryer Failure (Case 19)

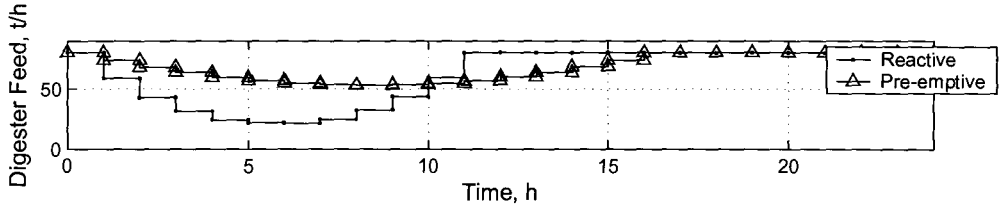

(a) Digester Feed

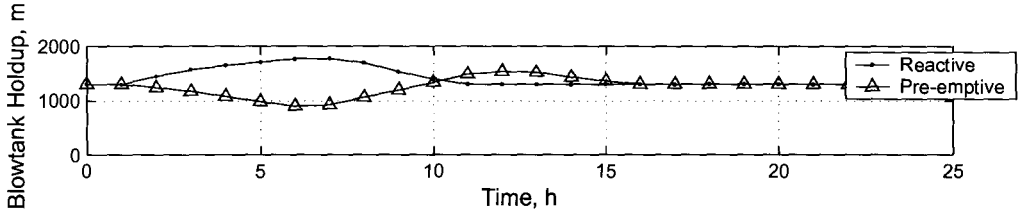

(b) Blowtank Volume

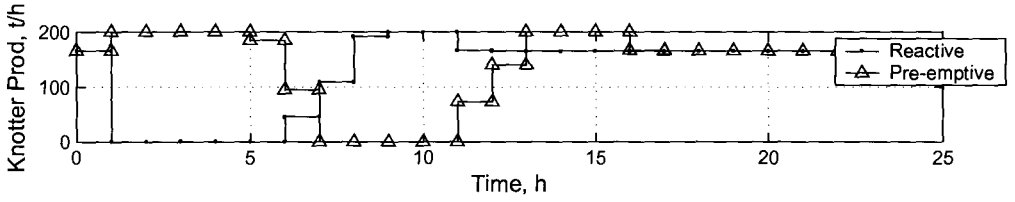

(c) Knotter Feed

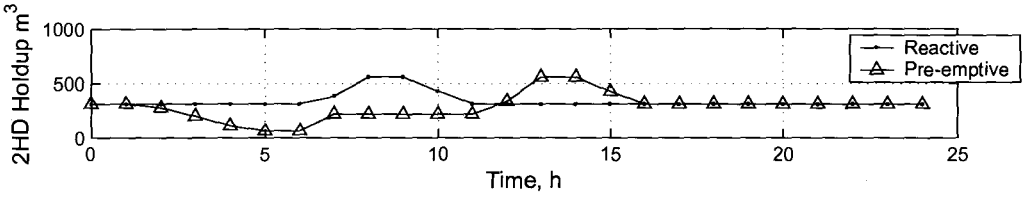

(d) 2HD volume

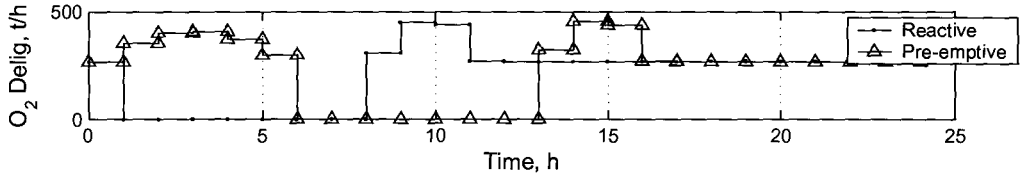

(e) O_2 Feed

Figure 5.15: Preemptive versus Reactive Scenarios for an Oxygen Delignification Outage

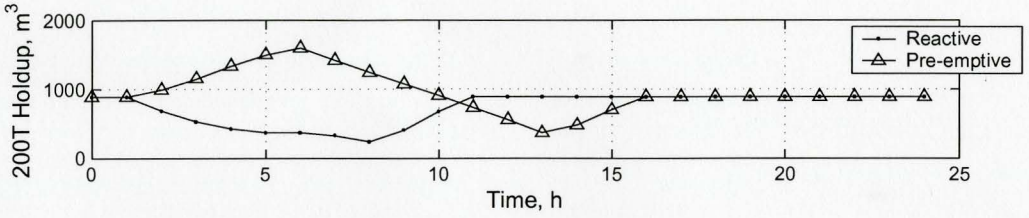

(a) 200T Volume

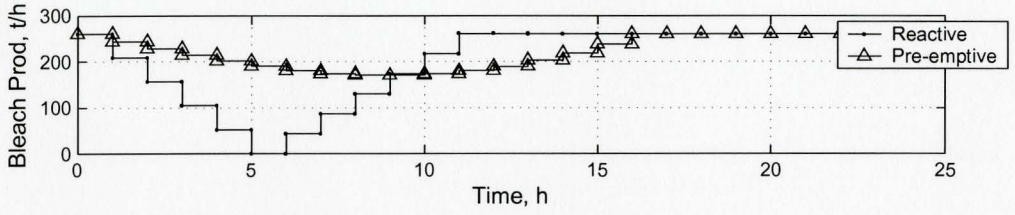

(b) Bleach Feed

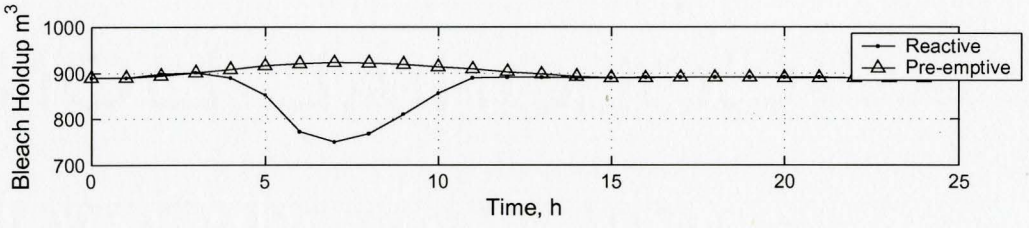

(c) Bleach Storage Volume

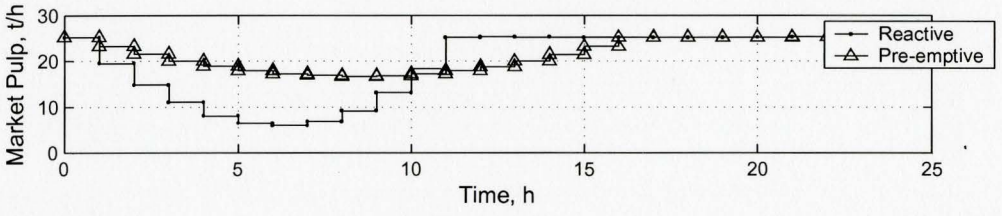

(d) Pulp Production

Figure 5.16: Preemptive versus Reactive Scenarios for an Oxygen Delignification Outage

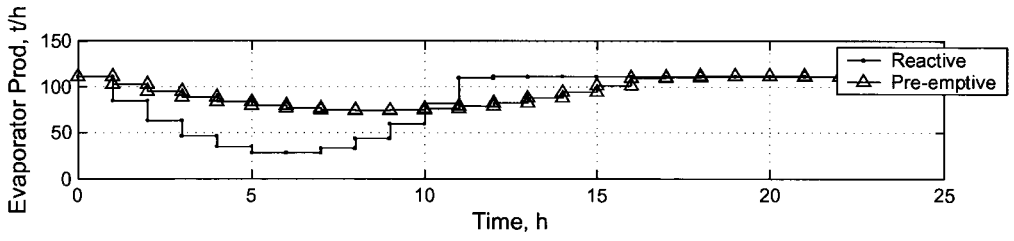

(a) Evaporator Production

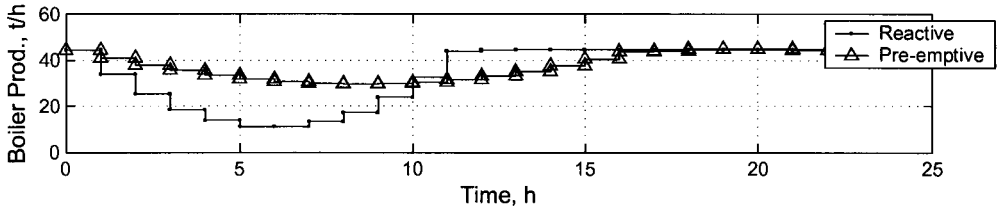

(b) Boiler Production

Figure 5.17: Preemptive versus Reactive Scenarios for an Oxygen Delignification Outage

5.5 Case Studies: Re-Optimization

In a true industrial setting, it is not likely that engineers and operators will know the exact length of either a scheduled or unscheduled shutdown. The studies described so far all assume that length of the shutdown is known exactly. Whether dealing with planned or unplanned scenarios, it is probable that the length of a unit shutdown will be different from the initial estimated downtime. Therefore, the failure-response scenarios can be optimized using an initial estimate of the downtime, and then re-optimized somewhere along the time-horizon using a re-estimation of the projected downtime. The initial values (of the operating variables) for the second optimization are those that define the operating point at the time when the re-estimation of the downtime is received (or when the re-optimization occurs).

Two possible situations exist, and they are as follows, where t_{est} is the estimated

shutdown length, and t_{real} is the true shutdown length:

$\mathbf{t_{est} \geq t_{real}}$ In this case, the shutdown time is overestimated, and operations are capable of resuming sooner than originally estimated. Options include:

Apply Initial Recipe The required maintenance would be completed, and the system would remain idle until the recipe directs appropriate input variables to return units back to steady-state. While this situation is feasible, it is clearly sub-optimal since production areas that have either slowed down or shutdown stay offline without producing pulp.

Re-Optimize Recipe At the time the re-estimated downtime is received, the system can be reoptimized such that units are brought back online in a co-ordinated fashion. This may results in a lower objective function value than if t_{real} was known a priori.

$\mathbf{t_{est} \leq t_{real}}$ In this case, the shutdown time is underestimated, and maintenance will be required for longer than originally estimated. Options include:

Apply Initial Recipe This option is infeasible. If original input trajectories were maintained, the shutdown department would begin receiving material from upstream storage capacities before it is ready to restart production.

Re-Optimize Recipe This scenario requires that the input trajectories be reoptimized and subsequently applied to the plant.

Therefore, as summarized above, an incorrect estimate of the shutdown duration leads to either an infeasible recipe in the case of an underestimated downtime, or a sub-optimal recipe in the case of an overestimated downtime. The following exploratory example, involving only two production departments separated by a single buffer capacity, illustrates some of the key issues. A modified digester, blowtank, and washing section is used for study. The goal of this small study is to illustrate the effects of

not knowing the shutdown length exactly, as well as ways to implement such a study in the computational environment. Note that these approaches can also be extended to address uncertain estimations in the preparation and restoration times.

5.5.1 Illustrating Example

SCENARIO: The subset of units is subject to a failure in the second unit. The initial estimated downtime is 8 hours; however, 6 hours into the shutdown, the shutdown length is extended to 10 hours. The allowable restoration time from the time of the end of the shutdown is 5 hours, at which the production rates and tank volume must return to the nominal operating point. The penalty-function formulation is used for this study.

Figure 5.18 illustrates three profiles for each of the variables of interest. The initial trajectories are smooth, and appear to be very much like those observed in the previous sections. For the first six-hours of the scenario, the initial and re-optimized trajectories are the same. However, the difference is of course after the downtime estimate is revised. After the re-estimation of the downtime length is received, the digester must be shutdown to maintain feasibility (end-point on blowtank volume). This is observed in Figure 5.18(a). Similarly, because of the reduced digester production, the washing section cannot ramp up quickly to catch up on production (Figure 5.18(c)). Because of the digester slow-down that is necessary to meet end-point constraints, production is lost and plant profit suffers.

The ideal trajectory in Figure 5.18 is that which would be followed had the true downtime length was known at the beginning of the failure. These trajectories, once again, characterize a smooth operation. Clearly, implementation of the initial trajectories would result in an infeasible situation because it prescribes the operation of the washing/screening operations prior to the true availability of these units.

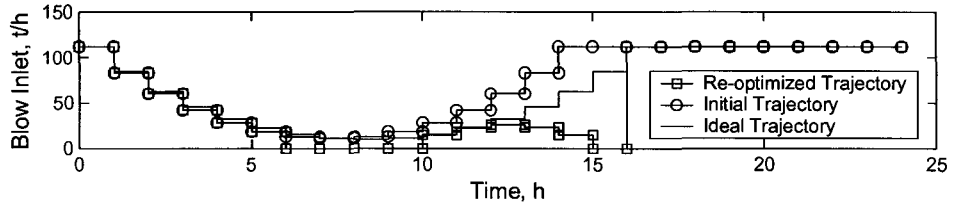

(a) Blowtank Inlet

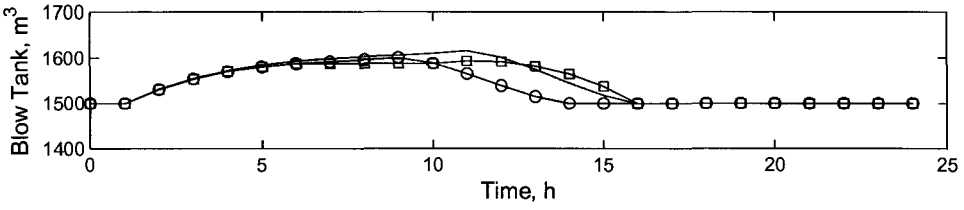

(b) Blowtank Holdup

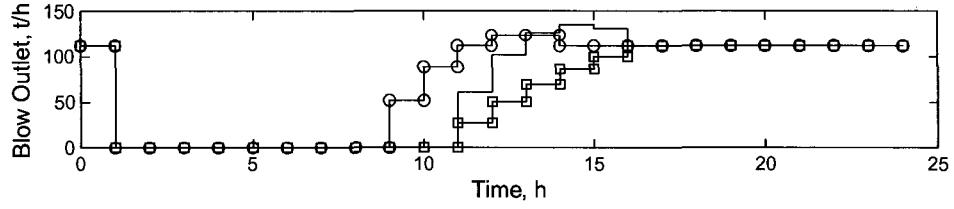

(c) Blowtank Inlet

Figure 5.18: Re-optimization after Downtime Re-estimation

5.6 Chapter Summary

This chapter has illustrated solutions for four common pulp mill failures. The key contributions and important considerations from these exercises are as follows:

- In Section 5.2, the benefit of preparation time was illustrated. When maintenance shutdowns are required to service equipment, the amount of preparation time will impact the plant profit. The main benefit is the ability to transfer buffer loads from upstream storage vessels to those downstream of the area to be shutdown. This leads to an operation that yields less variation in the production rates through the processing units. In Section 5.3, the impact of shutdown length and the lack of preparation time were illustrated. Longer shutdowns require more adjacent production areas to slow down and ultimately shutdown, to maintain feasibility in the optimization problem.

- To maintain both a smooth and economically favorable operation, it is desirable in all cases to coordinate all production departments in the event of a shutdown, either planned or unplanned. Mathematically, this was achieved through formulation of an optimization problem involving a profit-maximization objective as the first tier of the problem. The second tier involved moving along the hyperline that defined the maximum profit, to determine the minimum input usage. This was illustrated for all scenarios. In addition, the impact of alternate approaches including penalty and epsilon-constraint formulations were studied. The potential for over-constraining the problem, leading to sub-optimality was illustrated through a set of trade-off curves.

- Important constraints that must be incorporated into the model are the final tank levels after the failure has occurred. If the buffer levels are left lower or higher than the nominal value after a failure, the system may be incapable of rejecting subsequent disturbances.

Chapter 6

Optimization of Plant Design: Formulation and Solution

6.1 Introduction

As reviewed in Chapter 2 and repeated in Chapter 4, the overall formulation of the dynamic optimization problem involves the formulation of a constraint set involving the process inputs and process outputs, path and end-point constraints on these inputs and outputs, as well as the formulation of a meaningful objective function over which the process system is to be optimized. In this section, we extend the work from Chapter 5 to include design decisions. We analyze the process system using a parallel-model approach, and perform two different design studies. The first, involving only continuous variables, seeks the optimal steady-state buffer tank levels in addition to the optimal time-varying trajectories of the operating variables. The decision space of the second study includes those of the first study, as well as determining whether or not extra storage capacity would be beneficial at one of the existing buffer locations. The latter study results in a mixed-integer dynamic optimization problem.

6.2 Motivation

In many instances, surge tank levels are set to be around 50% as is the practice at several pulp and paper mills. The underlying assumption when using this approach is that the probability of the surge tanks having to empty (level decrease) is the same as the probability of it having to fill (level increase). This is, in practice, not true. The different production departments, and more specifically the individual processing units, will inevitably have varying levels of reliability. Issues such as varying equipment wear rates and differences in sensitivity to fluctuations in plant operation will lead to different reliability levels across production departments. For these reasons, it may not be appropriate to arbitrarily set the target surge tank levels at 50-60%, as commonly done in industry and in the literature [Dube [2000], Uronen *et al.* [1984] and Pettersson [1969]]. However, it is appropriate to gain an understanding of where the areas of low reliability exist in the plant, and determine the target steady-state surge tank levels accordingly. For example, consider the simple multi-unit processes depicted in Figure 6.1. Plant I and Plant II are identical in design, consisting of three pseudo-steady-state operating departments, separated by two intermediate buffer capacities. The key difference between Plant I and Plant II is in the reliability of production department 'B'. In Plant I, the reliability of each of the production departments is equal, and therefore, the frequency of failure on a normalized scale is 0.33. Stated another way, the probability of a failure in any of the three production departments is equal. This corresponds to the likelihood of the surge tanks having to fill or empty. Therefore, under the assumption that all failures carry the same economic cost, the surge tanks should be kept at 50% capacity. While the frequency distribution may be equal, if there is a difference in the relative economic impacts of the three possible failure scenarios, the steady-state surge tank levels would be adjusted accordingly. Conversely, in Plant II, the reliability of production department 'B' is inferior to those of production departments A or C. For example, the frequency

distribution may be such that it is twice as likely that there is a failure in production department B than it is in A or C. This corresponds to normalized frequencies of A=0.25, B=0.50, and C=0.25. Therefore, it is more likely that the first surge tank will need to fill rather than empty. Similarly, it is more likely that the the second surge tank will have to empty rather than fill. Once again, under the assumption that there is no difference in the relative economic impacts of the three failure types, the steady-state surge tank levels should be adjusted such that the plant is biased towards failures in production department B. Of course, in this hypothetical scenario, the assumption is that only one shutdown, and subsequent response and recovery, can occur at any given time.

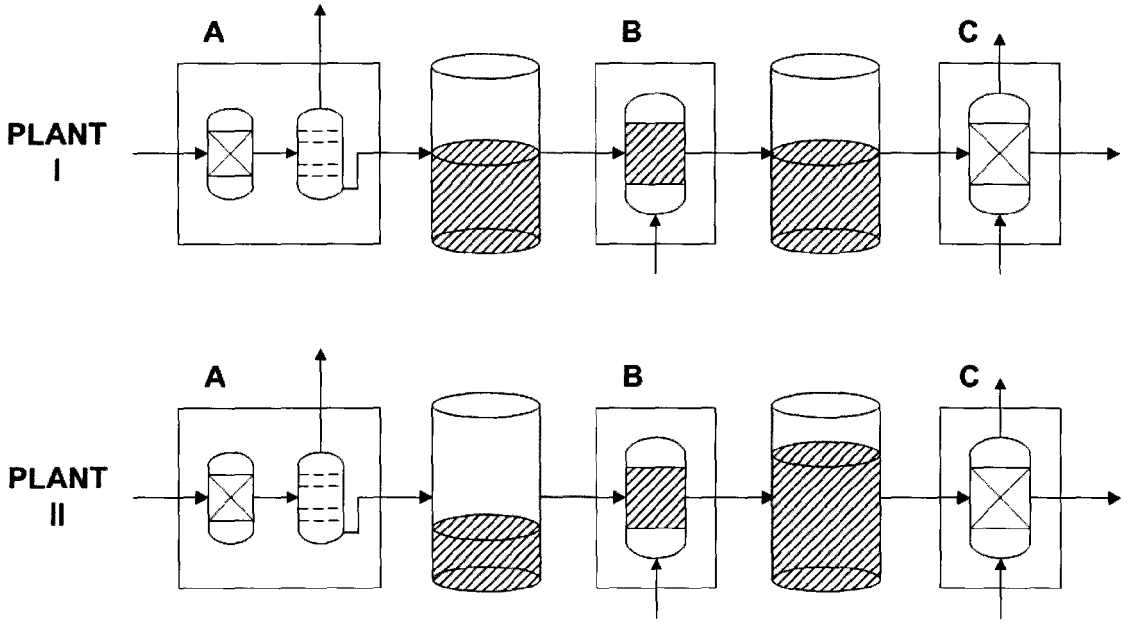

Figure 6.1: Reliability Example

These scenarios consider only the frequency distribution of the potential shutdown scenarios, without considering the economics of each scenario. For example, if a given failure scenario occurs at a very high frequency (say, everyday), but is accompanied by a negligible economic cost, it would have little bearing on the decision of what the nominal surge tank levels should be. This is why the economic impacts should be

considered.

6.2.1 Frequency of Disturbances

Downtime data were collected from an industrial partner for the period from 2000-2003. The downtime data were categorized into the most common shutdowns affecting the plant. Each category was then studied for a distribution in the lengths of the shutdowns. The nominal disturbance case was assumed to be the peak in this distribution of downtime lengths. Figure 6.2 illustrates a two-dimensional frequency table, where the types of shutdowns are listed as the rows, and the distribution of downtime-length is tabulated across each row. For the design case, only unplanned shutdowns were considered. For planned shutdowns, optimal storage levels can be achieved by preparing the plant during the period leading up to the shutdown. In other words, if sufficient preparation time is available, the operating point can be moved prior to the shutdown of equipment. In this study, we strive to determine the *nominal* operating point, with knowledge of the shutdown distribution a priori.

Once the frequency distribution was computed, the most common types/lengths of Kraft mill shutdowns were identified. These became the 'critical shutdown scenarios'. The issue illustrated by the frequency distribution is essentially a measure of the reliability of equipment, or groups of equipment, termed production departments. Differences in reliability upstream and downstream of storage capacities lead to the question of where target stock levels should be. For example, if an unreliable production department exists upstream of a storage capacity, the stock level should be kept fairly high. Therefore, in the event of a failure, the high inventory level can be used to keep downstream units running. Conversely, if an unreliable production department exists downstream of a storage capacity, the stock level should be kept fairly low to allow accumulation within in the event of a failure. The relative frequency of these

two events will aid in determining the nominal steady-state operating level.

For proper analysis, one must consider the entire plant for this study, due to the 'domino effect' and recycle effects that occurs when there is a failure within a pulp mill. When a plant failure occurs, adjacent production departments can be impacted immediately. As buffer capacities fill or empty to combat the disturbance (i.e., as constraints are hit during the time horizon), other units/departments are required to shutdown or at least slowdown. Moreover, due to strong interactions within a chemical plant due to recycle streams and reuse of process steams for energy transfer etc., otherwise distant production areas can be affected as well. For this reason, when computing optimal storage levels, one must consider the relative reliability of all departments within the plant, and not those that are just adjacent to the storage capacities themselves. It should be noted here that for the plant being investigated, the shutdowns that contribute the most to buffer tank design decisions are those that are adjacent to the buffer tank.

f_{11}	f_{12}	•	•	f_{1n}	•	•	f_{1N}
f_{21}	f_{22}						•
•		•					•
•			•				•
f_{n1}				f_{nn}			f_{nN}
•					•		•
•						•	•
f_{N1}	•	•	•	f_{Nn}	•	•	f_{NN}

Figure 6.2: Frequency Distribution of Downtimes

It is not difficult to understand that the bottlenecks during a transient event, such

as a unit failure or shutdown, are the intermediate storage capacities. Obviously, minimum throughput limitations on equipment limit the plant as well. However, these are ultimately limited by the amount of upstream inventory that is available when units further upstream have been shutdown. When a shutdown occurs, the tanks fulfill their true role as surge tanks. Surely, large capacities provide more time for the required maintenance to be performed, and to bring shutdown departments back online. Stated another way, larger storage capacities slow the above domino effect. However, larger tanks are limited by capital costs to implement them.

6.3 Formulation

Often times, it is the design decisions made during steady-state analysis that limit the operability of a chemical plant. These may relate to equipment sizing, target production rates, and the relationship between these. This chapter seeks to illustrate that steady-state design decisions can be inferior to those decisions made when accounting for the dynamic behaviour of the plant. Specifically, the dynamic behaviour of the plant is investigated as the system responds and recovers from a given set of failure scenarios. A technique that is used in the literature to compute optimal designs when accounting for dynamics, is the use of multiple plant models in the same optimization problem. This is sometimes referred to as scenario-based optimization [Abel and Marquardt, 2003]. The structures and parameter values of the parallel-models are identical. However, each model has its own set of state variables. The input forcing functions are also unique to each model, and are determined from the scenario being investigated. Of course, the design decisions are common to all of the models/scenarios. The set of scenarios chosen for study was not, and should not be arbitrary. To provide a meaningful study, the set of models and scenarios used to determine optimal designs were based on a distribution of downtimes, derived from

industrial downtime reports. The resulting matrix of failures allows one to isolate where the reliability issues exist in the plant being investigated, as described in Section 6.2.1. Once the set of scenarios of interest are determined, a parallel set-up of the models is prepared as shown in Figure 6.3. In the figure, there are N scenarios that have relative frequency weights, w_i and individual objective values, ϕ_i. The overall objective to the optimization problem, Φ will involve the weighted sum of the individual objectives.

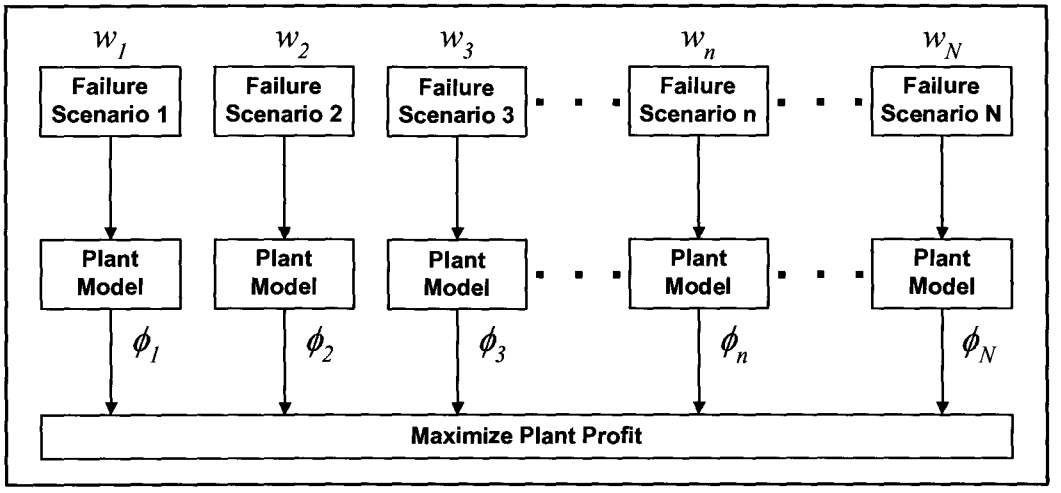

Figure 6.3: Parallel Model Strategy

As discussed in Section 6.1, two studies are of interest – one involving only continuous design decisions, and the second involving these and a binary design decision. The aspects that are common to both studies will first be presented, followed by a discussion of the items that are specific to each study. The overall formulation of the problem falls within the general formulation for dynamic optimization problems as presented in Chapter 2 and takes the following form which includes all parallel scenarios:

$$\max_{\mathbf{x^k}(t),\mathbf{u^k}(t),d} \phi(\mathbf{x^k}(t), \mathbf{u^k}(t), \mathbf{z^k}(t), \mathbf{p}, \mathbf{d}, t),$$

subject to

Model equations

$$\mathbf{0} = \mathbf{h}[\dot{\mathbf{x}}^{\mathbf{k}}(t), \mathbf{x}^{\mathbf{k}}(t), \mathbf{u}^{\mathbf{k}}(t), \mathbf{z}^{\mathbf{k}}(t), \mathbf{p}, \mathbf{d}, t]$$

$$\mathbf{0} = \mathbf{f}^{\mathbf{k}}[\mathbf{u}^{\mathbf{k}}(t)]$$

Path constraints

$$\mathbf{x}^{min} \leq \mathbf{x}^{\mathbf{k}}(t) \leq \mathbf{x}^{max}$$

$$\mathbf{u}^{min} \leq \mathbf{u}^{\mathbf{k}}(t) \leq \mathbf{u}^{max}$$

$$\mathbf{0} \leq \Delta\mathbf{u}^{\mathbf{k}}(t) \leq \Delta\mathbf{u}^{max}$$

End-point Constraints

$$\mathbf{x}^{\mathbf{k}}(t) = \mathbf{x}_0 \qquad \text{for } t > t_{end}$$

where the index k refers to the individual model/scenarios. The minimum and maximum bounds on the input and state variables are the same for all models. The end-point constraints are also the same for all models, as they are part of the design decisions common to all scenarios.

6.3.1 Issues: Study 1 - Optimal Operating Level

The first column of Table 6.1 summarizes the decisions to be made in Study 1. Steady-state production rates and other steady-state operating variables (for example, split fractions and chemical dosage rates) are assumed to be those described in Chapter 3. The only issue to be tackled, aside from the parallel-model formulation explained above and the general optimization formulation presented in Chapter 4, is the manner in which the overall objective function is computed.

The economic performance of each scenario is captured by an objective function, exactly as used in Chapter 5. These are then summed into one overall merit function.

However, to describe the relative importance of each scenario, the individual model objectives can be weighted using factors that correspond the the relative frequencies of the downtimes being considered. For example, an individual objective function is given generically as

$$\max_{F_{j,k}} \sum_{j=1}^{N} \sum_{k=1}^{t_f} c_j F_{j,k}, \tag{6.1}$$

where $F_{j,k}$ represents plant flow j at discrete time interval k, c_j is the economic coefficient associated with stream j, N is the total number of streams, and t_f is the time horizon. This is modified to

$$\max_{F_{i,j,k}} \sum_{i=1}^{M} \sum_{j=1}^{N} \sum_{k=1}^{t_f} w_i c_j F_{i,j,k}, \tag{6.2}$$

where w_i is the scenario weight based on the frequency distribution and M is the number of models being considered simultaneously. This is illustrated in Figure 6.3, where

$$\phi_i = \sum_{j=1}^{N} \sum_{k=1}^{t_f} c_j F_{j,k}. \tag{6.3}$$

For the design studies considered, feasibility is enforced for all failure scenarios. In the worst case, the optimizer may choose to shut the plant down, or at least sections of the plant. Based on the model and problem formulation, this is one feasible, but clearly sub-optimal solution, provided that the restoration time is sufficiently long for the end-point constraints to be met.

Table 6.1: Decision Variables for Design Studies

Study 1	Study 2
(1) Optimal trajectory of operating variables for each scenario.	(1) Optimal trajectory of operating variables for each scenario.
(2) Steady-state buffer-tank levels ($x(t_0) = x(t_f)$).	(2) Steady-state buffer-tank levels ($x(t_0) = x(t_f)$).
	(3) Location of additional storage.
	(4) Size of additional storage.

6.3.2 Issues: Study 2 - Optimal Placement of Capacity Addition

The second design study, involving the optimal placement of additional capacity is really an extension to the study involving only the optimal steady-state buffer levels. The second column of Table 6.1 summarizes the decisions to be made in Study 2. Once again, steady-state production rates and other steady-state operating variables (for example, split fractions and chemical dosage rates) are assumed to be those described in Chapter 3.

During transient events, plant performance can be improved by providing the plant a greater capability to buffer itself against transients caused by equipment failure, by increasing flexibility in the intermediate storage capacities. As discussed in Section 3.3.1, the tanks are not permitted to fill to capacity (V=100%), or run dry (V=0%). This is applied for safety and environmental reasons. Instead, the permissible volume range is given by

$$0.10\mathbf{V}_{max} \leq \mathbf{V} \leq 0.90\mathbf{V}_{max} \tag{6.4}$$

where $\mathbf{V}_{max}$ is the inner volume of the storage vessels. One option to achieve a small increase in flexibility is to relax these safety constraints. The benefit of employing this strategy is that it is purely a change in operating practice, carrying no economic penalty. However, safety and equipment protection are the motivating factors behind using these minimum and maximum constraints. Therefore, with safety and equipment protection issues paramount, relaxation of these constraints is not a viable option.

An alternate approach is to investigate the option of expanding buffer capacity in one or more locations throughout the plant. Naturally, this will involve some economic cost through the capital expenditure, as well as the cost incurred due to the downtime necessary to install the vessel and required infrastructure. However, these costs can be recovered through better handling of transient situations – the increased buffer capacity will lead to improved economics in times where additional storage would be beneficial. Therefore, two key issues exist that are unique to the second study. These are:

1. The treatment of integer variables in the optimization formulation.
2. The estimation of the capital cost of extra storage volume.

Treatment of Integer Variables

The amount of extra storage can be formulated as either a continuous or discrete variable in the optimization problem. The discrete formulation implies that the tank additions are available only in a finite number of sizes. For example, capacities may be available in volumes of 500 or 1000 m^3, but not available in sizes on the continuous range from 500–1000 m^3. The continuous formulation is the approach used in this study, and implies that tank additions are available in any size within a given range.

While no lower limit would normally exist, an upper limit on a volume addition may be due to the availability of plant property on which to build it. The assumed range of possible capacity addition is given by

$$0 \leq V_{add} \leq 1000, \tag{6.5}$$

where V_{add} is additional capacity purchased in m^3. The next key point in the formulation is the issue of *where* to add the capacity. Clearly, location is a discrete variable. The location of the additional capacity is assumed to be at one of the existing capacities, specifically, at one of the pulp tanks. In other words, this is a retrofit, in which one of the existing buffer tanks is to be expanded. Each location is deemed a candidate, y_l, in the optimization formulation, leading to a set of P candidate locations. The discrete constraint is given by

$$\sum_{l=1}^{P} y_l \leq 1 \tag{6.6}$$

which implies that if the economics are not favourable, the solution to the optimization problem can result in maintaining the plant flowsheet 'as is'. If economics are favourable, additional volume is to be added in, at most, one location. The actual implementation of these binary variables in the problem formulation is in constraints on the maximum tank volumes. Recall from the general formulation stated in Section 6.3, the tank volumes must obey the path constraint given by

$$\mathbf{x}^{min} \leq \mathbf{x}^{\mathbf{k}}(t) \leq \mathbf{x}^{max}.$$

The maximum limit is modified to include the potential volume addition, V_{add} and the binary decision variable, y_l. Given one of the buffer locations considered, l, the maximum allowable volume becomes

$$x_l^{max} = x_l^{max,nominal} + y_l V_{add}.$$

For convenience, it is assumed that the minimum constraint on volume, as well as the freeboard that is 10% of the nominal tank volume are maintained.

An alternate approach would be to pose a problem that involves the addition of a new vessel, as opposed to the expansion of an existing one. This would require a different formulation since it involves the introduction of additional dynamic equations. The integer variables would then be used to select the optimal location, as well as introduce or 'turn on' these required equations. The underlying assumption inherent in the formulation applied in this work (i.e., expansion of an existing buffer tank) is that the capital cost of the expansion is the same as the cost of purchasing a tank to be placed adjacent to the location chosen. The estimation of this capital cost is discussed in the next section.

Capital Cost Estimation

A flowsheet design or retrofit requires a modified objective function, so that the capital expenditure is included in the analysis. As described above, the problem postulated is to determine whether additional capacity would be beneficial where storage already exists. This is easily seen where the system hits capacity constraints in the operability scenarios in Chapter 5. Physically, these additions can be made to the existing physical structure. Alternatively, the additional tankage can be added adjacent to the existing storage capacity. In the chemical process industry, 'adjacent' may simply mean that the process flows from the main tank to that which is determined necessary by the optimization.

Table 6.2: Cost Estimation Data [Sinnott, 1993]

Data	Value	Units
S, Characteristic Size Parameter	50–8000	m^3
C, Cost Constant	1200	£
n, Equipment Index	0.55	–
M_f, Material Factor, Carbon Steel	1.0	–
P_f, Pressure Factor, Low Pressure	1.0	–
BM, Bare Module Factor	3.15	–

Sinnott [1993] provides a method for computing the purchased equipment cost. The equation required for the estimation is given by

$$C_e = CS^n(M_f)(P_f) \tag{6.7}$$

where C_e is the purchased equipment cost, S is a characteristic size parameter, C is a cost constant, n is the equipment index, M_f is the material factor, and P_f is the pressure factor. For storage tanks, Sinnott [1993] provides the required data, tabulated in Table 6.2.

Since carbon steel is assumed (M_f=1), and the storage tank is not required to act as a pressure vessel (P_f=1), Equation 6.7 reduces to 6.8, which includes the scale up for inflation and exchange from pounds to dollars. The exchange rates are based on those given by the Bank of Canada in the second quarter of 2005 (http://www.bankofcanada.ca). A 20% contractor and contingency allowance is assumed. The estimated equipment cost is therefore given by

$$C_e = CS^n(M_f)(P_f)\left(\frac{I_{2005}}{I_{1992}}\right)\left(\frac{\$2.265}{1£}\right) \times BM \times 1.20 \tag{6.8}$$

where $I_{2005} = 1233.2$ and $I_{1992} = 943.1$ are the cost indices for 2005 and 1992, respectively, which are used to adjust the cost for inflation. The indices used are the Marshall and Swift Equipment Cost Indices found in Zanetti [1994] and Chopey [2004]. Figure 6.4 illustrates the trend of capital cost with surge tank volume for the range of volumes that are appropriate for the estimation formula given in Equation 6.8.

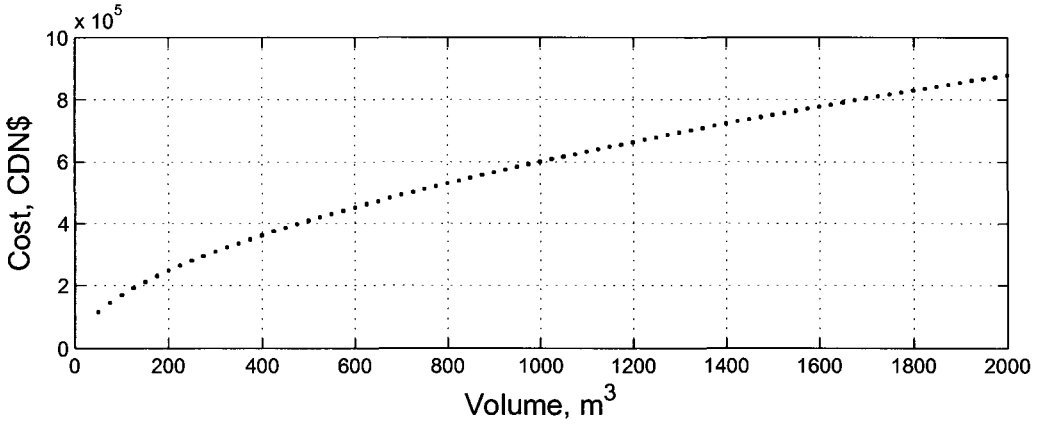

Figure 6.4: Cost of Surge Tank Addition

Revised Objective Function

Recall the objective function used for Study 1 (Equation 6.2), given by

$$\max_{F_{i,j,k}} \sum_{i=1}^{M}\sum_{j=1}^{N}\sum_{k=1}^{t_f} w_i c_j F_{i,j,k},$$

which represents the expected profit for a single operating day. The objective function for the MIDO problem will involve this expected profit function and the estimated

capital cost. In addition, a project life of $A = 30$ is and an absolute downtime frequency of 120 days/year are assumed. The latter is necessary to quantify the frequency at which any one of the scenarios would occur. These are the instances in which the added capacity would be utilized. During the remaining days of the operating year, the plant is assumed to be at steady-state, during which time the buffer capacities are assumed to be at a constant level. To account for the time value of money, a 14% interest rate is assumed. Based on tabulated values found in Park *et al.* [2001], a present worth factor, P was determined for use in the objective function. Assuming a project life of 30 years as stated above, and an interest rate of 14%, the present worth factor is $P = 7.0027$. Therefore, the revised objective function is given by

$$\Phi = (P+1) \times (120\ d/y) \left[\sum_{i=1}^{M} \sum_{j=1}^{N} \sum_{k=1}^{t_f} w_i c_j F_{i,j,k} \right] - \left[CS^n (M_f)(P_f) \left(\frac{I_{2005}}{I_{1992}} \right) \left(\frac{\$2.265}{1£} \right) \right], \tag{6.9}$$

where the first term includes the present worth factor, P, for years $n = 1$ to $n = 30$, plus the income at year zero.

6.3.3 GAMS Implementation

Each plant model in the multiple-model approach is used to mimic a realistic failure scenario. In the gPROMS environment, this is easily achieved by declaring an *array* of plant models. This study requires a similar approach in the GAMS environment, by adding an extra dimension to every plant variable. For example, $F_{j,k}$ may represent one flowrate variable at time interval k. This is sufficient for an optimization problem involving only one plant model. This approach was modified to include a second index, i, to represent the set of plant models/scenarios investigated simultaneously.

Table 6.3: Probability Distribution

Scenario #	Department	Failure Length (hrs)	Probability
1	Digester	8	0.09
2	Digester	12	0.09
3	Knotting/Washing	4	0.05
4	Knotting/Washing	8	0.05
5	Oxygen Delignification	4	0.09
6	Oxygen Delignification	8	0.09
7	Bleach Plant	9	0.10
8	Bleach Plant	13	0.10
9	Machine/Dryer	7	0.17
10	Machine/Dryer	11	0.17

Therefore, the flowrate variable above becomes $F_{i,j,k}$, and therefore if the original optimization problem involved P variables and Q equations, the multiple-model problem involves PM variables and QM equations. Every variable in the model is re-indexed as described here. Once again, MINOS and CONOPT2 were used for the computation of Study 1. The SBB solver was used for the MIDO problem (Study 2), with CONOPT2 used to solve the relaxed NLP problems at each node.

6.4 Case Studies: Optimal Designs

Table 6.3 identifies the relative frequency to be used in the design studies, which is approximately based on industrial downtime reports. It encompasses a short shutdown and a long shutdown for each department, which are assumed to occur at the same frequency.

For all scenarios stated above, a common restoration time of 9 hours was allowed. The scenarios were simulated in parallel, similar to the scenarios described in Section 6.3. Three separate optimization studies were postulated for which optimal control profiles and objective values were computed. These were:

(1) Nominal Case In this scenario, additional constraints were added to added to lock decisions on the steady-state level to their nominal values as applied in Chapter 5.

(2) Optimized Solution, no Capital Investment Optimized solution considering optimal steady-state buffer tank levels and operating variable trajectories.

(3) Optimized Solution with Capital Investment (MIDO) Optimized solution from (4) above, with added flexibility of capacity addition.

Table 6.4 describes the results from the optimization using parallel models. The three studies yield some interesting results. The nominal case serves as the baseline scenario for which to compare results. Study 1 illustrates the result for the steady-state levels, with no capital investment. The decision to keep the volume of the 2HD storage tank very low is not surprising. It is the smallest of the pulp tanks, and among the smallest storage vessels throughout the plant, and most of the plant is downstream. Therefore, with the majority of the failure distribution in downstream production departments, it is optimal to keep this stock level low. Moreover, its proximity to the digester makes it available to accumulate the maximum amount of pulp without causing premature outages at the digester.

Study 2 illustrates the optimization results found when capital investment is permitted. Because the storage is only permissible in one location, the mixed-integer formulation described in Section 6.3.2 is applied. The option of merely replacing the unreliable equipment (i.e., instead of purchasing additional storage) is not considered in this case.

Table 6.4: Results for Design Problems

	Constraints		Steady-State Levels		
Tank	Minimum (m^3)	Maximum (m^3)	(1) Nominal (m^3)	(2) Study 1 (m^3)	(3) Study 2 (m^3)
Blowtank	205	1845	1025	1460	1129
2HD	62	558	310	180	205**
200T	178	1602	890	392	516
1HD	178	1602	890	1285	1269
Obj. ($/day)	—	—	99,598	104,974	107,818
CPU Time	—	—	—	44.34 min	79.21 min

** = site of capacity addition

While the stock level in the 2HD tank is kept low, the upper constraint remains a limiting factor, and therefore this is the location of the capital investment, as indicated by the asterisks in Table 6.4. This is not surprising as it is very small relative to the other three pulp tanks. The capital outlay, using Equation 6.8 is $375,043, based on an addition of 389 m^3 of tank volume.

Figures 6.5 and 6.6 illustrate the limiting cases for the two optimization studies. The most critical scenarios are those where the downtime is very long, namely scenarios 2, 4, 8, and 10 from Table 6.3. The two scenarios that contribute to the 2HD buffer being the critical storage location are the 8-hour outage at the knotting/washing department and the 8-hour outage at the oxygen delignification department. These are used in the following illustration. Please refer to Figure 3.1 to clarify the location of the various buffer capacities. Figure 6.5 illustrates the results for Study 1. During the knotting/washing shutdown, the 2HD buffer capacity (downstream of outage) empties in an attempt to keep the pulping line running. Conversely, during the

oxygen delignification outage, the 2HD capacity (upstream of outage) must fill to minimize shutdowns upstream (Figure 6.5(b)). As reviewed in Chapter 5, shuts at the digester cripple the plant, and lead to very poor economics. Because the 2HD tank is very small, shutdowns upstream of it quickly impact the downstream areas, and vice versa. This is seen in Figures 6.5(a) and (c), where either failure requires a shutdown on the other side of the buffer storage to properly reject the failure and obey end-point constraints. Figure 6.5(b) illustrates the limitations at constraints for the case in which only optimal steady-state buffer levels are computed. This is especially true at the upper bound, where the capacity is attempting to buffer the washing/knotting section and more importantly, the digester, from the downstream shutdown at the oxygen delignification department.

Figure 6.6(b) illustrates the availability of extra storage capacity. Therefore, during the time horizon, the new upper bound on the storage is contacted only for one point in time, and then the volume returns to the revised steady-state level to obey the end-point constraints. The previous upper bound is illustrated by the dotted line in Figure 6.6(b). The availability of the extra capacity allows the knotting department to ramp up faster than the previous case (Figure 6.5(a) versus Figure 6.6(a)), and maintain higher production rates. The higher throughput is required to maximize production, and bring the blowtank level down to obey end-point constraints. Downstream of the extra storage capacity, the difference in the production profile is that it can operate at slightly higher levels during the transients. This is observed for the oxygen delignification and bleaching departments, which operate at the high throughputs during the restoration period (Figures 6.6(c)-(d)). This is in contrast to the varying throughputs through these areas in the case without capacity addition, Study 1 (Figures 6.5(c)-(d)). Ultimately, this results in a higher market pulp output as illustrated in Figure 6.6(e), as compared to the lower throughput seen in Figure 6.5(e), for the oxygen delignification failure.

Under the conditions considered, the economics of the capital-expenditure problem are very attractive – the potential profit increase from the addition based on the postulated scenarios is quite substantial, relative to the cost of the equipment.

6.5 Chapter Summary

This chapter has provided a framework in which one can utilize a parallel plant-model scheme to compute optimal steady-state operating points alone, or together with flowsheet design changes. It was shown that through careful capital cost-estimation and use of a frequency distribution of shutdowns, potential plant improvements can be computed through use of multiple models, yielding improved operating profits.

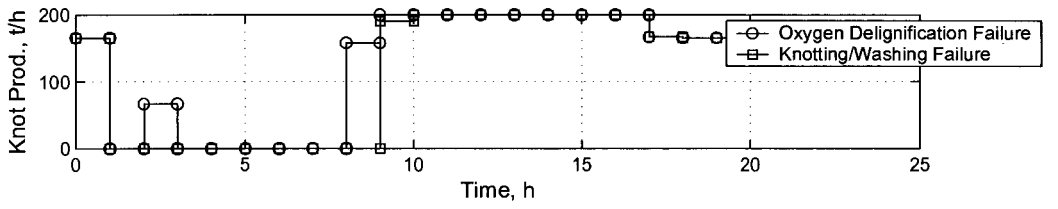

(a) Knot/Wash Production

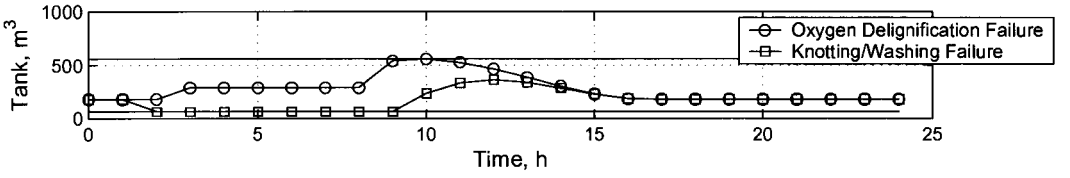

(b) 2HD Holdup

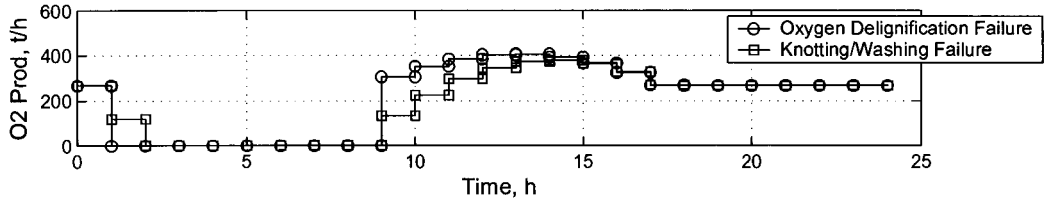

(c) O2 Delig Prod.

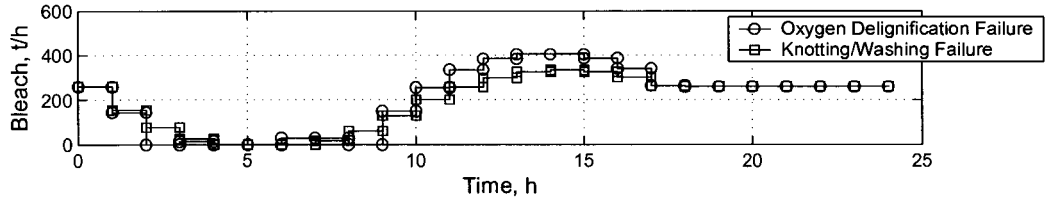

(d) Bleach Prod.

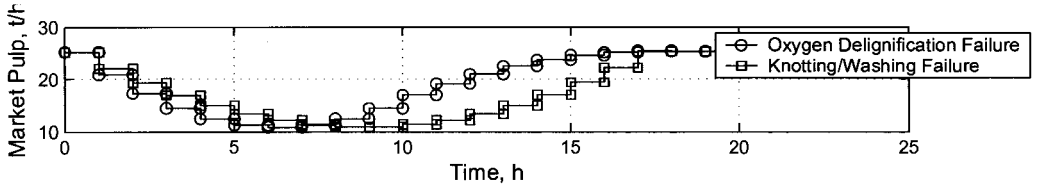

(e) Market Pulp

Figure 6.5: Limiting Cases - No Capacity Addition

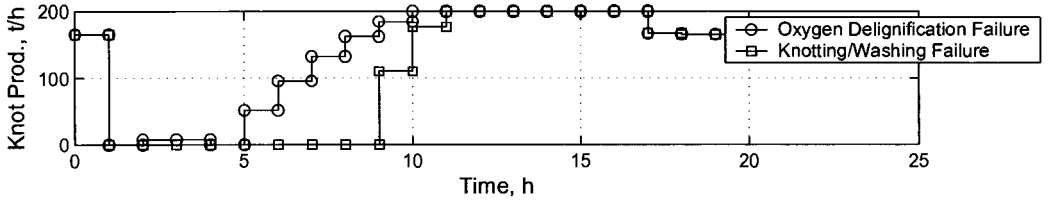

(a) Knot/Wash Production

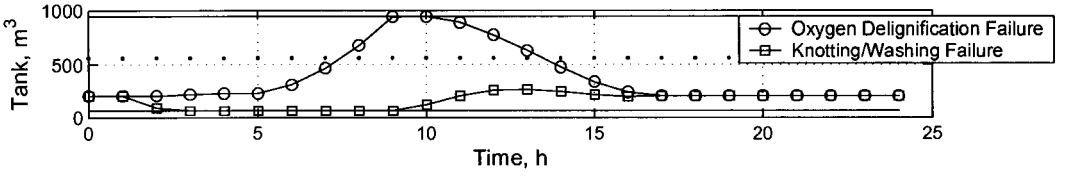

(b) 2HD Holdup

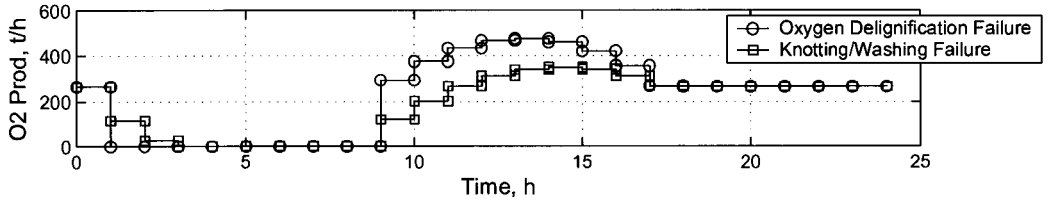

(c) O2 Delig Prod.

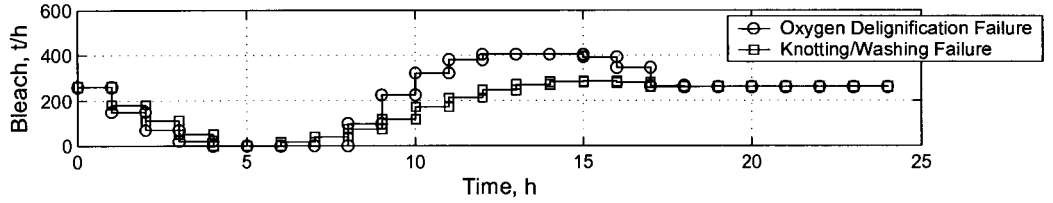

(d) Bleach Prod.

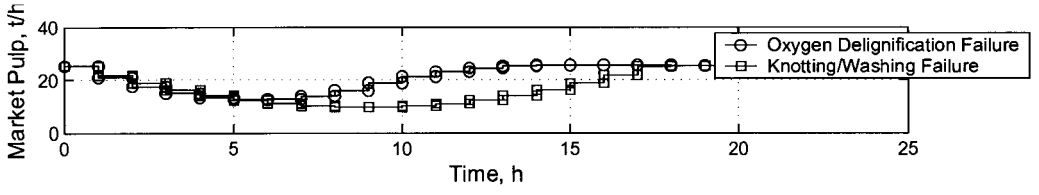

(e) Market Pulp

Figure 6.6: Limiting Cases - Capacity Addition

Chapter 7

Conclusions and Recommendations

7.1 Conclusions

The formulation of an optimization problem involving a multiple-unit system with inventory dynamics was described and implemented in this work. Investigation of the impacts of transient events such as scheduled versus unscheduled shutdowns was illustrated through several case studies. The contribution of preparation time, shutdown duration, and available restoration time to the solution of many of the scenarios is also illustrated, as were the effects of end-point constraints.

Key findings from this work include:

1. When the plant is provided with knowledge of a shutdown prior to the outage, the preparation time is beneficial in improving plant economics. This is especially important when studying long shutdowns. This preparation time allows the plant to move operating rates and storage tank levels to more advantageous points within the operating window to best buffer the plant from the outage.

2. Naturally, as the shutdown duration increases, the economic objective degrades whether the shutdown was was planned or unplanned. The increased availability of preparation or restoration time helps to minimize the economic impact of this situation.

3. The restoration time is another important time variable considered in this studied. The restoration time has two related contributions to the system. First, it allows areas of the plant to come back online and 'catch-up' on some of the lost production. Secondly, the increased amount of freedom (in terms of control intervals) allows some departments to spread the loss of production across the time horizon, avoiding the shutdown of more sections of the plant.

4. A short investigation into the effect of an uncertain shutdown length is investigated. Re-optimization based on re-estimations of downtime length are necessary to maintain feasibility, and improve economics. It is shown that economics and operability are both improved if the downtime estimate is known exactly.

5. Through the use of probability distributions of the most common shutdowns to hit each of the sections, a parallel-model was developed and used to determine both optimal steady-state buffer tank operating levels. Through extension of this to a mixed-integer dynamic optimization problem, the additional decision of where best to implement additional storage volumes, as well as the size of that addition, was determined. The result was not surprising, based on the assumed design of the nominal plant.

When studying systems involving many degrees of freedom, the presence of non-unique optima is possible, as is the case with ill-conditioned MPC systems. In these cases, there may be a variety of input combinations that yield the same objective value, while obeying system constraints. The ill-conditioning can also lead to erratic

plant movement. While the primary focus in this study was on plant economics, and equally important aspect in any process system is to develop a control strategy that promotes a smooth operation, even in the face of changing plant conditions. A two-tiered optimization method, focusing first on economics and then operability, was developed and used for all case studies presented in this work.

7.2 Recommended Future Work

This section provides some interesting avenues of research, which serve as extensions to this work.

7.2.1 Addition of Controller Dynamics

For the studies that have been completed, the plant is assumed to operate under open-loop optimal control. Also, regarding the trajectories of flowrates between units, all steps are assumed to be perfect. An interesting addition would be to consider PI or constrained model predictive control loops around some of the process equipment. The addition of these control will change the dynamics of the plant, and will therefore impact the optimal dynamic response to a plant failure.

7.2.2 Optimization with State Estimation

In order to compute the optimal trajectory of the critical plant variables during a failure scenarios, it is necessary to have accurate knowledge of their values. However, often times in a plant setting, one of the following situations can arise:

1. Poor measurement due to sensor failure, or failure in signal transmission

2. Multi-rate system in which some variables are sampled more often than others. For example, lab tests on pulp viscosity or Kappa number will be available much less frequently than temperature or consistency data.

3. There may be no direct measurement for a variable (such as Kappa Number). Related to the previous point, this data is then dependent on the sampling rate of the variables used to observe the unmeasured quality variable.

To overcome these situations, some variables may require estimation based on data that is readily available. State estimation ideas can be applied in these cases.

7.2.3 Oxygen Delignification Model

The fundamental model used for the oxygen delignification can be extended and used in a control system design study. Preliminary work has included the validation of the model against published industrial data. The application of linear model predictive control on both the nonlinear system, as well as a linearized model, have been studied [Soliman *et al.*, 2004]. The model was developed in a SIMULINK/MATLAB framework, and should be converted to a GAMS or gPROMS/gOPT for studies involving optimization. Set point optimization and control structure selection would be interesting issues to address. Similar studies have already been completed for the fundamental digester model used in this work. The connection of the above to this thesis is to investigate the impact of failures of a different type – these are those in the control systems.

7.2.4 Alternate Models for Storage Capacities

With respect to the intermediate storage capacities, there may be alternate methods of modelling the dynamic behavior within the tanks. The present model assumes

perfectly mixed storage tanks for all capacities. In other words, the storage tanks have been modelled as stirred-tanks, which assumes perfect axial mixing. However, it has been suggested that the tanks may be better modelled as plug flow vessels, because the assumption of axial mixing may not be valid at slower throughputs. This can be improved by implementing spatial dynamics in the formulation, or assume a tanks-in-series approach to approximate plug-flow behaviour.

7.2.5 Cogeneration and Discontinuous Costs

One aspect neglected in the objective function used in this study is the possibility of contributing electrical energy to the public grid. In addition, when failures occur, liquor shortage often results. When oil and gas prices are too high, resulting in a situation where it it unattractive to produce electricity in-house, power must be purchased from the grid. The issue of peak-demand pricing should be addressed. This is a situation in which a consumer of electricity is charged a premium when the usage over some period of time passes a threshold. This premium is applied to the total consumption, and not on the increment above the threshold. This leads to a discontinuity in the price that may be included in the objective function.

List of References

ABEL, O. AND MARQUARDT, W. (2003). Scenario-integrated on-line optimisation of batch reactors. *Journal of Process Control*, **13**, 703–715.

AGARWAL, S., COLE, B., GENCO, J., AND MILLER, W. (1998). Medium Consistency Oxygen Delignification Kinetics and Tower Design. *AIChE Symposium Series*, **94**(319), 32.

ALLISON, B. (2004). Averaging Level control for Surge Tanks in Series. In *Control Systems Conference*, pp. 159–167. Technical Association of the Pulp and Paper Industry Press.

ARMAOU, A. AND CHRISTOFIDES, P. D. (2002). Dynamic Optimization of dissipative PDE systems using nonlinear order reduction. *Chemical Engineering Science*, **57**, 5083–5114.

BANSAL, V., PERKINS, J. D., AND PISTIKOPOULOS, E. N. (2002). A Case Study in Siumltaneous Design and Control Using Rigorous, Mixed-Integer Dynamic Optimization Models. *Industrial and Engineering Chemistry Research*, **41**(4), 760–778.

BARLOW, R. AND HUNTER, L. (1960). Optimum Preventative Maintenance Policies. *Operations Research*, **8**, 90–100.

BARROSO, J., BARRERAS, F., AMAVEDA, H., AND LOZANO, A. (2003). On the optimization of boiler efficiency using bagasse as a fuel. *Fuel*, **82**, 1451–1463.

BIEGLER, L. T., CERVANTES, A. M., AND WÄCHTER, A. (2002). Advances in simultaneous strategies for dynamic process optimization. *Chemical Engineering Science*, **57**, 575–593.

CERVANTES, A. AND BIEGLER, L. T. (2001). Optimization Strategies for Dynamic Systems. In Floudas, C. A. and Pardalos, P. M. (Eds.), *Encyclopedia of Optimization*, Vol. 4, pp. 216–227. Kluwer Academic Publishers.

CHAPRA, S. C. AND CANALE, R. P. (1998). *Numerical Methods for Engineers.* McGraw-Hill, New York.

CHOPEY, N. P. (2004). Economic Indicators. *Chemical Engineering*, **111**(2), 79–80.

DEDOPOULOS, I. AND SHAH, N. (1996). Long-term maintenance poloicy optimization in multipurpose process plants. *Chemical Engineering Research & Design*, **74**, 307–320.

DUBE, J.-F. H. (2000). Pulp Mill Scheduling - Optimal Use of Storage Volumes to Maximize Production. Master's Thesis, McMaster University.

FAUCONNIER, W. (1993). Peak Load Control for a pulp and paper mill. *Pulp and Paper Canada*, **94**(11), 56–59.

FLOUDAS, C. A. (1995). *Nonlinear and Mixed-Integer Optimization.* Oxford University Press, New York.

GANI, R. AND GRANCHAROVA, A. (1997). Dynamic Optimization of Differential-Algebraic Systems Through teh Dynamic Simulator DYNSIM. *Computers and Chemical Engineering*, **21**, S727–S732.

GEANKOPLIS, C. J. (2003). *Transport Processes and Unit Operations.* Prentice-Hall, Inc., New Jersey, fourth edition.

GEORGIADIS, M., SCHENK, M., PISTIKOPOULOS, E., AND GANI, R. (2002). The interactions of design, control and operability in reactive distillation systems. *Computers and Chemical Engineering*, **26**, 735–746.

GRACE, T. M., LEOPOLD, B., AND MALCOLM, E. W. (1989). *Pulp and Paper Manufacture - Alkaline Pulping*, Vol. 5. The Joint Texbook Committee of the Paper Industry, Montreal, Quebec, Canada, third edition.

GROSSMAN, I. AND MORARI, M. (1983). Operability, Resiliency and Flexibility – Process Design Objective for a Changing World. In *Proceedings of the Second Inernational Conference on Foundations of Computer-Aided Process Design*, pp. 931–1030.

GÜMÜŞ, Z. H. AND FLOUDAS, C. A. (2001). Global Optimization of Nonlinear Bilevel Programming Problems. *Journal of Global Optimization*, **20**, 1–31.

INCROPERA, F. P. AND DEWITT, D. P. (1996). *Fundamentals of Heat and Mass Transfer, 3rd Edition.* John Wiley & Sons, Inc.

IRIBARNE, J. AND SCHROEDER, L. (1997). High-Pressure Oxygen Delignification of Kraft Pulps. *Tappi Journal*, **80**(10), 241.

KAYIHAN, F. (1997). Process systems managment in the pulp and paper industries: An optimization approach. *Pulp and Paper Canada*, **98**(8), 37–40.

KAYIHAN, F., GELORMINO, M. S., HANCZYC, E. M., DOYLE, F. J., AND ARKUN, Y. (30 June - 5 July, 1996). A Kaymyr Continuous Digester Model for Identification and Control. *13th IFAC World Congress, San Francisco*, **1**, 999.

KEMPE, M. J. (1995). Dynamic Modelling of a Vacuum Drum Washing System. Master's Thesis, McMaster University.

LASSLETT, N. (2000). Production Sheduling for Pulp Mills. In *Control Systems Conference*, pp. 53–57. Technical Association of the Pulp and Paper Industry Press.

LEIVISKÄ, K., AURASMAA, H., AND URONEN, P. (1979). The premises for a computer-based production control system of a sulphate pulp mill. *Computers and Chemical Engineering*, **3**(4), 575–579.

LEIVISKÄ, K., JUTILA, E., URONEN, P., AND SAKARI, H. (1980). Production Control of Complex Integrated Mills. *Computers In Industry*, **1**(4), 225–233.

MOHIDEEN, M. J., PERKINS, J. D., AND PISTIKOPOULOS, E. N. (1996). Optimal Design of Dynamic Systems under Uncertainty. *AIChE Journal*, **42**(8), 2251–2272.

MYERS, M. AND EDWARDS, L. (1989). Development and Verification of a Predicitive Oxygen Delignification Model for Hardwood and Softwood Kraft Pulp. *Tappi Journal*, **72**(9), 215.

NILSSON, K. AND SÖDERSTRÖM, M. (1992). Optimizing the operating strategy of a pulp and paper mill using the mind method. *Energy*, **17**(10), 945–953.

PARK, C. S., PELOT, R., PORTEOUS, K. C., AND ZUO, M. J. (2001). *Contemporary Engineering Economics, Second Canadian Edition.* Pearson Edulcation Canada Inc., Toronto.

PERRY, R. H. AND GREEN, D. W. (1997). *Perry's Chemical Engineers' Handbook.* McGraw-Hill, New York, seventh edition.

PETTERSSON, B. (1969). Production Control of a Complex Integrated Pulp and Paper Mill. *Tappi Journal*, **52**(11), 2155–2159.

PETTERSSON, B. (1970). Optimal Production Schemes Coordinating Subprocesses in a Complex Integrated Pulp and Paper Mill. *Pulp and Paper Canada*, **71**(5), 59–63.

PISTIKOPOULOS, E. N. AND SAKIZLIS, V. (2001). Simultaneous Design & Control Optimization under Uncertainty in Reaction/Separation Systems. In *Chemical Process Control 6, January 7–12, Tuscon, Arizona*, pp. 223–238.

PISTIKOPOULOS, E. N., VASSILIADIS, C. G., AND PAPAGEORGIOU, L. G. (2000). Process design for maintainability: an optimization approach. *Computers and Chemical Engineering*, **24**, 203–208.

PULKKINEN, P. (2004). Designing operator decision support system for TMP production-based on dynamic simulation and optimization. In *Control Systems Conference*, pp. 215–218. Technical Association of the Pulp and Paper Industry Press.

QIN, S. AND BADGWELL, T. (2003). A Survey of Industrial Model Predictive Control Technology. *Control Engineering Practice*, **11**(7), 733–764.

RAY, A. K. AND SINGH, P. (2000). Simulation of Multiple Effect Evaporator for Black Liquor Concentration. *Quarterly Journal of Indian Pulp and Paper Technical Association*, **12**(3), 53–63.

ROSS, R., PERKINS, J., PISTIKOPOULOS, E., KOOT, G., AND VAN SCHIJNDEL, J. (2001). Optimal design and control of a high-purity industrial distillation system. *Computers and Chemical Engineering*, **25**, 141–150.

RUIZ, J., MURATORE, E., AYRAL, A., AND DURAND, D. (1990). Kraft pulp and paper mill production managment with Optimill. *Pulp and Paper Canada*, **91**(4), 54–58.

SAKUMA, S., IWASE, H., AND SOTOBAYASHI, H. (1987). High-Consistency Oxygen Bleaching with Low Purity Oxygen. In *TAPPI Proceedings, International Oxygen Delignification Conference.*

SANMARTI, E., ESPUNA, A., AND PUIGIANER, L. (1997). Batch production and preventative maintenance scheduling under equipment failure uncertainty. *Computers and Chemical Engineering*, **21**, 1157–1168.

SARIMVEIS, H., ANGELOU, A., RETSINA, T., RUTHERFORD, S., AND BAFAS, G. (2003). Optimal energy management in pulp and paper mills. *Energy Conversion and Management*, **44**, 1707–1718.

SCHWEIGER, C. A. AND FLOUDAS, C. A. (1998). Interactions of Design and Control: Optimization with Dynamic Models. In *Optimal Control: Theory, Algorithms, and Applications*, pp. 388–435. Kluwer Academic Publishers.

SINNOTT, R. (1993). *Chemical Engineering Design*, Vol. 6. Butterworth-Heinemann Ltd., Oxford, second edition.

SMOOK, G. A. (1992). *Handbook for Pulp & Paper Technologists, 2nd Edition.* Angus Wilde Publications.

SNOW, C. A. AND REALFF, M. J. (1998). Mill steam and power optimization in a real-time pricing environment. *Tappi Journal*, **81**(12), 142–151.

SOLIMAN, M., BALTHAZAAR, A. K. S., AND SWARTZ, C. (2004). Modeling and Model-Based Control of an Oxygen Delignification Unit. In *Control Systems 2004 Conference Preprints*, pp. 87–90. Technical Association of the Pulp and Paper Industry Press.

TATSUISHI, H., HATANO, T., IWAI, T., AND KOVASIN, K. (1987). Practical Experiences of Medium-Consistency Oxygen Delignification by Rauma-Repola and Sumitomo Heavy Industries. In *TAPPI Proceedings, International Oxygen Delignification Conference.*

THAMARAISELVAN, P. AND SIVALINGAM, A. (2003). Optimization of Steam Economy in Multiple Effect Evaporator. *Quarterly Journal of Indian Pulp and Paper Technical Association*, **15**(4), 69–78.

URONEN, P., LEIVISKÄ, K., AND POIKELA, T. (1984). Economic Justification of Production Control Systems. *Pulp and Paper Canada*, **85**(9), 36–38.

VASSILIADIS, C. G. AND PISTIKOPOULOS, E. N. (2001). Maintenance scheudling and process optimization under uncertainty. *Computers and Chemical Engineering*, **25**, 217–236.

VICENTE, L. AND CALAMAI, P. (1994). Bilevel and Multilevel Programming: A bibliography review. *Journal of Global Optimization*, **20**, 2–31.

VISWANATHAN, J. AND GROSSMAN, I. (1990). A combined Penalty Function and Outer Approximation Method for MINLP Optimization. *Computers and Chemical Engineering*, **14**, 769–782.

WANG, R., TESSIER, P., AND BENNINGTON, C. (2003). Modeling and Dynamic Simulation of a Bleach Plant. *AIChE Journal*, **41**(12), 1707–1718.

WISNEWSKI, P. A. AND DOYLE, F. J. (1998). Control structure selection and model predictive control of the Weyerhaeuser digester problem. *J. Proc. Cont.*, **8**(5–6), 487–495.

WISNEWSKI, P. A. AND DOYLE, F. J. (2001). Model-Based Predictive Control Studies for a Continuous Pulp Digester. *IEEE Transactions on Control Systems Technology*, **9**(3), 435–444.

ZANETTI, R. J. (1994). Economic Indicators. *Chemical Engineering*, **101**(9), 197–198.

Appendix A

Kraft Models

A.1 Overview

This appendix contains many of the modelling details that were inspired or taken from the work of Dube [2000].

A.2 Blow-tank Storage Capacity

See Figure 3.4 for notation. The blowtank is divided into two pseudo steady-state sections and one dynamic section. The top of the blow tank, where steam is vented, is assumed to operate at steady-state. In addition, the agitated bottom of the blowtank is assumed to operate at steady-state, where dilution liquor is added to control outlet consistency. The middle portion is assumed to be above the point at which dilution liquor is added. The component balances around the first steady-state section are given by

$$F_{10}^{P} = F_{6}^{P}, \tag{A.1}$$

$$F_{10}^{W} = F_{6}^{W} - F_{7}^{W}, \tag{A.2}$$

$$F_{10}^{DS} = F_{5}^{DS}, \tag{A.3}$$

$$F_{7}^{W} = 0.02F_{6}^{W}, \tag{A.4}$$

where it is assumed that 2% of the incoming water stream is lost as steam for blow-tank pressure relief Dube [2000]. The middle section of the blowtank is modelled dynamically as a buffer capacity, as discussed in Section 3.3. The mixing point at dilution liquor is added is assumed to exist at the agitated section of the blowtank. The dilution liquor is recycled back from the first brown-stock washer seal tank. These balances are

$$F_{9}^{P} = F_{11}^{P}, \tag{A.5}$$

$$F_{9}^{W} = F_{11}^{W} + F_{8}^{W}, \tag{A.6}$$

$$F_{9}^{DS} = F_{11}^{DS} + F_{8}^{DS}. \tag{A.7}$$

A.3 Knotting Department

In this section, the knotters are modelled using steady-state mass balances. The function of the knotters is to remove large undigested pieces of wood. These are then collected and recycled to the digester with the chip load (not modelled). See Figure 3.7 for notation.

A.3.1 Primary Knotter

The mass balances are given by (based on Figure 3.7)

$$F_{12}^{P} + F_{13}^{P} = F_{9}^{P}, \tag{A.8}$$

$$F_{13}^{W} + F_{12}^{W} = F_{9}^{W} + F_{15}^{W}, \tag{A.9}$$

$$F_{13}^{DS} + F_{12}^{DS} = F_{9}^{DS} + F_{15}^{DS}, \tag{A.10}$$

where the feed of wash liquor for dilution (F_{15}) is set to be proportional to the incoming pulp stream, F_9, using the empirical constant, α_{dil1}=0.05 [Dube, 2000]. It is assumed that some pulp are lost in the reject stream (F_{13}). This is defined via an empirical constant, $\alpha_{knotrej1}$=0.10 [Grace *et al.*, 1989]. There are also additional equations to be constrain the pulp/water and water/dissolved solids ratios to be the same for accepts and rejects from the primary knotter. The balances are given by

$$F_{13}^{P} = \alpha_{knotrej1} \times F_{9}^{P}, \tag{A.11}$$

$$F_{12}^{W} F_{13}^{P} = F_{12}^{P} F_{13}^{W}, \tag{A.12}$$

$$F_{13}^{W} F_{12}^{DS} = F_{13}^{DS} F_{12}^{W}. \tag{A.13}$$

A.3.2 Secondary Knotter

Equations A.14-A.17 specify the component balances around secondary knotter. The feed of wash liquor for dilution (F_{16}) is set to be proportional to the incoming pulp stream, F_{13}, using the empirical constant, α_{dil2}=0.10. The rejects from the secondary knotter are sent to the knot tank, while the accepts are recycled back to the inlet of the primary knotter. The balances are given by

$$F_7^P = F_{13}^P - F_{14}^P, \tag{A.14}$$

$$F_{14}^P = 0.05 F_{13}^P, \tag{A.15}$$

$$F_{14}^W + F_7^W = F_{13}^W + F_{16}^W, \tag{A.16}$$

$$F_{14}^{DS} + F_7^{DS} = F_{13}^{DS} + F_{16}^{DS}, \tag{A.17}$$

$$F_{14}^W + F_{14}^{DS} = \alpha_{moist} \times (F_{14}^P + F_{14}^{DS} + F_{14}^W), \tag{A.18}$$

$$F_{14}^W F_7^{DS} = F_{14}^{DS} F_7^W. \tag{A.19}$$

where Equation A.18 specifies the amount of liquor (water and dissolved solids) lost with the dumped knots, through $\alpha_W = 0.10$

A.4 Brownstock Washers

For clarity, the mass balances will be shown only for one stage, using the nomenclature from Figure 3.8. At the header of the first stage, the pulp stream from the knotting department is combined with filtrate from the first stage's seal tank. The header outlet consistency is assumed to be perfectly controlled at 1.5% (Dube [2000] and Grace *et al.* [1989]), as stated in Equation A.23. See Figure 3.8 for notation.

A.4.1 Header

At the header, the pulp stream is combined with wash liquor from the first seal tank. The balances are given by

$$F_{17}^{P} = F_{12}^{P}, \tag{A.20}$$

$$F_{17}^{W} = F_{12}^{W} + F_{22}^{W}, \tag{A.21}$$

$$F_{17}^{DS} = F_{12}^{DS} + F_{22}^{DS}, \tag{A.22}$$

$$F_{17}^{P} = 0.015(F_{12}^{P} + F_{12}^{W} + F_{12}^{DS}). \tag{A.23}$$

A.4.2 Vacuum Drum Washing Unit

The vacuum drum washing unit requires component three component mass balances, and an expression for the washing efficiency. Consider Figure A.1, depicting just a single vacuum drum washer. The pulp is assumed to pass through the washer, with no loss. The water and associated dissolved solids each enter at two points (F_1 and F_2) and exit at two points (F_3 and F_4). The washing efficiency is defined at the ability to remove dissolved solids from the liquor in the pulp stream, and is assumed to be 90% for all washers in the system.

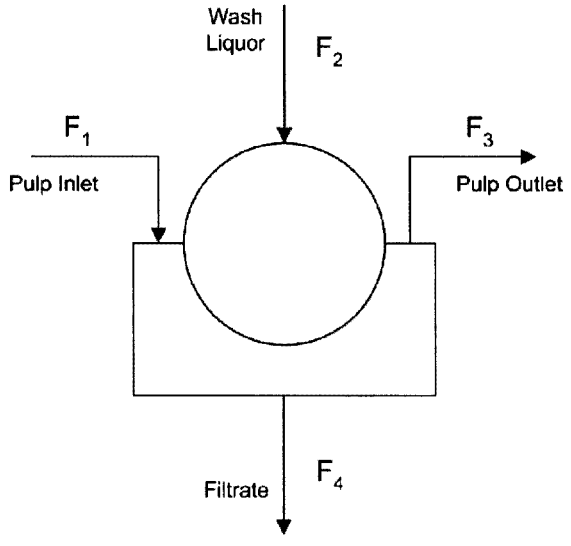

Figure A.1: Vacuum Drum Washing Unit

Returning to the stream numbering in Figure 3.8, component mass balances around the vacuum drum washer are given by

$$F_{18}^{P} = F_{17}^{P}, \tag{A.24}$$

$$F_{18}^{W} = F_{17}^{W} + F_{31}^{W} - F_{19}^{W}, \tag{A.25}$$

$$F_{18}^{DS} = F_{17}^{DS} + F_{31}^{DS} - F_{19}^{DS}, \tag{A.26}$$

$$F_{18}^{P} = 0.10(F_{18}^{P} + F_{18}^{W} + F_{18}^{DS}). \tag{A.27}$$

A.4.3 Seal Tank and Downstream Split-Point

There is assumed to be no accumulation in the seal tank, and therefore Equations A.28 and A.29 are simple steady-state mass balances. Equations A.30-A.32 are balances about the split point between the seal tank and the header. Equation A.32 specifies that the dissolved solids are split in the same ratio as the water (perfect liquor split), with the overall volume split governed by the consistency control at the header. The balances are

$$F_{20}^{W} = F_{19}^{W}, \tag{A.28}$$

$$F_{20}^{DS} = F_{19}^{DS}, \tag{A.29}$$

$$F_{22}^{W} = F_{20}^{W} - F_{21}^{W}, \tag{A.30}$$

$$F_{22}^{DS} = F_{20}^{DS} - F_{21}^{DS}, \tag{A.31}$$

$$F_{22}^{DS} F_{21}^{W} = F_{22}^{W} F_{21}^{DS}. \tag{A.32}$$

There are two brownstock washers between knotting and screening. Seal tanks are assumed to operate at steady state. The filtrate liquor from the last washing stage

is split between the blowtank (outlet consistency control) and the weak-black liquor tanks (recovery).

A.5 Screening Mass Balances

See Figure 3.9 for notation. While the primary screens section is presented, the secondary and tertiary screens follow the same structure as given here.

A.5.1 Mixing Point

The balances around the primary mixing point are the following.

$$F_3^P = F_1^P + F_9^P, \tag{A.33}$$

$$F_3^P = 0.03(F_3^P + F_3^W + F_3^{DS}), \tag{A.34}$$

$$F_3^W = F_1^W + F_2^W + F_9^W, \tag{A.35}$$

$$F_3^{DS} = F_1^{DS} + F_2^{DS} + F_9^{DS}. \tag{A.36}$$

At the primary screen, there is a 5% pulp loss due to the presence of the shives. The accepted product is diluted to 4.5% consistency and sent to the oxygen delignification department.

A.5.2 Screens

The balances around the primary screens are

$$F_5^P = F_3^P - F_6^P, \tag{A.37}$$

$$F_5^P = 0.95F_3^P, \tag{A.38}$$

$$F_5^P = 0.045(F_5^P + F_5^W + F_5^{DS}), \tag{A.39}$$

$$F_6^{DS} = F_3^{DS} + F_4^{DS} - F_5^{DS}, \tag{A.40}$$

$$F_6^W = F_3^W + F_4^W - F_5^W, \tag{A.41}$$

$$F_5^P F_6^W = F_5^W F_6^P, \tag{A.42}$$

$$F_5^P F_6^{DS} = F_5^{DS} F_6^P. \tag{A.43}$$

A.6 Oxygen Delignification

This section presents the model equations for the oxygen delignification department. See Figure 3.10 for notation.

A.6.1 O2 Feed Press

In the O2 Feed Press, a feed at 4.5% consistency is raised to 30% consistency. No pulp is lost in the press. Therefore, the simple mass-balances are

$$F_{81}^P = F_{80}^P, \tag{A.44}$$

$$F_{81}^W = F_{80}^W - F_{82}^W, \tag{A.45}$$

$$F_{81}^{DS} = F_{80}^{DS} - F_{82}^{DS}, \tag{A.46}$$

$$F_{81}^P = 0.30(F_{81}^P + F_{81}^W), \tag{A.47}$$

$$F_{81}^{DS} F_{82}^W = F_{81}^W F_{82}^{DS}. \tag{A.48}$$

where (A.44) and (A.46) are the mass balances around pulp and water. Equation A.47 specifies the outlet consistency from the press and equation A.48 follows the assumption that the dissolved solids are split in the same ratio as the water.

A.6.2 O2 Feed Press Filtrate Tank

There is assumed to be no accumulation in the O2 Feed Press Filtrate Tank.

$$F_{83}^{W} = F_{82}^{W}, \tag{A.49}$$

$$F_{83}^{DS} = F_{82}^{DS}. \tag{A.50}$$

A.6.3 Mixer

The mixer is the site at which the pulp is mixed with fresh caustic (for delignification), magnesium sulphate (for pulp protection), and steam. The pulp and chemicals are assumed to enter the mixer at 25°C. To raise the temperature to the required reaction level of 100°C, medium pressure steam is added. Therefore, the mixer requires 3 component mass balances and 1 energy balance. These are given as

$$F_{87}^{P} = F_{81}^{P}, \tag{A.51}$$

$$F_{87}^{DS} = F_{81}^{DS} + F_{84}^{DS} + F_{85}^{DS}, \tag{A.52}$$

$$F_{87}^{W} = F_{81}^{W} + F_{84}^{W} + F_{85}^{W} + F_{86}^{ST}, \tag{A.53}$$

$$F_{84}^{DS} = 0.020 F_{81}^{P} \tag{A.54}$$

$$F_{84}^{W} = \frac{0.92}{0.08} F_{84}^{DS} \tag{A.55}$$

$$F_{85}^{DS} = 0.002 F_{81}^{P} \tag{A.56}$$

$$F_{85}^{W} = \frac{0.955}{0.045} F_{85}^{DS} \tag{A.57}$$

$$F_{86}^{ST} = \frac{(F_{84}^{i} + F_{85}^{i}) c_{p,water} (T_{in,chem} - T_{set}) + (F_{87}^{P} c_{p,pulp} + F_{87}^{W} c_{p,water})(T_{in,pulp} - T_{set})}{c_{p,water}(T_{set} - 273) - H_{mps}} \tag{A.58}$$

where the F_{84}^{i} are the flows of water and dissolved solids in the 8% sodium hydroxide solution added, and F_{85}^{i} are those for the 4.5% magnesium sulphate solution. It is also assumed that the specific heat capacity of the chemicals is that of water. The dosages of sodium hydroxide, magnesium sulphate, steam, and oxygen are found in [Grace *et al.*, 1989], and are stated in Table 3.6. The steam addition will be a function of the inlet pulp flow and corresponding chemical additions. The steam rate is calculated by the energy balance stated in Equation , where T_{set} is the desired temperature in the oxygen delignification reactor.

A.6.4 Reactor

In the oxygen delignification reactor, pulp shrinkage occurs. A nominal shrinkage factor of 2.3% exists, based on typical pulp losses (lignin removal), as found in industrial studies by Sakuma *et al.* [1987] and Tatsuishi *et al.* [1987]. This factor is based on a drop in Kappa number from K_{in}=30 to K_{out}=12. However, this value will change

as production rates increase and decrease to combat disturbances and unit failures. Therefore, the shinkage factor is a function of a production factor, ζ, and is discussed in detail in Section 3.6.4.

$$F_{88}^{P} = (1 - \alpha_{O2})F_{87}^{P}, \tag{A.59}$$

$$F_{88}^{DS} = F_{87}^{DS} + \alpha_{O2}F_{87}^{P}, \tag{A.60}$$

$$F_{88}^{W} = F_{87}^{W} \tag{A.61}$$

where α_{O2} is the regressed shrinkage factor calculated using Equation 3.36, which is restated below.

$$\alpha_{O2} = -0.0113\alpha_{prod}^{3} + 0.0116\alpha_{prod}^{2} - 0.0022\alpha_{prod} + 2.301 \tag{A.62}$$

A.6.5 O2 Blowtank

There is assumed to be no accumulation in the O2 blowtank due to the very small volume of the vessel.

$$F_{89}^{P} = F_{88}^{P}, \tag{A.63}$$

$$F_{89}^{DS} = F_{88}^{DS}, \tag{A.64}$$

$$F_{89}^{W} = F_{88}^{W}. \tag{A.65}$$

A.6.6 Post-Oxygen Washer

In the post-oxygen washer POW), all dissolved solids are removed, and the pulp exists at 10% consistency. The underlying assumption for the removal of all the dissolved solids is that the washer is 100% efficient. It is assumed that no pulp is lost in the washer filtrate. The mass balances are given by

$$F_{91}^{P} = F_{89}^{P}, \tag{A.66}$$

$$F_{91}^{W} = F_{89}^{W} + F_{108}^{W} - F_{92}^{W}, \tag{A.67}$$

$$F_{92}^{DS} = F_{89}^{DS} + F_{108}^{DS}, \tag{A.68}$$

$$F_{91}^{P} = 0.10(F_{91}^{P} + F_{91}^{W}) \tag{A.69}$$

where the first three statements are the component mass balances, and the final equation is the constraint on the exit consistency. The washer shower liquor is comprised of the liquor from the bleach department, plus make-up water in the event of a bleach plant outage.

A.6.7 Post-Oxygen Filtrate Tank

There is assumed to be no accumulation in the Post-Oxygen Filtrate Tank.

$$F_{93}^{W} = F_{92}^{W}, \tag{A.70}$$

$$F_{93}^{DS} = F_{92}^{DS}. \tag{A.71}$$

A.7 Bleach Plant

A.7.1 Mixing Point

Before entrance to the bleaching tower, the pulp stream is first mixed with chlorine and chlorine dioxide. The mixing equations are therefore given by the following. See Figure 3.14 for notation.

$$F_5^P = F_1^P, \tag{A.72}$$

$$F_5^W = F_1^W + F_2^W + F_3^W + F_4^W \tag{A.73}$$

$$F_5^{DS} = F_1^{DS} + F_2^{DS} + F_3^{DS} \tag{A.74}$$

where steams F_2^i and F_3^i are the necessary chemical additions at each stage, and the proportion of water and dissolved solids is determined by the concentration of the chemical added. Note that at any given stage, there are no more than two chemicals added. The steam injection is given by F_4^W. Steam is injected at the same rate (kg/tonne O.D. pulp) at stages 2-5 - the D100 stage has no steam injection. Table 3.7 outlines the necessary chemical and steam addition at each bleaching stage [Wang *et al.*, 2003]. Within the reaction tower, shrinkage of the pulp occurs. A shrinkage factor, α_{D100}, is used to determine with component balances given by

A.7.2 Bleach Tower

$$F_6^P = (1 - \alpha) \times F_5^P, \tag{A.75}$$

$$F_6^W = F_5^W, \tag{A.76}$$

$$F_6^{DS} = F_5^{DS} + \alpha F_5^P, \tag{A.77}$$

where α is the proportion of pulp that is removed (bound lignin removed) and enters the dissolved solids phase. The α for each stage is set according to the typical drop in Kappa number/brightness for an industrial process [Wang *et al.*, 2003], and are tabulated in Table 3.8. Based on the shrinkage factors and Kappa number reduction, it becomes evident why the first two stages are the true stages and the subsequent stages are termed brightening stages.

A.7.3 Bleach Washer

The balance around the washer header is given by component balances

$$F_7^P = F_6^P, \tag{A.78}$$

$$F_7^W = F_6^W + F_{13}^W, \tag{A.79}$$

$$F_7^{DS} = F_6^{DS} + F_{13}^{DS}, \tag{A.80}$$

$$F_7^P = 0.015(F_7^P + F_7^W + F_7^{DS}), \tag{A.81}$$

where the amount of seal tank water recycled is governed by the consistency requirement defined by Equation A.81. The washer utilizes filtrate liquor from the upstream stage as well as fresh water as necessary. The washer is assumed to be 100% efficient in the removal of dissolved solids, and it is assumed that no pulp is lost in the filtrate stream. Balances are given by

$$F_{10}^P = F_7^P, \tag{A.82}$$

$$F_{10}^P = 0.10(F_{10}^P + F_{10}^W), \tag{A.83}$$

$$F_{11}^W = F_7^W + F_8^W + F_9^W - F_{10}^W, \tag{A.84}$$

$$F_{11}^{DS} = F_7^{DS} + F_9^{DS}. \tag{A.85}$$

The washer shower flow (in this case, F_9^i) originates from downstream bleaching stages, and the make-up water rate is adjusted to meet the consistency requirement, as well as aid in the event of downstream outages.

A.7.4 Seal tank and split-point

There is no accumulation in the seal tank. The component balances are given by

$$F_{12}^W = F_{11}^W, \tag{A.86}$$

$$F_{12}^{DS} = F_{11}^{DS}, \tag{A.87}$$

The filtrate from the seal tank is split into two streams, having the same composition. The split ratio is determined via a consistency constraint on the feed to the washers. The remainder of the stream is sent to the upstream bleaching stage. In the case of the first stage, the remaining filtrate is sent to the post-oxygen washer in the oxygen delignification department.

$$F_{12}^W = F_{13}^W + F_{14}^W, \tag{A.88}$$

$$F_{12}^{DS} = F_{13}^{DS} + F_{14}^{DS}, \tag{A.89}$$

$$\frac{F_{13}^W}{F_{14}^W} = \frac{F_{13}^{DS}}{F_{14}^{DS}}. \tag{A.90}$$

At the outlet of the bleach-plant, there exists a 300-tonne high-density storage vessel. It is modelled as a dynamic storage capacity, as discussed.

A.7.5 Chemical and Steam Usage

For ease of use in the objective function and steam production model, the chemical usages and steam requirements are summed.

$$F_{Cl_2,Total} = \sum_{i=1}^{5} F_{Cl_2,i}, \tag{A.91}$$

$$F_{ClO_2,Total} = \sum_{i=1}^{5} F_{ClO_2,i}, \tag{A.92}$$

$$F_{NaOH,Total} = \sum_{i=1}^{5} F_{NaOH,i}, \tag{A.93}$$

$$F^{Bleach}_{Steam,Total} = \sum_{i=1}^{5} F_{Steam,i}, \tag{A.94}$$

where i identifies the stage number.

A.8 Drying Section

This section presents the model equations for the dry end of the pulp stream. See Figure 3.16 for notation.

Headbox

The headbox is modelled as

$$F_{D2}^{P} = F_{D1}^{P}, \tag{A.95}$$

$$F_{D2}^{W} = F_{D1}^{W} + F_{D5}^{W}, \tag{A.96}$$

$$F_{D2}^{W} = x_{H2O,headbox}(F_{D2}^{P} + F_{D2}^{W}). \tag{A.97}$$

Machine

The machine model is given by

$$F_{D6}^{P} = F_{D2}^{P}, \tag{A.98}$$

$$F_{D6}^{W} = F_{D2}^{W} - F_{D3,W}, \tag{A.99}$$

$$F_{D6}^{W} = x_{H2O,dryer}(F_{D6}^{W} + F_{D6}^{W}), \tag{A.100}$$

$$F_{D5}^{W} = F_{D3}^{W} - F_{D4}^{W}. \tag{A.101}$$

Dryer

The dryer models are

$$F_{D8}^{P} = F_{D6}^{P}, \tag{A.102}$$

$$F_{D8}^{W} = F_{D6}^{W} - F_{D7}^{W}, \tag{A.103}$$

$$F_{D8}^{W} = x_{H2O,market}(F_{D8}^{W} + F_{D8}^{W}). \tag{A.104}$$

- The energy balance around the dryer is formulated using a steam economy that states the mass of steam required is equal twice the amount of water driven off in the dryer (Table 3.9, Dube [2000]).

$$F_D^{ST} = 2 \times F_{D7}^W, \tag{A.105}$$

$$F_D^{COND} = F_{D,ST}. \tag{A.106}$$

A.9 Recausticizing

All steady-state mass balances in this section are based on the mass balance over the typical recausticizing plant, as given by Grace *et al.* [1989]. See Figure 3.20 for notation.

A.9.1 Dissolving Tank

$$F_{R1}^{DS} = F_{R3}^{DS} + F_{R4}^{DS}, \tag{A.107}$$

$$F_{R2}^W = F_{R3}^W + F_{R4}^W, \tag{A.108}$$

$$F_{R2}^W = 9.2 F_{R1}^{DS}, \tag{A.109}$$

$$F_{R4}^{DS} = 0.01 F_{R1}^{DS}, \tag{A.110}$$

$$F_{R3}^{DS} F_{R4}^W = F_{R3}^W F_{R4}^{DS}. \tag{A.111}$$

A.9.2 Dregs Filter

$$F_{R5}^{DS} = F_{R4}^{DS}, \tag{A.112}$$

$$F_{R6}^W = F_{R4}^W, \tag{A.113}$$

$$F_{R2}^W = F_{R6}^W + F_{R7}^W, \tag{A.114}$$

A.9.3 Slaker Causticizer

$$F_{R9}^{DS} = 0.67F_{R8}^{DS}, \tag{A.115}$$

$$F_{R8}^{DS} + F_{R9}^{DS} = F_{R10}^{DS} + F_{R11}^{DS}, \tag{A.116}$$

$$F_{R8}^{W} + F_{R9}^{W} = F_{R10}^{W} + F_{R11}^{W}, \tag{A.117}$$

$$F_{R10}^{DS} = 0.02(F_{R8}^{DS} + F_{R9}^{DS}), \tag{A.118}$$

$$F_{R10}^{DS}F_{R11}^{W} = F_{R10}^{W}F_{R11}^{DS}. \tag{A.119}$$

A.9.4 White Liquor Clarifier

$$F_{R11}^{DS} = F_{R12}^{DS} + F_{R13}^{DS}, \tag{A.120}$$

$$F_{R11}^{W} = F_{R12}^{W} + F_{R13}^{W}, \tag{A.121}$$

$$F_{R13}^{DS} = 0.52(F_{R11}^{DS}), \tag{A.122}$$

$$F_{R13}^{DS} = 0.212(F_{R13}^{W} + F_{R13}^{DS}). \tag{A.123}$$